

Load Hiding of Household's Power Demand

Master's thesis
submitted by

Christoph Prokop

supervised by:
Assoc.-Prof. Dipl.-Ing. Dr.techn. Udo Bachhiesl

Institute of Electricity Economics and Energy Innovation
Graz University of Technology

and:
Dipl.-Ing. Dominik Egarter

and:
Univ.-Prof. Dipl.-Ing. Dr.techn. Wilfried Elmenreich

Institute of Networked and Embedded Systems
Alpen-Adria-Universität Klagenfurt

April 2014/Graz

Statutory Declaration

I declare that I have authored this thesis independently, that I have not used other than the declared sources / resources and that I have explicitly marked all material which has been quoted either literally or by content from the used sources.

.....
date

.....
(signature)

Acknowledgement

Foremost, I would like to thank all those people around me, who made this thesis possible for me.

First of all, I would like to express my sincere gratitude to my adviser Assoc.Prof. Udo Bachiesl. Although there were some busy months due to the organization of the 13th symposium energy innovation in Graz in February 2014, he agreed to supervise my Master's thesis anyway.

This thesis would not have been possible without the help and support of my co-adviser Prof. Wilfried Elmenreich who also made the proposal for this thesis.

My sincere thanks is also owed to Dominik Egarter for his personal support and great patience at all times.

Last but not least, I would like to thank Anna Cmaylo for proofreading this thesis, my girlfriend for her patience at all times and my parents for their continuous support - not only materially.

Abstract

In a context of an ongoing transformation process of the electricity market, the rollout of smart meters will be one part of a modernized electricity system.

Such intelligent meters have potential benefits, but also raises new concerns regarding privacy protection. The frequent real-time data transmission of the end-users' electricity demand to the utility would allow for disaggregating the aggregated load profile to retrieve information about which device is operating and when. The disaggregation of the load profile into composite appliance profiles allow for determining activities such as the end users' wake and sleep cycles.

In order to maintain a satisfying level of privacy protection, implementing a load hiding system can be one meaningful approach. The installation of a battery system allows for flattening the metered load to reduce the information that can be gleaned from the load profile.

This thesis evaluates the effectiveness of state-of-the-art battery-based load hiding algorithms by analyzing the accuracy of a disaggregation technique. Moreover, accompanying issues such as the battery dimensioning and the practical feasibility will be discussed. Furthermore, this work proposes a new load-based load hiding system. Similar to the battery system, a controllable load like a domestic hot water boiler allows the system to manipulate the household's power demand by consuming power at strategic times. Finally a comparison between the load-based and battery-based system points out the difference of the effectiveness of these methods.

Kurzfassung

Im Rahmen der fortwährenden Umgestaltung des Elektrizitätsmarktes bildet auf Verbraucherseite die Installation der Smart Meter einen wesentlichen Teil eines modernen und stärker vernetzten Elektrizitätsversorgungssystems.

Die Einführung dieser intelligenten Zählwerke bringt nicht nur potentielle Vorteile mit sich, sondern es nehmen auch Bedenken bezüglich der Privatsphäre zu. Die hochaufgelöste Echtzeitübermittlung des aktuellen Energiebedarfs eines jeden Endkunden an das EVU wird dabei besonders kritisch betrachtet. So ermöglichen Algorithmen die das gemessene Lastprofil in die Betriebszustände der angeschlossenen Haushaltsgeräte zerlegen können weitreichende Erkenntnisse über das Kundenverhalten. Beispielsweise können anhand der Daten Gewohnheiten wie der Wach-/Schlafrythmus ermittelt werden.

Um dem damit einhergehenden Privatsphärenverlust entgegen zu können, wurden Verschleierungssysteme entwickelt. Diese Systeme versuchen direkt auf Endkundenseite das Lastprofil gezielt zu beeinflussen. So kann ein Batteriesystem durch intelligente Ansteuerung das elektrische Lastprofil des Netzkunden derart abflachen, dass kaum mehr Informationen daraus gewonnen werden können.

Diese Masterarbeit testet aktuelle Batterieverschleierungsalgorithmen anhand eines Simulationsmodells. Um die Effektivität dieser Systeme vergleichen zu können, wird anschließend die Erfolgsrate eines Algorithmus zur Zerlegung des Lastprofils in die einzelnen Haushaltsgeräte ausgewertet. Dazu passend wird auf Fragestellungen wie das Dimensionieren des Batteriesystems und eine mögliche praktische Realisierung eingegangen. Des Weiteren wird ein neues lastbasiertes System vorgeschlagen. Ähnlich dem Batteriesystem könnten steuerbare Lasten wie elektrische Warmwasserboiler gezielt eingesetzt werden, um den Strombedarf des gesamten Haushalts beeinflussen zu können. Schließlich wird die Effektivität eines solchen lastbasierten mit den batteriebasierten Systemen verglichen.

Contents

1	Introduction	9
1.1	Smart Grids and Smart Meter	9
1.2	Potential of Smart Metering	12
1.3	Threats of Introducing Smart Meter	13
1.4	Possible Solutions to Privacy Loss	15
1.5	Nonintrusive Load Monitoring	16
1.6	Load Hiding Systems	18
1.7	Time-Based Pricing	19
2	Battery-Based Load Hiding	21
2.1	Introduction	21
2.2	Algorithms	22
2.2.1	Best Effort Algorithm	22
2.2.2	Stochastic Algorithm	25
2.2.3	Non-Intrusive Load Leveling	25
2.2.4	Stepping Framework	27
2.3	Battery Configuration	28
2.4	Implementation	31
3	Load-Based Load Hiding	32
3.1	Introduction	32
3.2	Algorithm	33
3.3	Load Configuration	35
3.4	Implementation	36
4	Evaluation Setup	37
4.1	Measuring Privacy Protection	37
4.1.1	Relative Feature Mass	37
4.1.2	Root-Mean-Square Error	38
4.1.3	F-Measure	39
4.2	Data Setup	40
4.2.1	Database	40
4.2.2	Data Preparation	42
4.2.3	Load Profile	42
4.2.4	Dynamic Pricing	45

4.3	Battery-Based Load Hiding	45
4.3.1	Battery Configuration	45
4.3.2	Simulation Model	47
4.3.3	Assumptions	49
4.4	Load-based Load Hiding	50
4.4.1	Load Configuration	50
4.4.2	Noise Generation	50
4.4.3	Simulation Model	51
4.4.4	Assumptions	51
5	Results	53
5.1	Battery-Based Load Hiding	53
5.1.1	Net Demand vs. Metered Load	53
5.1.2	Battery Configuration	59
5.1.3	Current Ratings vs. Battery's Capacity	62
5.1.4	Potential Savings	64
5.1.5	UPS Capability	66
5.1.6	Implementation	67
5.2	Load-Based Load Hiding	69
5.2.1	Net Demand vs. Metered Load	70
5.2.2	Load Configuration	73
5.2.3	Implementation	76
6	Comparison and Discussion	78
6.1	BLH Battery Setup	78
6.2	BLH Algorithms	81
6.3	LLH Algorithms	83
6.4	BLH vs. LLH	84
7	Conclusion and Outlook	87

Acronyms

BE Best Effort

BLH Battery-based Load Hiding

DOD Depth of Discharge

HMM Hidden Markov Model

ICT Information and Communications Technology

iid independent and identically distributed

LLH Load-based Load Hiding

NILL Non-Intrusive Load Leveling

NILM Nonintrusive Load Monitoring

PDF Probability Density Function

RFM Relative Feature Mass

RMSE Root-Mean-Square Error

SF Stepping Framework

SOC State of Charge

1 Introduction

1.1 Smart Grids and Smart Meter

In times where climate change, energy efficiency and scarcity of resources are widely discussed issues, innovations with regards to energy production, transportation and consumption side become more and more important. This is where smart grids and smart meters come into play.

“A Smart Grid is a modern electricity system. It uses sensors, monitoring, communications, automation, and computers to improve the flexibility, security, reliability, efficiency, and safety of the electricity system.” [60]

The European Parliament forces the liberalization of the electricity market via the third energy package with the directive 2009/72/EC¹ in order to transform the electricity markets from vertical integrated electric utilities to a more competitive market with independent market players. Together with the strongly promoted and subsidized expansion of renewables, this led and still leads to a more decentralized energy supply with excess but smaller gensets. Compared to centralized systems in the past, decentralization increases the requirements to the system operator to maintain a good quality of supply.

Electric energy is characterized by being difficult to store which means that the level of supply must equal usage all the times. As supply has to keep up with usage, the transformation process towards decentralization brings up challenges: on the one hand renewables like photovoltaic and wind energy are supply-dependent, whereas a mix of conventional power plants based on hydro power, nuclear power or fossil fuels allow better control in a need-based matter. This uneven load of renewables must be forecasted and the gap between supply and usage has to be compensated by conventional power plants, e.g. combined cycle plants or pumped storage hydro power stations.

High subsidies for renewables and the nearing end of the design life of conventional power plants, especially with regards to the current situation in Germany conventional power plants are more and more advised out of the market, which increases the problem of attempting to maintain the balance between supply and usage at all times. This challenge can be minimized by reducing the gap between the load demanded by the customers and the given supply of the renewables.

Furthermore, electrical power grids and the generation system need to be dimensioned for the maximum load that can be expected during normal operation. A glance at

¹Directive 2009/72/EC of 13th of July 2009 concerning common rules for the internal market in electricity and repealing Directive 2003/54/EC

Austrian load profiles shows that the power demand increases during cold and extreme hot seasons and, on a smaller time scale, on weekdays at midday and in the early evening. The entire generation system (or rather imports) must be able to cover the maximum demanded load, which necessitates running power plants with a limited time of operation, though this results in high costs holding enough power generation units available for covering peak times. Maintaining a more constant load for conventional power plants would reduce the system costs. The electrical energy produced by these plants must also be transmitted to the customers. If power plants are built hundreds of kilometers away from the majority of the customers this may overload the grid, especially during those peak loads. To tackle such congestions, system operators may activate utilities such as phase-shifting transformers, or they may choose to redispatch the power plant deployment. Due to the limits of this loophole it seems to be necessary to strengthen the power grids, however, the projects are delayed or even doomed by the resistance of the affected landowners very often.

In order to solve both problems, customers need information and incentives when to consume energy, such as time-based pricing models. In a worst-case scenario, customers would be restricted to a maximum load or suffer from partial/total disconnection from the power grid during a congestion. This asks for a better communication between the suppliers, the grid operator and the customers. Large power plants are already well connected with the transmission grid in terms of working communication infrastructure, which essentially grasps the meaning of a smart grid, the situation in medium high voltage and low voltage systems looks more bleak. So-called smart grids necessitate the extension of Information and Communications Technology (ICT) between customers, power grid operators and suppliers in order to handle various challenges.

On the customer side this is where smart meters come into play. Since the introduction of the electromechanical induction watt-hour meters, complete with manual readout technology, in 1888, there was no significant development regarding electricity meters until the 1990s when the South African Electricity Supply Commission introduced digital readout meters [66]. Further enhancements led to electricity meters that are now known as smart meters.

Smart meters are electronic devices that record consumption, not necessarily solely of electricity but also of gas, water, heating and hot water in intervals of, for example, 15 min or even one second. This data should be provided to the customers in order to motivate a change in habits dependent on actual congestions on the power generation system side or the power grid side and, moreover, to save energy [51]. Furthermore, the data are meant to be sent to the utility for monitoring purposes, customer information and forecasting but also for billing purposes.

The concrete requirements of a smart meter depend on the region. In Austria they are listed in the ordinance “E-Control Ordinance Determining the Requirements for Smart Meters 2011,” see [30] published by E-Control, the Austrian energy markets regulator.

Corresponding to the ordinance and the associated annotations [29] the functionality of smart meters should comprise the following itemization:

- Two-way communication via Powerline, GRPS, ADSL, xDSL, wireless or similar

to be able to send and receive data to and from the system operator or a third party.

- Secured state-of-the-art communication to prevent access by non-entitled parties.
- The possibility to encrypt the display to avoid unwarranted readings by neighbours, etc.
- Data readings of the consumed energy with a timestamp of the balanced active power or balanced active energy every 15 minutes, 15 minutes, which allows the installation of electricity generators such as photovoltaic systems without the installation of a second electricity meter.
- Save the aggregated daily consumption.
- Store readings for a maximum of 60 days.
- To send all data until midnight of each day to the system operator via a communications interface daily no later than 12:00 on the following day.
- Prepaid tariffs or the possibility to remotely disable the connection of the customer facility and to restrict the maximum load; in case of a resetting the customer has to reactivate the current flow for safety reasons itself.
- A secured and encrypted communications interface to communicate with external devices such as other quantity metering devices for energy management purposes.
- An internal clock and calendar with remote synchronisation.
- To support status and/or error logs and access logs and the meters shall be equipped with a manipulation detection function.
- Remote software updates.
- The smart meters have to comply with the provisions of metrology and calibration law and data protection.

The legal framework for smart metering is based on the directive 2009/72/EC and is also mentioned in 2006/32/EC².

As per the directive 2009/72/EC:

“Where roll-out of smart meters is assessed positively, at least 80 % of customers shall be equipped with intelligent metering systems by 2020.”

²Directive 2006/32/EC of 5th of April 2006 on energy end-use efficiency and energy services and repealing Council Directive 93/76/EEC

Based on a cost-benefit-analysis, an outsourced PricewaterhouseCoopers Austria study in 2010 [65] concludes that the implementation of smart metering in Austria would be beneficial from an economic point of view. In contrast to that, an outsourced Ernst & Young study in Germany in 2013 [35] concludes the opposite, claiming the smart meter installation costs exceed the expected benefits.

Due to the ordinance for the implementation of intelligent meters in [18] system operators are obligated to install at least 10 % of their metering points with smart meters by 2015, 70 % by 2017 and 95 % by 2019 with a few exceptions due to already installed load profile and smart meters, for further information see [18].

1.2 Potential of Smart Metering

Aside from easing the progress of decentralization, the installation of smart meters may offer the potential for further benefits.

As environmental matters have gained more importance, greater energy efficiency and savings are central steps to reducing greenhouse gas emissions as outlined by Europe 2020 targets. Smart metering can be one of the many factors used to meet these targets. As per [65] the realtime reading of the consumed energy and the possibility to compare the development of consumption via a feedback system of the system operator using websites or mailings should force customers to adjust their consumption behaviour. As per [29] customers with yearly settlements are confronted with annual data of their energy consumption, sometimes even based on calculations and not on manual readings. Smart meters should enable better control of the consumption like providing monthly settlements [29]. [65] expects that such a system should be able to reduce electricity consumption by 3.5 %. The disaggregation of an end-user's load profile into the appliance's profiles can help realize large-scale and cost-effective energy savings [51]. Using such a disaggregation technique, a so-called Nonintrusive Load Monitoring (NILM) algorithm, allows for direct feedback as well as automated personalized recommendations to the end-user.

A project commissioned by Ofgem³ “was designed to help better understand how domestic customers react to improved information about their energy consumption over the long term” [15]. The project began in 2007, finished in 2010 and used different combinations of measures, including four energy supply companies with more than 60.000 households. The energy companies were able to find statistically significant energy savings from smart meters depending on the feedback and interventions of the supply companies [15].

On the customer side there are numerous benefits such as greater transparency and comprehension of energy consumption levels and furthermore increased ease in change of supplier due to remote readouts [65].

In addition smart meters will enable remote control to minimize electricity theft and allows a dynamic pricing scheme, with more than just one fixed off-peak tariff during

³Ofgem: Office of Gas and Electricity Markets, the government regulator for electricity and natural gas markets in Great Britain

nights and the regular tariff. There are different approaches to implement time-based pricing such as the so-called Tarif Bleu Option Tempo in France. The electricity market in France is distinguished due to both a high share of nuclear energy providing base load and a high number of electric heaters. This results in high peaks during cold season. To master the situation the French energy supplier EdF⁴ offers several tariffs such as the Tarif Bleu Option Tempo. French customers are informed via SMS, television, radio, internet, etc., about the tariff levels on a specific day: blue days refer to lower priced electricity, whereas electricity on red days is priced much higher, sometimes fivefold the rate on a blue day. This system helps minimize the peak loads and referring to [26] the system is quite successful.

Summing up, as [66] depicts:

“The idea is that smart meters will enable customers to conserve energy and adapt usage to supply conditions.”

1.3 Threats of Introducing Smart Meter

Smart metering systems provide high resolution and realtime end user power consumption data for utilities for monitoring, controlling, managing and billing purposes [22]. Besides the advantages of fine grained data for customers, for system operators, power plants and billing companies, smart metering data could be used to analyze the end-user's habits when applying a NILM algorithm. For example, researchers in [58] have shown that power consumption data with an sampling interval of max. 15 s allows detailed information on customer activities such as whether someone is home and reading the appliances use-status of the microwave, stove, water heater, TV etc., can determine the sleep/wake cycle and other events like showers, breakfast, dinner and parties.

Such fine grained data could answer the following questions [13], [20], [33], [38]:

- Were you home during your sick leave?
- Did you sleep well?
- How often do you eat microwave dinner?
- How many hours of TV do you watch?
- Do you eat breakfast, if so - a cold or hot one?
- Are you a devout muslim?

Furthermore there are agencies, organizations and individuals that may have motives to use power consumption data such as [37], [58], [66], [73]:

⁴EdF: Électricité de France SA

- Law enforcement agencies: e.g. to use records to seek out drug producers (e.g. the Austin Police Department as a special case even without a search warrant) relying on the fact that the heat lamps and watering systems increase the consumption far beyond the norm.
- Marketing: energy management tools like Google PowerMeter⁵ and Microsoft Hohm⁶ may feature their tools by using metering information for advertisements for repairs or new products if the customer's device gets broken. Moreover, this helps sellers adjust their prices to the customer's needs.
- Supply companies: combined with time-based pricing the data could allow supply companies to engage in predatory pricing and pursue exploitative contracts as the utilities exactly know the customers behaviour and needs.
- Insurance companies: could use information about customers' life patterns to charge those with "unhealthy" patterns more. They could also use the data to check if people on a sick leave are staying at home and to determine care premiums based on unusual behaviour indicating illness.
- Criminal activities: having information about the user's presence at home facilitates burglary and helps identify the presence of high-priced appliances.
- Creditor: usage patterns could provide information on the credit-worthiness of the customer.
- Press: to collect information on celebrities and other people in the public eye.

The 2010 Austrian study concluding with the view that the implementation of smart metering would be beneficial from an economic point of view [65] suggests the use of a web portal summarizing the data provided by smart meters and in agreement with the customers to transmit that data to third parties like energy consultants, suppliers or energy providers.

Anderson [66] argues that implementing remote off switches in smart meters to minimize electricity theft and defaults in payment may be hazardous, as cyber terrorists or wartime enemies could be able to shut electricity down. Furthermore, he sees another risk if a region faces a supply crunch as old power stations are near the end of their design lives. Will ministers cut off households who fail to meet saving targets or the most profligate household in each street?

Supporting the seriousness of this privacy threat, in 2009 the Dutch court decided that the mandatory collection of nonessential fine grained metering data is contrary to article 8, ECHR⁷ [23].

The NIST report on Smart Grid Interoperability Standards [61] states:

⁵Google PowerMeter: project to track electricity usage to save energy, announced in 2009, discontinued in 2011

⁶Microsoft Hohm: web application by Microsoft to analyze energy usage based on recommendations, announced in 2009, discontinued in 2012

⁷ECHR: European Convention on Human Rights, entered into force on 3rd of September 1953

“The major benefit provided by the Smart Grid, i.e. the ability to get richer data to and from customer meters and other electric devices, is also its Achilles’ heel from a privacy viewpoint.”

1.4 Possible Solutions to Privacy Loss

Privacy is “someone’s right to keep their personal matters and relationships secret” as per Cambridge Dictionary⁸.

With regards to this definition, smart metering may result in a conflict with privacy. Nevertheless reporting energy usage accurately is essential for the smart grid. [22] specifies some requirements considering a smart meter framework taking privacy preservation into account as well:

- to fully protect user’s privacy
- without sacrificing the resolution of smart meter data for actual load management usage
- to provide a verifiable billing method
- without a trusted third party.

[37] categorizes the effort to meet privacy issues into the following classes:

- Anonymization of metering data to separate the data from customer IDs which necessitates a third-party involved.
- Metering data obfuscation to mask the energy consumption profile, e.g. with local battery buffers, the so called Battery-based Load Hiding (BLH).
- Privacy-preserving metering data aggregation, e.g. sums the data of many customers up prior to sending the data to the utility.

The first category aims to address the privacy issue by anonymizing the customer’s identity through using an escrow service as a third party, as proposed by Efthymiou and Kalogridis in [19]. In fact, the authors state that this proposal may not offer sufficient smart metering protection, but it contributes an additional layer of privacy protection. The problem remains that the necessity to trust a third party should be avoided due to the framework requirements above.

In order to address these issues, several researcher developed systems that fit into the third category, see [22], [36], [38] and [49]. Using this method of data aggregation includes the encryption of the data, followed by an aggregation prior sending the data to the utility. With regards to an encryption system, many papers suggest some sort

⁸Cambridge Dictionary: Cambridge Advanced Learner’s Dictionary and Thesaurus, Cambridge University Press, online: <http://dictionary.cambridge.org/dictionary/british/privacy?q=privacy>, accessed on 7th October 2013

of homomorphic encryption which allows the summing up of ciphertext (so that each individual's contribution remains encrypted) which equals after the decryption the sum of the same operation using plaintext. Due to a random factor such homomorphic encryption techniques are indeterministic, i.e. they are resistant to dictionary attacks [36].

Acs and Castelluccia [39] follow a similar approach of aggregating a cluster of thousands of smart meters using a modulo addition-based encryption scheme, which is arguably easier to adopt than homomorphic encryption. Prior applying this encryption technique, they implement a Laplacian Perturbation Algorithm, which modifies the measure by adding noise. The noisy and encrypted measure will be sent to the supplier that is only able to decrypt the noised aggregated electricity consumption of the cluster without gaining access to individual values. The aggregate is noised just enough to provide privacy to each user, while still providing a low data error [39].

Moreover the third category can offer the advantage of reducing the amount of data that is generated due to the summation of many metering points. This scheme can satisfy all four requirements to a smart meter framework [22] but raises new concerns such as electricity theft that would be impossible to detect. Referring to [40] this solution is the most relevant one to protect smart grid privacy at the moment.

Aside from these schemes, the second class of metering data obfuscation seems promising as well. While it currently lacks in efficiency, the idea of BLH is to install a control system in combination with a rechargeable battery between the metering point and the internal wire to obfuscate the actual power consumption with characteristic peaks by modifying and smoothening the load profile, as proposed by [27], [40], [70] and [74]. Obfuscating metering data could also be done on the customer's load side for powerful interruptible processes that are not time-critical and adjustable in their power consumption, with the same result of modifying or smoothening the total load. Such a process could be a domestic electric hot water boiler, an electric heater, or perhaps even an electric vehicle charger. In the remainder, systems using such a variable load will be shortened by Load-based Load Hiding (LLH), inspired by BLH.

1.5 Nonintrusive Load Monitoring

NILM or Nonintrusive Appliance Load Monitoring demonstrates how the information gleaned through metered energy data can be used to track appliance usage patterns [40]. As early as 1992, Hart defined [41]:

“A nonintrusive appliance load monitor determines the energy consumption of individual appliances turning on and off in an electric load, based on detailed analysis of the current and voltage of the total load, as measured at the interface to the power source.”

Following, NILM algorithms decompose load profiles into composite appliance profiles based on either known or learned signatures [70]. Based on [14] the NILM approach is illustrated in Figure 1.1. As [14] explains: the first step is to acquire the aggregated

load measurement by the smart meter. After applying some preprocessing such as filtering, the next module extracts features from the load profile data. Referring to [47] such features could be switching transients (ON/OFF-events), the current waveform, active and reactive power, harmonics, eigenvalues of the current waveform, the instantaneous admittance or power waveform. Then the load identification attempts to identify appliance-specific states from the aggregated measurement. The last step is the system training process. The learning process can be divided into supervised and unsupervised learning approaches. Supervised mechanisms require labeled data sets to train the classifier [14]. This approach incurs extra human effort, whereas the unsupervised method tries to achieve disaggregated energy sensing without a-priori information [14].

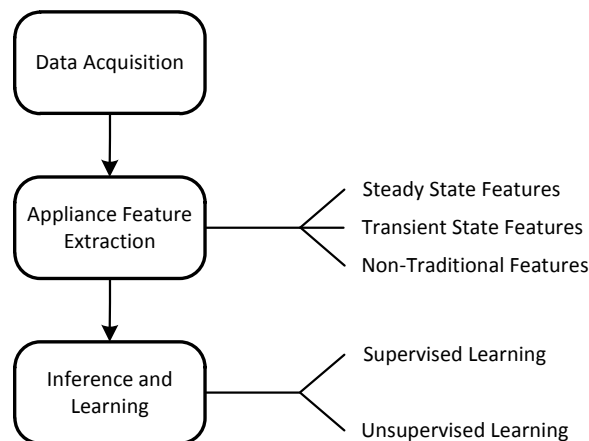


Figure 1.1: NILM approach to disaggregate the load profile [14]

[48] demonstrates that the use of multiple features increases the disaggregation accuracy remarkable. For a more cost-effective NILM solution [57] lists some methods that base on very few data. As an example [57] lists a heuristic approach that uses real power data with a 15 min. sampling interval.

Referring to [74] various NILM approaches are based on edge detection:

Traces of discrete changes in energy use can be mapped directly to ON/OFF events of appliances. NILM matches sister features (ON/OFF events with the same amplitude) against known profiles, e.g. a light bulb, to uncover usage patterns by extracting such appliance profiles from the household's load profile where the appliance's power signatures are aggregated [70]. Techniques that reconstruct the usage pattern have been shown to be highly accurate in practise [32], [58], [59]. Such a result is illustrated in Figure 1.2.

Aside from edge detection, another important approach is to determine the appliance's ON/OFF-state for each sampling interval by evaluating the most likely combination of the appliances that are turned ON. One idea is to model each appliance as an Hidden Markov Model (HMM), which is a model in which the states are not directly observable but are characterized by a probability density function. In order to model the aggregated load profile using the HMM a Factorial Hidden Markov Model (FHMM) can be used [76].

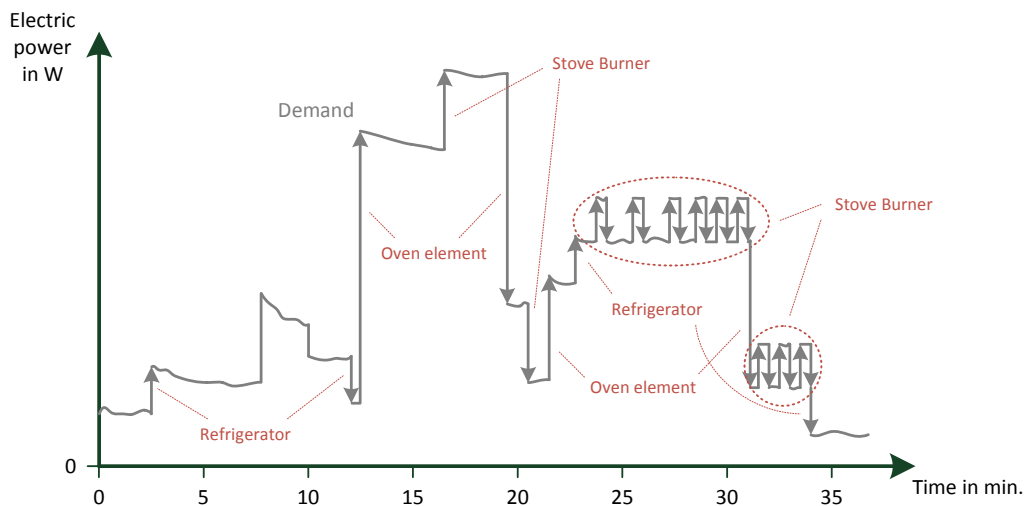


Figure 1.2: Exemplary load changes due to individual appliance events, reproduced from [41]

The idea is to find the combination that results in an aggregated signal that is as close as possible to the observed signal [48]. Such an algorithm that determines these hidden states via a probability distribution using a particle filter was proposed by Egarter et al. [24]. In the remainder this NILM algorithm will be used to evaluate the effectiveness of the load hiding systems.

To gain high success rates of decomposing load profiles necessitates a high sampling rate at the current state of research. [40] claims that, within the near future, use of less fine-grained data, e.g., intervals of 15 min., will allow data readers to predict the operation of certain home appliances. [73] argues that when using long sampling periods like 15 min., fast switching appliances can no longer be recognized, but measuring active and reactive power helps in identifying certain appliances once again.

Note that NILM algorithms do have useful applications, such as informing electricity customers about their usage patterns, which may help conserve energy as demonstrated in [51]. However, analyzing a user's electric load profile to deduce the appliances that are being used can be done remotely without the knowledge of the household's residents [74].

1.6 Load Hiding Systems

The idea behind a load hiding system is to obfuscate the fine-grained energy consumption data measured by the smart meter. In principle net demand, which is the demand of all appliances except the load hiding system, could be modified by hiding, obfuscating or smoothing, as illustrated in Figure 1.3 [40].

The state-of-the-art technique of a load hiding system is BLH. It uses a rechargeable battery that gets charged and discharged at strategic times, attempting the modification

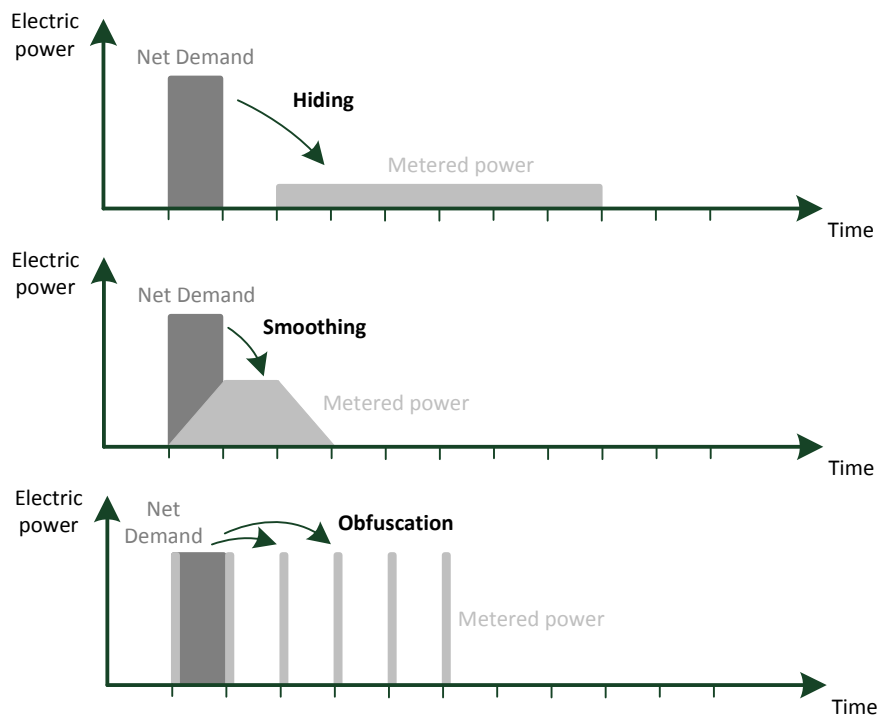


Figure 1.3: Different load shaping strategies as per [40]

of net demand. As a new approach this work proposes a LLH system using a variable load such as a domestic hot water heater. Conversely to BLH, that allows to increase but also decrease the energy consumption that is measured by the smart meter, a LLH system only allows to increase the energy consumption.

1.7 Time-Based Pricing

Time-based pricing is the idea of moving from time-invariant electricity prices to prices that are more closely tied to the variation in the marginal costs of generating electricity [64] as an incentive for the end-users to adjust their energy consumption to the supply-dependent resources.

As [64] depicts, the marginal costs of electricity vary widely over time because of both varying demand and the uneconomical nature of electricity storage in most applications. Base load capacity with high construction costs and low marginal operating costs, intermediate capacity with lower construction costs and higher marginal operating costs and peaking capacity with the lowest construction costs and the highest marginal operating costs must always balance supply and demand. As long as demand is low it is cleared with base load capacity, but as demand rises, generating capacity with higher marginal operating costs are called upon to meet the condition supply equals demand.

If customers face retail prices that reflect these variations, they will consume less during peak periods and more during off-peak periods [64]. This possibility is one reason

for introducing the smart meter as a gentle modification of consumption.

There are different approaches for time-based pricing, including real-time, or dynamic pricing, whereby prices may change on an hourly basis, and critical peak pricing, whereby prices increase only during certain peak periods. The time-of-use principle sets specific electricity prices during a specific time period in advance. For further information see [25].

Under such pricing schemes battery-based load hiding may be beneficial as it usually moves the end-user's peak load towards off-peak periods.

2 Battery-Based Load Hiding

2.1 Introduction

The idea behind BLH is to obfuscate the actual household's energy demand. Therefore a battery with an intelligent control system must be installed between the smart meter and the internal wiring without the necessity of any further modifications on the smart grid side or the smart meter itself. Moreover, as explained in [40], BLH can co-exist with other privacy protection solutions which may increase the effectiveness of each solution. Figure 2.1 illustrates a BLH system with arrows indicating possible load flows for pure customers without any power generation units, based on the work of Kalogridis et al. [40].

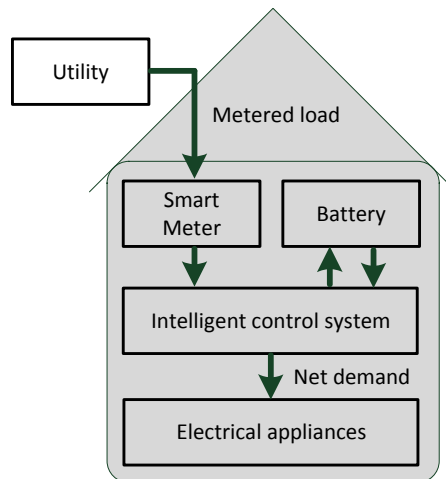


Figure 2.1: Schematic representation of BLH based on [40]

The aim is to hide or obscure load signatures so that appliance usage events and usage patterns cannot be detected [40]. To reach a level of perfectly hidden load signatures, the customer's load would have to be zero all the time, so that both the average and changes in energy consumption are hidden. In case of customers with at least one appliance and without electricity generation units and due to physical limitations of the battery's capacity it would be impossible to reach a zero energy consumption level at all times. The second-best solution for providing privacy would be to maintain a constant consumption which would only leak the average. Such an idealized BLH system without any constraints is diagrammed in Figure 2.2.

In practise there are physical limitations of batteries such as a maximum charging

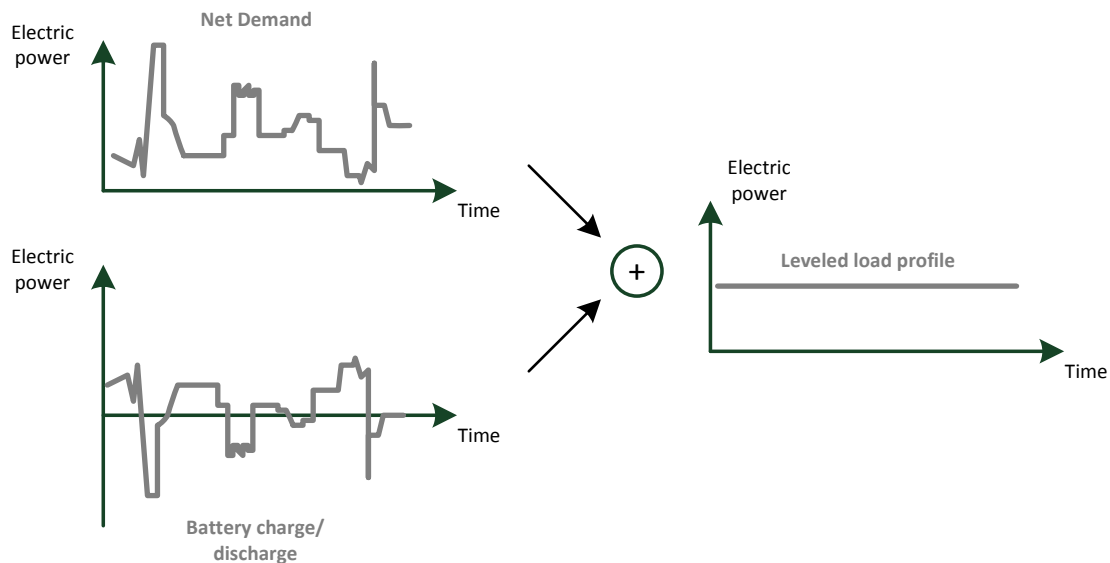


Figure 2.2: Idealized battery-based load hiding based on [70]

and discharging rate or the limited capacity of the battery. Taking high battery prices and limited battery capacity into account, providing the second best solution would be inefficient. This leads to an optimization problem minimizing the leakage of information using feasible battery sizes. Therefore several algorithms have already been studied as mentioned in [74].

The aim of BLH algorithms is to minimize the residence's leak of information by charging or rather discharging a battery at strategic times [74]. This allows the removal of one part of the basic information needed by NILM algorithms to identify appliances, thus thwarting further analysis [74]. BLH algorithms have to cope with physical limitations of the battery system and with varying consumption patterns in net demand [74].

The basic strategy of existing BLH algorithms is to flatten the load profile to a constant value as often as possible [74]. The algorithms are currently designed to mask short-term energy usage patterns and not to mask longer periods of inactivity by emulating appliances.

2.2 Algorithms

2.2.1 Best Effort Algorithm

The first proposal of a BLH algorithm was the so-called Best Effort (BE) algorithm, suggested by Kalogridis et al. [40] in 2010. The BE algorithm aims to hold the external load measured by the smart meter constant whenever possible. If net demand changes, the battery should make up the difference.

The explanations of the following 4 cases are based on [74]. In [40] only the latter two cases are described precisely.

- Case 1: the battery's State of Charge (SOC) gets too low.
- Case 2: SOC gets too high.
- Case 3: the charge rate is too weak.
- Case 4: the discharge rate is too weak.

The best effort algorithm always attempts to maintain the metered load that is transmitted to the utility at a constant level for as long as possible. If the battery should discharge to hold the metered load constant but the SOC is too low, the battery can't provide more energy to maintain a constant power level, thus the metered load will increase to the level of net demand. Such a case is illustrated in Figure 2.3.

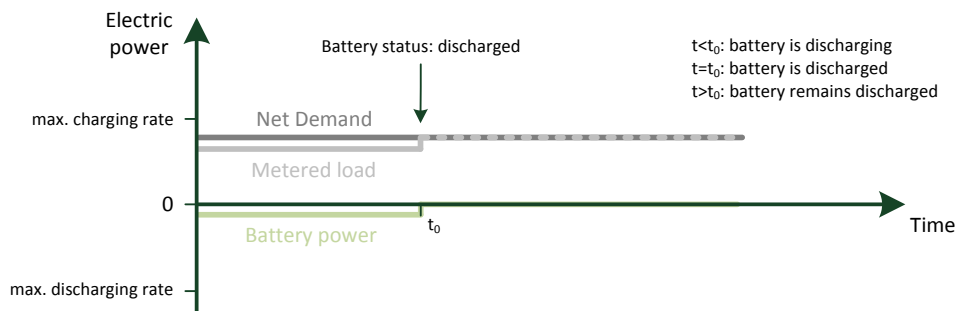


Figure 2.3: BE algorithm: SOC is too low, the battery idles

Note that the authors in [74] argue the opposite, or that the metered load will decrease. One of the authors, Mr. Weining Yang, confirmed their fault in their paper by mail.

If the opposite happens, maintaining the load would overcharge the battery, the metered load will decrease to the level of net demand and again the battery idles.

Furthermore there are two situations regarding battery rate constraints where the BLH system cannot provide enough power to maintain a constant metered load, where the first one is plotted in Figure 2.4.

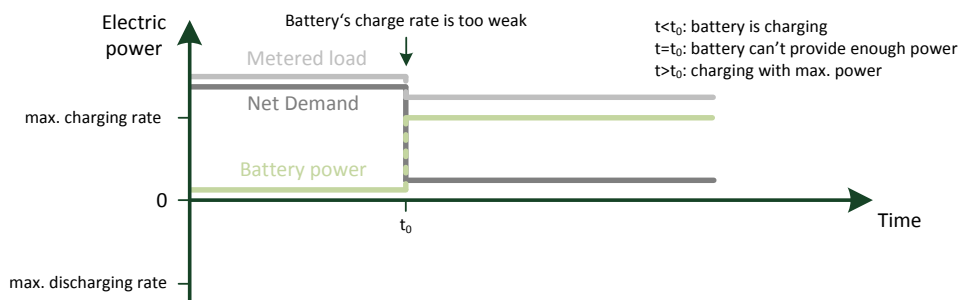


Figure 2.4: BE algorithm: if the charge rate limits the system the metered load will decrease

If net demand decreases by an amount that cannot be covered by charging the battery, the metered load will decrease by the difference that cannot be hidden. The battery will be charged at its maximum rate until it reaches the upper level of SOC.

Again the opposite happens if the increase in net demand cannot be covered by the battery system. The metered load will increase as the discharging rate of the battery is too low, as plotted in Figure 2.5. Similarly the battery will be discharged at its maximum rate until the battery's SOC gets too low.

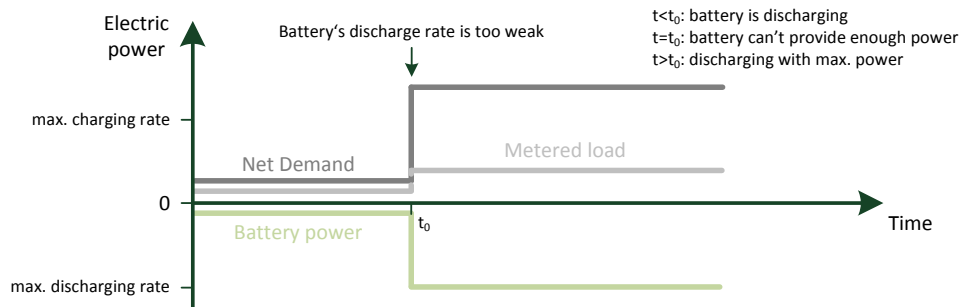


Figure 2.5: BE algorithm: if the discharge rate limits the system, the metered load will increase

Yang et al. [74] observed that this algorithm can leak information as plotted in Figure 2.6.

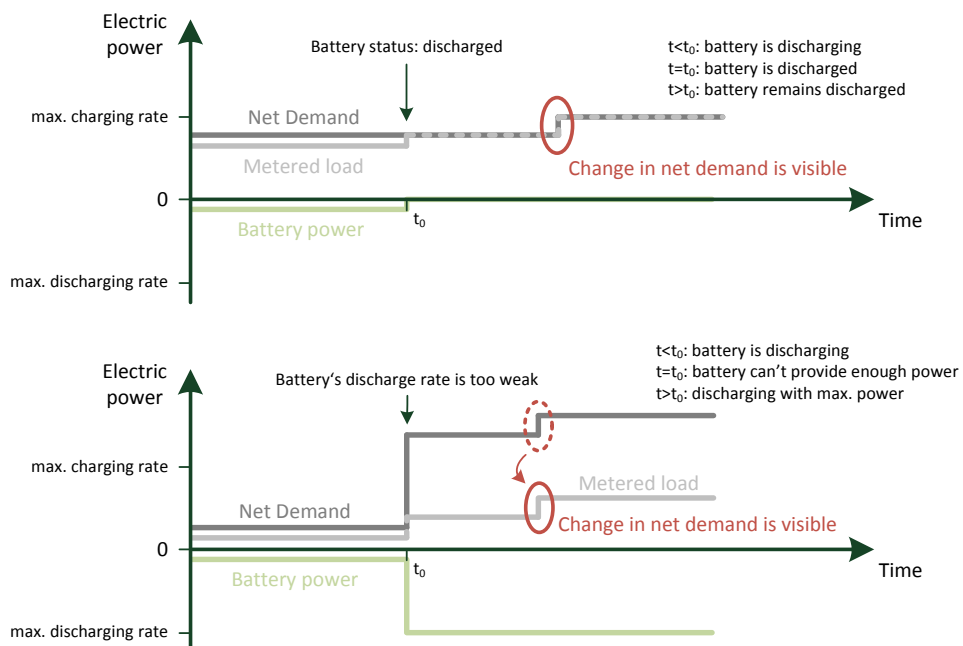


Figure 2.6: Information leakage using best effort algorithm

If the metered load increases, it can be either case 1 (upper SOC limit) or case 4 (exceeding max. charging current) [74]. In this situation the metered load equals net

demand (case 1) or net demand minus the maximum discharging rate of the battery (case 4) [74]. Imagine the observation of the load profile changes of the metered load. If two consecutive changes having the same direction occur, e.g. (up, up), the possibility is high that these changes were caused by the same constraint, either case 1 or 4 [74]. Hence the second change most likely reveals the increase in net demand which may be useful for decomposing the profile [74]. Certainly, BE can also leak information if the metered load decreases.

2.2.2 Stochastic Algorithm

In 2011, a stochastic battery policy was proposed by Varodayan and Khisti in [27]. The authors suggest that it would be possible to minimize information leakage compared to BE algorithm. This new abstract algorithm considers a binary-load binary-battery model in which net demand and the metered load are independent and identically distributed (iid). Using such a model means that the appliances (binary load) consume either 1 or 0 units of power at a discrete time or rather the utility provides 1 or 0 units of power. Moreover, the battery (binary battery) has two states: 1 = charged and 0 = discharged. For example, if the battery is fully discharged and net demand is 1, the utility must provide 1 and the battery's SOC remains low. If the appliances consume 0 either the battery can be charged (utility = 1) or remains discharged (utility = 0). The decision whether to load the battery or to stay at the same level bases on stochastic probabilities [27].

With regards to this algorithm, the work does not go into further details due to the limitation of this simple binary-load binary-battery model. For proper simulation results such a model requires further enhancements. Furthermore, compared to that compared to more advanced algorithms, particularly the stepping framework, the benefits of this algorithm are not readily apparent.

2.2.3 Non-Intrusive Load Leveling

McLaughlin et al. proposed the so-called Non-Intrusive Load Leveling (NILL) algorithm [70]. NILL tries to maintain a constant target load similar to the BE algorithm using a more complex system differing three states. The NILL approach attempts to provide privacy for all appliances under all battery states [70], even if the battery's SOC is too low or too high.

The following explanations of the NILL algorithm are based on [70] and [74]:

NILL algorithm distinguishes between the following three states:

- Stable State: NILL will always attempt to set the metered load to this state, which is the forecasted average load; if the battery's charge or discharge rate is too weak to maintain a constant level, the metered load will change and the battery be used with its maximum power (remaining in stable state)
- High recovery state: occurs if the battery's SOC is insufficient to hold the metered load on a constant level under light net demand (upper SOC limit)

- Low recovery state: similar, with battery's SOC being too low to maintain the metered load under heavy net demand

The algorithm maintains a stable state until either a high or a low recovery state occur. If the system returns to a stable state from either a high or a low recovery state, the new stable state level is updated to the exponential weighted moving average of the most recent stable state and the average load during the last high or low recovery state ($\alpha \cdot average + (1 - \alpha) \cdot last\ stable\ state$) where α is chosen to be 0.5 in experiments [70]).

If the battery reaches the upper limitation of SOC, it changes from a stable state to a high recovery state and sets the new metered load just below the most recent net demand to discharge the battery slightly, e.g. a discharge current of 0.5 A. The system remains at this high recovery state level as long as no new overloading situation occurs or rather one of the following two cases: if net demand is 5 A higher than the current level of high recovery state, the system returns to a stable state with a new level based on the weighted average. Also if the battery is discharged to 50 % of its usable capacity, it returns to a new stable state (note that the usable capacity may be between 20 % and 90 % of the battery's total capacity, so 50 % would be $0.5 \cdot 20\% + 0.5 \cdot 90\% = 55\%$ of total capacity). Both cases are illustrated in Figure 2.7.

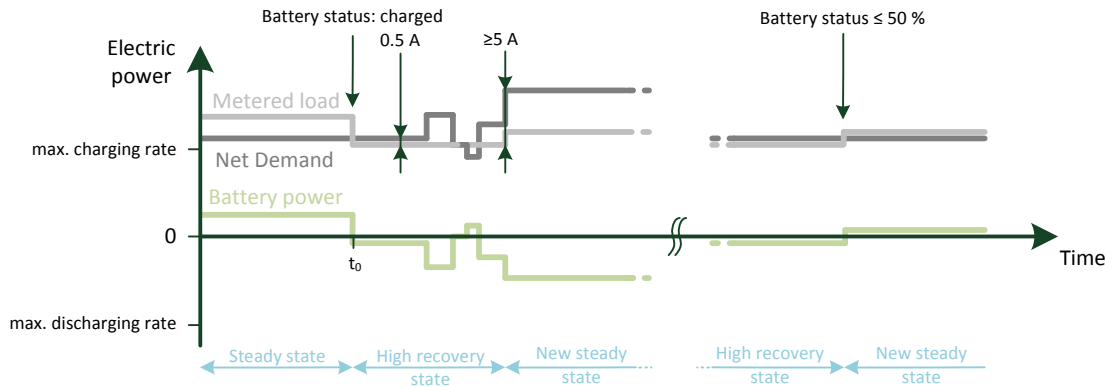


Figure 2.7: NILL algorithm: situations under a high recovery state

If the battery's SOC gets too low, the system switches to a low recovery state where the metered load is set to the maximum charging rate of the battery, hence a low recovery state can mask events with amperages less or equal to this maximum rate. A low recovery state attempts to gradually recharge the battery. In order to make this understandable, the authors of NILL assume that the maximum charge rate of the battery is higher than the expectable load of net demand. In the case when the battery is in danger of discharging once again while maintaining a constant metered load, the battery idles and the metered load is set to net demand. The system remains in a low recovery state until the SOC reaches 80 %.

As with BE algorithm, Yang et al. [74] observed that NILL algorithm can leak information in the stable state if the battery's charge or discharge rate is too low, and in a low recovery state if net demand exceeds the maximum charging rate. The latter case is illustrated in Figure 2.8.

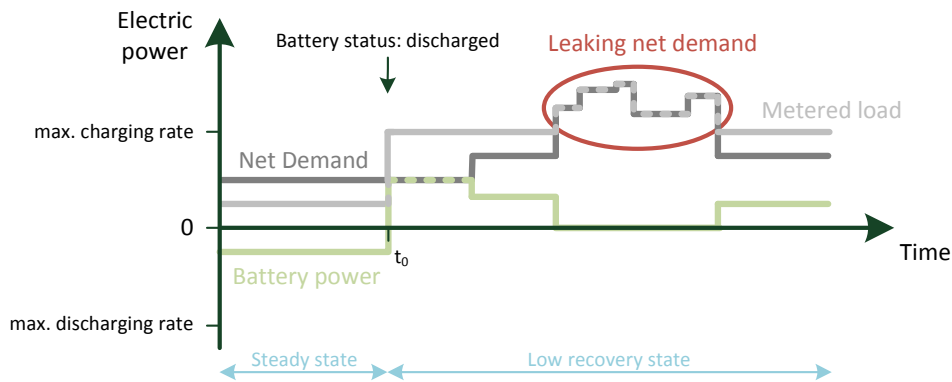


Figure 2.8: Information leakage using NILM algorithm

With regards to the NILM algorithm, identifying this information leakage is tricky as it necessitates the prediction of the system's state. Referring to [74] this may be feasible as the stable state is maintained for an extended period of time and e.g. sustained peak periods in net demand will cause the system to enter a low recovery state. It would be hard to identify if the metered load varies because the system is in a low recovery state and net demand is too high or because it is limited by the maximum current rating in a stable state.

2.2.4 Stepping Framework

Finally, Yang et al. [74] proposed a new framework for BLH algorithms which they call Stepping Framework (SF). This algorithm aims to coarse-grain the value dimension of the metered load by quantizing it to a step function, hence the name [74].

Based on [74] SF makes the metered load to be integer multiples of a constant value, chosen on the battery's parameters. To specify it, the constant value is the minimum of the maximum of the allowed charging and discharging rate. Therefore for any possible net demand there exists a multiple of this constant satisfying the battery constraints. For each level of net demand one can choose either the level just higher than net demand, which will charge the battery, or the level just lower than net demand which will discharge the battery. If the battery's SOC gets too high then the system chooses the lower level and the reverse when the battery's state gets too low.

During normal operation the decision of whether to choose the upper or lower level is task of the SF. Yang et al. consider the following algorithms:

- *Lazy Stepping 1*: keep the metered load constant if possible, otherwise if the battery's usable capacity is below half, charge the battery by choosing the higher level and discharge it otherwise.
- *Lazy Stepping 2*: keep the metered load constant if possible, otherwise randomly choose the upper or rather the lower level.

- *Lazy Charging*: keep the charging state constant if possible (until the SOC is too high or low), otherwise change it.
- *Random Charging*: randomly choose the charging state whereas the expectation of the randomizing function should be adjusted according to the actual SOC (e.g. the probability for choosing the lower level to discharge the battery equals to: $\frac{\text{actual SOC} - \text{min. SOC}}{\text{max. SOC} - \text{min. SOC}}$).

After applying the SF, the uncertainty of predicting net demand is two times the constant value that is the charging/discharging rate (which can be determined by observers). This is plotted in Figure 2.9. Note that *Lazy Charging* is more predictable as the actual charging state divides the possible range into half.

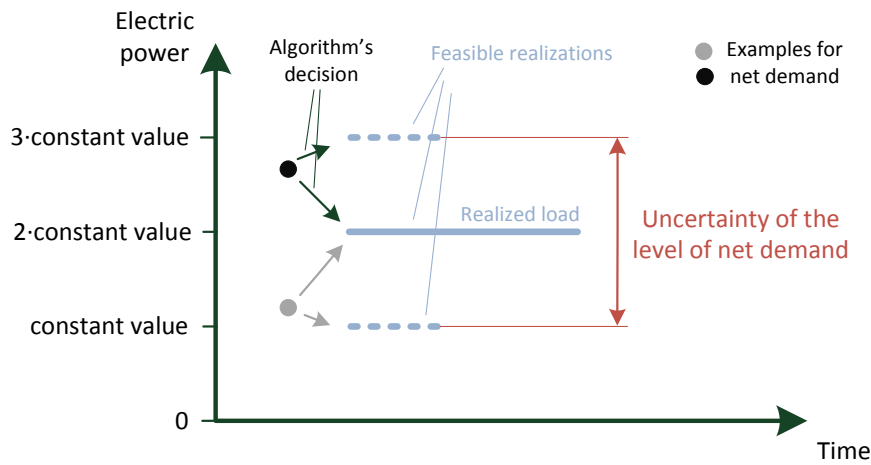


Figure 2.9: The uncertainty of predicting net demand using stepping framework

One strength of SF is that one always obtains some degree of privacy protection. Predicting the charging state halves the possible range of net demand. Highly accurate load change detection due to information leakage, as it was demonstrated for BE and NILL under certain circumstances, is impossible for SF.

The authors conclude that the *Lazy Stepping 2* algorithm in particular significantly and consistently outperforms other algorithms. For this reason this work bases the application of the stepping framework on *Lazy Stepping 2* using the acronym SF.

2.3 Battery Configuration

The battery is the central element of a BLH system. Referring to [21] the battery requirements can be compared with batteries used in combination with photovoltaic systems as they experience deep cycling and are sometimes left in low states of charge for extended periods of time.

Table 2.1 compares some typical battery types. Considering our battery setup, a long cycle life, a high round trip efficiency and a low price are the most important parameters.

Lio-ion as well as LiPo provide the highest round trip efficiency, but a cycle life that does not outperform lead acid batteries significantly. Regarding cycle life, the high temperature molten salt Zero Emission Battery Research Activities (ZEBRA) battery provides the best results.

	Lead acid	Li-ion	LiPo	NiMH	ZEBRA
Energy density in Wh/l	70	200-730	300	170-240	160
Specific power in W/kg	75-412	250-1500	100-315	150-250	150
Round trip efficiency in %	85	>95	>95	65	91
Cycle life	>200	>400	>400	>300	>3000

Table 2.1: Battery type comparison [1], [2], [5], [6], [10], [11], [43], [46], [52], [54]

A study in 2011 [28] suggests that lead acid and lithium-ion batteries in particular are the most qualified decentralized storage units in dwellings. Lithium-ion batteries cost approximately 750 €/kWh [28] but it is expected that the costs for stationary batteries decrease to 250 €/kWh within several years due to further improvements and economies of scale [28]. Lead acid batteries cost approximately 100-250 €/kWh and it is expected that the costs will reduce to 80 €/kWh [28], but compared to other types it offers a moderate efficiency with high maintenance requirements and a long lifetime [21].

Neovoltaic AG, a company seated in Hartberg in Styria, has developed their own storage unit "neostore compact". It is used in combination with a photovoltaic system providing a capacity of 5 kWh using lithium-iron phosphate batteries (a kind of lithium-ion batteries). These batteries have a life cycle of over 6000 and a Depth of Discharge (DOD)¹ of 80 % with an output power of 3500 W or rather a short-term output power of 10500 W [8]. Unfortunately this system is not feasible for BLH systems as it necessitates a power generation unit and does not offer the possibility of modifying the charger according to the BLH algorithm which was confirmed by the CEO of neovoltaic AG, Mr. Werner Posch.

Another Styrian company, Everto Photovoltaik-Energie KG, seated in Leibnitz-Leitring, uses storage units developed by VARTA Storage using the same type of lithium-iron phosphate batteries with a capacity between 3.7 and 13.8 kWh, a cycle life of 6000 and a DOD of 90% with a single phase output power of 1.33 kW [9].

Inspired by McLaughlin et al. [70] this work assumes the use of deep-cycle lead acid batteries.

Common starting lead acid batteries are designed for a low DOD of a just a few % of the battery's capacity. Deep-cycle lead acid batteries are designed for DODs of up to 80% with a cycle life of several thousand [21]. Modifications to the electrolyte such as Absorbent Glass Matting include the ability to be deeply discharged without affecting lifetime, allowing high charge/discharge rates and an extended temperature range for operation [21]. Such a modification is accompanied by higher initial costs and the need

¹DOD: Depth of Discharge, which specifies the battery's usable capacity in % [21]

for more carefully controlled charging regimes [21]. These improvements are very helpful when implementing a BLH system at home.

For all battery types, specific charging strategies exist to maintain an optimum capacity during the lifecycle. For lead acid batteries one possible strategy is the iu-charging method, which loads the battery with a constant current up to 80 % and with a constant voltage above this level until the battery is fully charged. Such a procedure is not feasible for BLH systems as they necessitate a particular load at a particular time.

One of the limitations that necessitates the use of specific BLH algorithms to maintain some degree of privacy is the charging/discharging rate of the battery system. Setting this rate affects the rated battery capacity, higher currents reduce the capacity and furthermore it decreases the battery's lifetime due to a higher temperature [21]. [70] assumes the use of ten 50 Ah batteries (500 Ah in total) with a maximum charging or rather discharging current of 60 A, chosen because of a specific solar charge controller with this current setting. 60 A for a 500 Ah battery system means that the current is approximately 0.12 of the rated capacity: the notation 0.12C (or rather the inverse C8.33) stands for $0.12 h^{-1} \cdot 500 Ah = \frac{500 Ah}{8.3 h} = 60 A$.

While the charging current for small lead-acid batteries should be set between 0.1C and 0.3C (e.g. 0.3C: 600 mA for a 2 Ah type), larger batteries should generally be charged at lower current ratings [44]. [72] recommends a current less than 0.1C to avoid the battery's voltage from exceeding the level where the gassing process increases severely. Doubtless higher current ratings reduce the usable capacity, [34] states that even with currents up to 8C (e.g. 300 A for a 37 Ah battery) they could not find evidence that fast-charging has detrimental effects on cycle life of a battery, as temperature didn't increase dramatically. The manual of the Xtender inverter/charger-combination² of Studer Innotec recommends charging currents between 0.1C and 0.2C.

An overview of deep cycle batteries such as Multipower MP100-12C (100 Ah, 12 V)³, Ritar RA12-260D (260 Ah, 12 V)⁴ and Ultracell UCG 120-12 (120 Ah, 12 V)⁵ demonstrates that all of these batteries support charging current rates of 0.3C. The maximum 5 s short-time discharging currents are 12C for the 120 Ah battery and 10C for the 260 Ah.

Aside from the maximum current rating, another important parameter when dimensioning the battery setup is the capacity itself. The choice of the battery's capacity is connected with two important effects: Firstly, a greater capacity allows higher charging/discharging currents. Secondly the time until the battery gets fully charged or discharged increases with capacity, which results in a longer design life as one charge/discharge cycle describes a longer time interval. Conversely, the required space and expenses in-

²Xtender inverter/charger combination of Studer Innotec as per <http://www.studer-inno.com/upload/temp/Benutzerhandbuch%20Xtender%20Serie.pdf>, accessed on 29th of November 2013

³Multipower MP100-12C: http://www.akkusolar.de/data/datenblatt_0000038_1.pdf, accessed on 7th of November 2013

⁴Ritar RA12-260D: http://www.maurelma.ch/Produkte/Batterien/Hausmarke/Datenblatt_RA12_260D_260Ah.pdf, accessed on 7th of November 2013

⁵Ultracell UCG 120-12: <http://www.blei-akkus.com/Multipower-MP100-12C-12V-100Ah-Blei-Akku-Zyklentyp>, accessed on 7th of November 2013

crease as the battery's capacity increase.

2.4 Implementation

Aside from simulating a BLH system, the implementation of a working system would be of interest to get an idea if such a system would be practicable and feasible.

In the previous sections, the necessary components for building an elementary BLH system were already discussed. The combination of a charger and an inverter with the integrated DC-AC and AC-DC conversion must allow a power flow into both directions, the battery stores the energy and the control system, which may be a PC, a Raspberry PI, a μ Controller like an Arduino etc. sets the actual charging/discharging current for the inverter/charger-combination on the basis of the BLH algorithm.

Developing a BLH system requires several specifications to be satisfied. After designing the system based on a harmonized system of the battery and the inverter/charger-combination, must allow the realtime-adjustment of the battery's current remotely. Therefore, the control system necessitates some input parameters such as the actual SOC of the battery and the battery's voltage to calculate the charging or rather discharging current based on the power level that was chosen by the BLH algorithm. Moreover, it is essential to measure net demand.

3 Load-Based Load Hiding

3.1 Introduction

Proposing an alternative load hiding system one could theoretically reach similar results using fully controllable loads. The reason for considering a rather new approach beyond BLH bases upon the high implementation and maintenance costs, but also the power losses of the battery and the inverter/charger-combination when applying a BLH system. The schematic of such a load-based load hiding system is demonstrated in Figure 3.1.

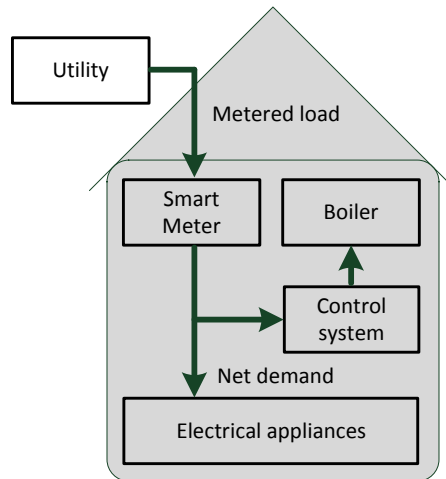


Figure 3.1: Schematic representation of LLH based on the BLH system in [40]

An interruptible load such as that of an electric water boiler would allow to defer the power consumption of heating water. Reproduced from Figure 2.2, Figure 3.2 shows a constant metered load using LLH instead of BLH. Note that LLH can only increase but not decrease the level of the metered load compared to the corresponding net demand. This is limited by the maximum power of the appliance used as a variable load and moreover by the necessary energy consumption of the device during a day.

Developing a LLH system profits by previous works of demand side management. In [31] the authors attempt to develop a control strategy for demand side management of electric boilers to smooth the aggregated household's demand by improving the existing ripple control in Switzerland. LLH would require similar engagement but on a much smaller scale - namely a single household, a shorter interval of control and adjustments beyond ON/OFF-time. As per [63] electric water heaters in EU-27 accounted for 8.7% of total electricity consumption in 2009. In 2007, estimations show that in the EU-27

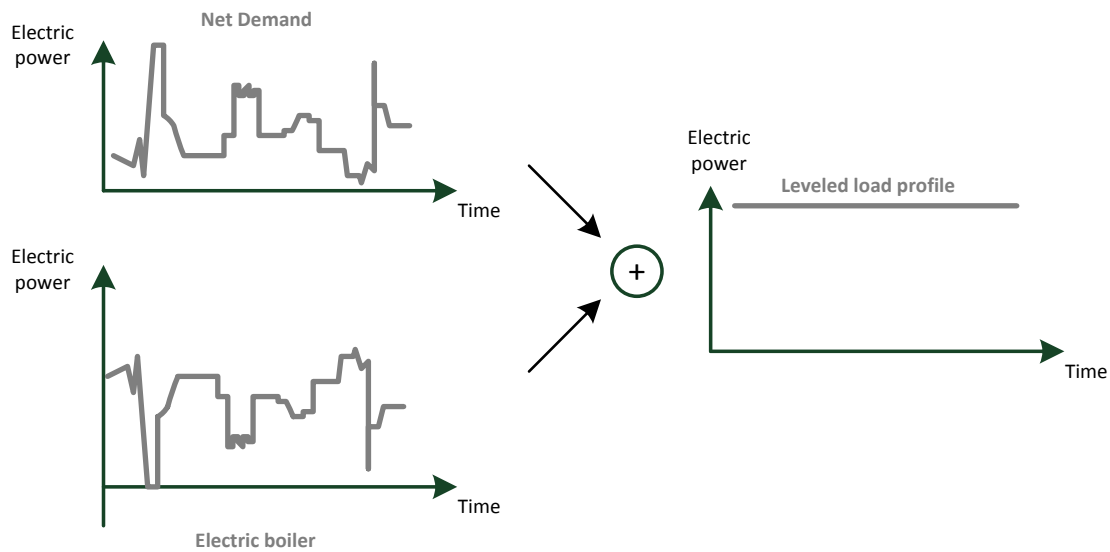


Figure 3.2: Idealized load-based load hiding

about 119 million electric water heaters were installed, whereas 29 million units were electric instantaneous and 90 million of those units were heaters with storage systems as per [63]. This illustrates the widespread use of domestic electric boilers that could be used as variable loads.

3.2 Algorithm

To the best of our knowledge there exists no LLH system/algorithm or similar privacy preserving approach. The following algorithm is the first attempt of a load hiding system using variable loads such as an electric hot water boiler. As the use of an electric boiler must be based upon the customer's needs, the algorithm must take this into account. For this system a sampling interval of one second is assumed.

For the sake of simplicity, this work assumes a daily target energy consumption disregarding the amount, temperature or time of use of the hot water as the boiler's end product. Taking these effects into account would require a dynamic model with further assumptions like setting the temperature and the time and amount of using hot water. A simple dynamic thermal model of a 150 l 2.2 kW boiler based on experiments can be found in a paper proposed by Amann et al. [62]. The authors analyze possible savings and the demand side management potential of electric boilers, but in their paper the boiler can either be turned on with the maximum power or turned off with zero power which distinguishes the use of the boiler compared to LLH. From a demand side management point of view there exist several other dynamic thermal models of electric water heaters like in [31], [45], [50], [53] and [56]. As a first approach, a dynamic model does not seem necessary as the consumed energy will be set in advance.

Two main targets of developing a LLH algorithm are the simple implementation and a

high level of privacy protection. A novel implementation does not require any changes in the household's internal wiring and furthermore necessitates no extra measurements like the actual level of net demand (demand apart from the variable load) which is necessary in case of a BLH system.

The target model is a completely passive electric boiler without any knowledge of the internal wiring, the appliances in use, net demand or the metered load. Without any data of net demand, maintaining a constant metered load is impossible. Additionally, holding a constant value like under BLH would necessitate some kind of forecast to fill the gap between net demand and the constant load to still meet the targeted energy level at the end of each day without leaking too much information. The basic idea of this proposal is to overlay net demand by a probabilistic signal i.e. artificial noise which impedes the detection of the appliance's states. Figure 3.3 plots net demand that is overlayed by a probabilistic load of the electric boiler.

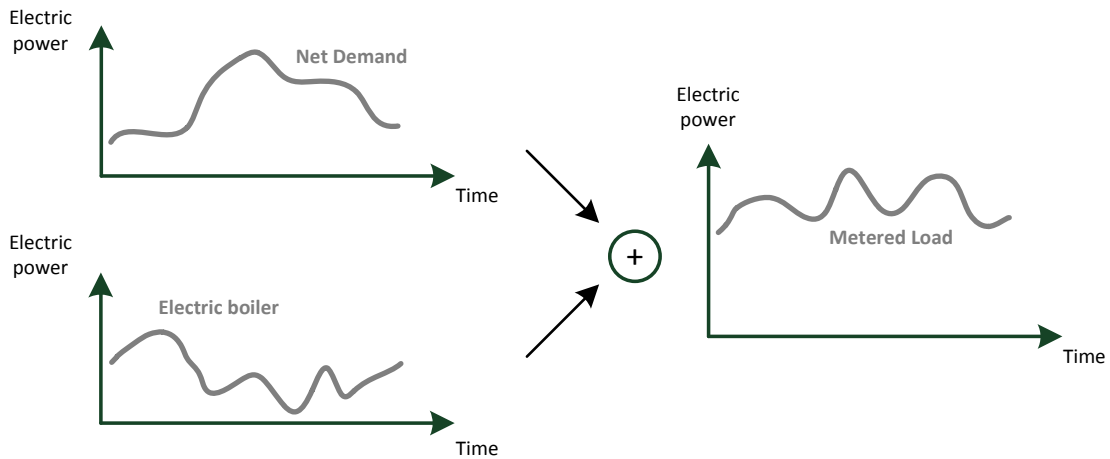


Figure 3.3: Sketchy: net demand overlayed by artificial noise to obfuscate net demand

The basis of this artificial noise is a Probability Density Function (PDF) which describes the range and probability of the realizations. The realizations must lie within the interval $[0 P_{max}]$ where P_{max} is the maximum power of the variable load. In order to meet the target energy consumption, the mean of the distribution function and the comparable constant load must be balanced, e.g.: a daily energy target of 5 kWh can be realized by a constant load of $\mu_{set} = \frac{5000 Wh}{24h} = 208.3 W$ but also by realizations of a random variable X based on a PDF with the same mean. Figure 3.4 plots a signal of 1440 realizations which are held constant for 60 s each. The dark grey line illustrates the (true) mean of the signal. The underlying PDF is a beta distribution with $\alpha = 0.7$, $\beta = 7.028$ and $P_{max} = 2300 W$ with an expectation of $208.3 W$. The corresponding histogram is plotted on the left. This concrete realization results in an energy consumption of 5.1 kWh.

In this paper both a beta and a truncated normal distribution will be used. In addition to these two basic distributions, a modified beta distribution should test potential privacy protection improvements. The reason for testing another distribution is the pre-

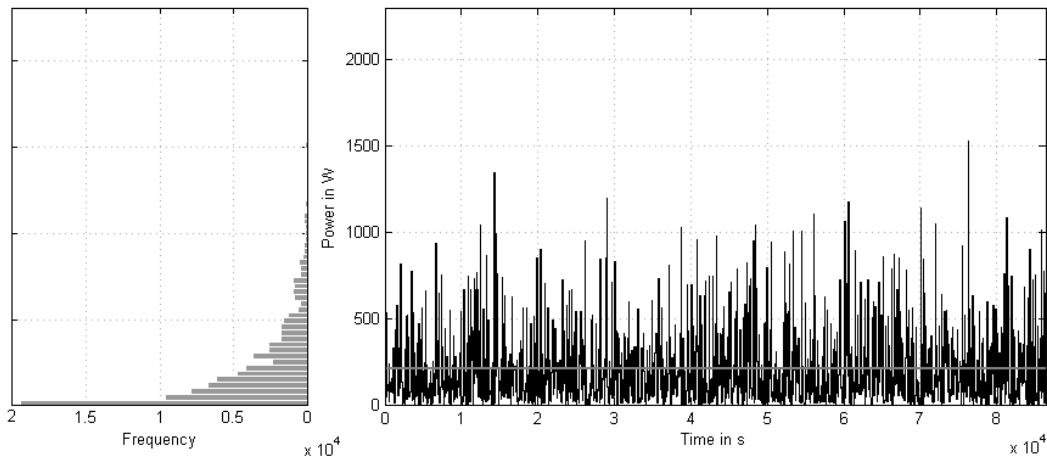


Figure 3.4: Artificial noise using a beta distribution

processing of the NILM algorithm which uses filters such as applying a running median filter prior to applying the actual algorithm. The higher the level of randomization of the artificial noise is, the worse the effectivity of the filter should be.

Figure 3.5 plots 3 histograms for a specific parameter set with $\mu_{set} = 208.3 \text{ W}$.

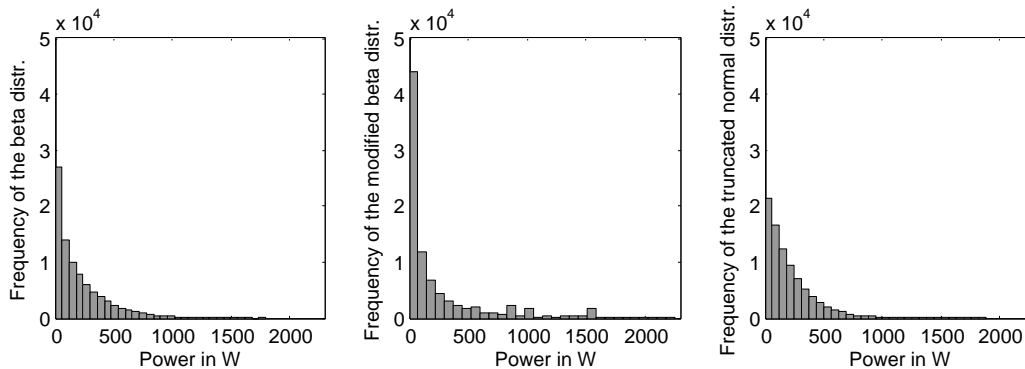


Figure 3.5: Histograms of a beta, truncated normal and a modified beta distribution with an expectation of 208.3 W

The left diagram shows a beta distribution, the center diagram the modified beta distribution and the right diagram the truncated normal distribution. The realizations with the highest values accompany with the modified beta distribution with a few outliers. Furthermore, the beta distribution is steeper than the truncated normal distribution.

3.3 Load Configuration

In contrast to the battery system of BLH, the variable load of a LLH system must be dimensioned in a need-based matter. In this work, the controllable load is assumed to be

an electric boiler that must provide a specific temperature for a given volume of water. Whereas an electric boiler using off-peak electricity heats the boiler up to a specific temperature set by the customer, other types of electric boilers usually try to maintain a given temperature level within a hysteresis. To implement a LLH system using an electric boiler necessitates some knowledge about the customer's behaviour and the hot water demand.

Measurements in a flat share in Graz over a period of 76 days (16th of May until 31st of July 2013) showed an average energy consumption of 5 kWh per day for an off-peak electric boiler with 150 l. At a rough estimate this should represent about $m = \frac{5 \text{ kWh} \cdot 3600 \frac{\text{s}}{\text{h}}}{4.184 \frac{\text{kJ}}{\text{kgK}} \cdot (37-12) \text{ K}} = 172 \text{ kg}$ of water of body temperature referring to the formula $Q = m \cdot c \cdot \Delta T$ where Q is the energy content, m the mass, c the specific heat capacity and ΔT the temperature difference. The inlet temperature of water is assumed to be 12°C. As per [71] 4 persons consume about 120-200 l of water of body temperature per day for showering purposes only. To take a full bath [71] specifies a water demand of 150-180 l of body temperature per person.

This work assumes a target energy consumption of 2.5-10 kWh per day.

3.4 Implementation

Compared to a BLH system, the realization of a LLH system requires less effort. There are two essential elements for implementing a LLH system: the electric boiler and an electronic device with a simple control system that allows the adjustment of the voltage level provided to the heating element of the electric boiler as illustrated in Figure 3.6. In Figure 3.6 the electronic device is a Phase-Fired Controller (PFC) which allows the adjustment of the root mean square value of the voltage. Note that $P \sim U^2$ as $P = \frac{U^2}{R}$ where R can be assumed to be constant. In reality, the control system should set the voltage based on the actual temperature, the set temperature and the LLH algorithm that will be used.

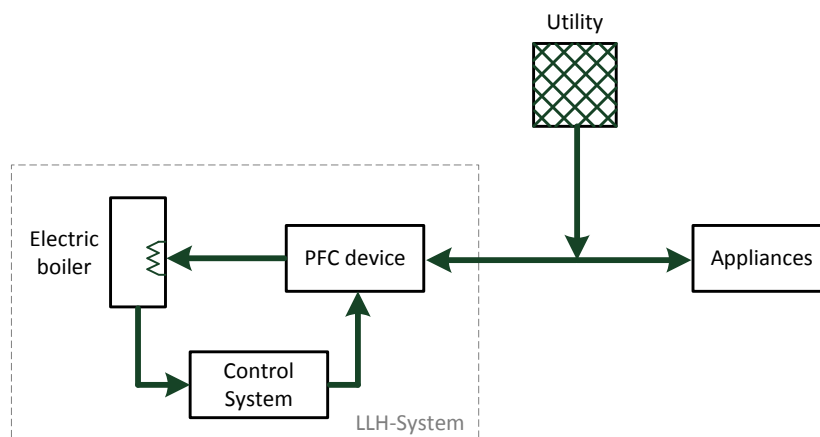


Figure 3.6: Model of a LLH system

4 Evaluation Setup

4.1 Measuring Privacy Protection

In connection with the discussion of the simulation results, it is convenient to compare the efficiency of different load hiding systems using some kind of quantity measuring the efficacy of privacy protection. In similar works the authors favor different metrics such as empirical and relative entropy in [40] and [70], relative feature mass in [70], mutual information measures in [27] and [74] and finally cluster classification in [40]. While the idea of each measure is to quantify the information content, the approaches are very different. This work focuses on metrics that can be easily calculated and do not necessitate restrictive assumptions like the independence assumption of the time series.

The idea of the first metric, the relative feature mass, is to measure the efficacy of a BLH algorithm to hide load changes as edge detection is the key information for many NILM algorithms. The second metric is the Root-Mean-Square Error (RMSE) which is well known for measuring the accuracy of forecasting models. In this work, RMSE should quantify the deviation between the original time series of net demand and the metered load profile after applying a load hiding system. The last quantity is the direct comparison of the success rate of a NILM algorithm of net demand and the metered load.

4.1.1 Relative Feature Mass

Inspired by [70] the first measure is Relative Feature Mass (RFM) which quantifies the improvement of the number of changes in the load profile during a specified time window of the time series after applying an algorithm compared to the original time series. The following explanations regarding this measure are based upon [70]:

Imagine a load profile with 6 realizations $p(t)$: 0, 10, 5, 15, 15, 30 for t_0 up to t_5 . A differentiation at lag 1 yields the changes in the load profile $dp(t) = p(t) - p(t-1)$: NaN, +10, -5, +10, 0, +15 for t_0 up to t_5 . Samples with no changes, i.e. $p(t) - p(t-1) = 0$ are no features and ignored for relative feature mass. The next step is to count the number of non-zero changes in the load profile, this number is called the feature mass (FM). For the given example feature mass is 4. For discrete sample sets with length ω $D = (dd_0, dd_1, \dots, dd_\omega)$ (time series of the changes in net demand) and $E = (de_0, de_1, \dots, de_\omega)$ (time series of the changes in the metered load) the feature mass for a given time windows ω can be calculated as:

$$FM(\omega, D) = \sum_{i=1}^{\omega} (dd_i \neq 0)$$

$$FM(\omega, E) = \sum_{i=1}^{\omega} (de_i \neq 0)$$

The relative feature mass for a time window of size ω is the ratio of the two feature masses, in this application it is the quotient of the metered load divided by the original time series of net demand:

$$RFM(\omega, D, E) = \frac{FM(\omega, E)}{FM(\omega, D)}$$

whereas $RFM(\omega, D, E) \geq 0$. [70] uses a sliding time windows of size $\omega = 1 h$. In this work the time windows is set to $\omega = 86400 s$, as a result RFM provides just a single measure per day. As NILM algorithms most likely won't analyze very small variations in power consumption due to noise and measuring inaccuracy, this work assumes all load changes below 5 W to be zero. The reason for choosing 5 W is based upon the load with the lowest possible power consumption, which is a smartphone charger that only consumes approximately 6 W referring to tracebase database [68] that will be described in section 4.2.1.

When applying a BLH system, a smaller RFM is better, as BLH tries to avoid load changes. When developing a LLH system, a constant target load must not be the best choice. As opposed to attempting to flatten the metered profile overlying disturbances by randomly adjusting the variable load may be beneficial as it necessitates no measurements of net demand. In this case a high RFM would suggest a better result.

RFM is significant as both of the other measures, the RMSE and the F-measure fail to describe the level of modifying load changes directly which is important as many NILM algorithms are based on edge detection.

4.1.2 Root-Mean-Square Error

While the first metric measures the change in the number of load changes, the RMSE aims to measure the deviation between the original time series and the time series after applying a load hiding system. This should quantify the information loss of the actual level of net demand, as opposed to the load changes in particular. The absolute value of RMSE is not significant as it changes with the sample length and other characteristics of the time series considered. Using this metric, only comparisons between different algorithms using the same sample length, sampling interval and the same time series of net demand is meaningful.

$$RMSE = \sqrt{\frac{1}{n} \sum_{i=1}^n (d_i - e_i)^2}$$

- d_i ... discrete time series of net demand
 e_i ... discrete time series of the metered load
 n ... sample length to be considered, i.e. 86400 s

4.1.3 F-Measure

The final metric is the success rate of decomposing the customer's load profile using a specific NILM algorithm by Egarter [24]. The NILM algorithm is not based on edge detection but on state estimation. It estimates the appliance's states with the help of particle filtering where appliances are modeled as a HMM. The algorithm chooses the most likely combination of appliances that are turned ON for each one of the 86400 samples per day. For a higher success rate only sampling intervals of one second will be applied, and furthermore a simplified load profile using only 7 appliances will be used.

The possible decisions of the NILM algorithm are listed in Table 4.1. When observing a specific sample, the head line describes the actual state of the appliance (ON or OFF) and the first column the estimated state using the NILM algorithm. If the appliance is turned ON and NILM detects it correctly as ON, the result is true-positive (shortened T_p), whereas if the algorithm detects it as OFF the result would be false-negative F_n . This ON/OFF-state estimation must be repeated for all the samples analyzed and moreover for all of the appliances that are adopted. When analyzing one day of 86400 samples, the aggregated T_p can be interpreted as the number of times an appliance is correctly detected as ON in our case. F_n -rate describes the number of times an appliance is wrongly detected as OFF, F_p the number of times an appliance is wrongly detected as ON and T_n characterizes the number of times an appliance is correctly detected as OFF.

	Appliance is ON	Appliance is OFF
NILM detects appliance as ON	T_p	F_p
NILM detects appliance as OFF	F_n	T_n

Table 4.1: Possible decisions of the NILM algorithm to detect the appliance's state

The effectivity of the NILM algorithm can be described by 2 measures commonly known in information retrieval: precision and recall. Precision is the positive predictive value and defined as $precision = \frac{T_p}{T_p + F_p}$. Recall is the sensitivity, hit rate or the true positive rate and defined as $recall = \frac{T_p}{T_p + F_n}$. Use of only one of these measures does not necessarily produce a meaningful result. Imagine a load profile of 1 appliance with 10 measurements where the appliance is turned ON for the first half of the samples and is

OFF for the second half. If the NILM algorithm decides that the appliance is always turned ON ($T_p = 5$, $F_n = 0$, $F_p = 5$) then the recall is $\frac{5}{5+0} = 1$ and the precision $\frac{5}{5+5} = 0.5$. For this case the measure recall does not seem very promising. Conversely, if the NILM algorithm detects the readings on the interval $[2, 5]$ to be ON ($T_p = 4$, $F_n = 1$, $F_p = 0$), recall is $\frac{4}{4+1} = 0.8$ and precision is $\frac{4}{4+0} = 1$. These examples demonstrate that, as an exclusive metric, neither the precision nor the recall are significant values in describing the efficiency of the algorithm. One approach to solving this problem is to combine these measures into one measure, as is true with the so-called F-measure, which is defined as the harmonic mean of precision and recall:

$$F = \frac{2 \cdot \textit{precision} \cdot \textit{recall}}{\textit{precision} + \textit{recall}}$$

As the NILM algorithm aims to detect more than just one device, the precision, or rather the recall, are derived for every appliance using 86400 samples. Hence each appliance includes two measures per day. Subsequently they are averaged over all devices to get the total precision and recall rate to finally calculate the total F-measure.

4.2 Data Setup

4.2.1 Database

The following databases concerning the load profiles for a household's demand have been considered for the evaluation (all listed databases are freely available):

- <http://www.tracebase.org/>: Tracebase [68] is a dataset provided by Technische Universität Darmstadt. It includes 43 types of devices such as refrigerators, TVs or WiFi routers with one or several appliances for each type with a total of more than 1800 traces (accessed on 28th of Oct. 2013). Such a trace includes a 24 h load profile measurement of active power using a sampling interval of one second or up to four seconds, but note that sometimes the sampling frequency varies within the same trace.
- <http://redd.csail.mit.edu>: The American REDD dataset in [75] is provided by Z. Kolter and M. Johnson and can be split into two parts: The high frequency part contains one voltage and two current measurements for 2 houses (accessed on 28th of October) recorded with a sampling frequency of 15 kHz. Due to the high frequency readings, the authors use a specific compression system to reduce the necessary memory capacity. The second part of the REDD database are low frequency apparent power measurements based on a sampling rate of approximately one second for a total of 6 houses with different device setups for several days each (accessed on 28th of October). The apparent power measurements are divided into up to 24 channels with individual circuit measurements such as lighting, refrigerator and another 2 extra channels for the whole house due to the split-phase electric power system.

- <http://ampds.org/>: The AMPds dataset is provided by S. Makonin and include recordings of a single household in Canada for an entire year from April 2012 until March 2013. The data records one minute read intervals measuring inter alia real, reactive and apparent power and energy. The recordings regarding electricity are split into 19 sub-meters and one meter for the whole house. Due to unmetered loads, the sum of all 19 sub-meters differ from the readings from the whole house. For the accompanying paper see [69].
- <http://nilm.cmubi.org/>: BLUED [16] is a electricity disaggregation dataset provided by INFERLab, a group at Carnegie Mellon University. The dataset consists of a voltage and two current measurements (two active wires) for a single-family residence using approximately 50 appliances in the United States over the course of a week, sampled at 12 kHz (accessed on 21st of Feb. 2014). The included csv-files contain the current and voltage measurements, the included mat-files contain active and reactive power data.
- <http://traces.cs.umass.edu/>: The UMass Smart* Home and the UMass Smart* Microgrid datasets [17] are provided by the Laboratory for Advanced System Software at the University of Massachusetts. The Smart* Home dataset includes a variety of traces of 3 homes in the United States. For example the measurements of home C contain aggregated electrical data (active power, sampling interval of one second), environmental data (temperature, humidity, windspeed, etc., sampling interval of 60 s) and power generation data from a battery system, three solar panels and two micro wind turbines (sampling interval of 5 s) over a period of approximately 3 months. Home A is the most deeply instrumented home with motion sensor data, electricity data of each circuit, heating sensors, etc. The Smart* Microgrid dataset includes electrical active power data from over 400 homes in the United States over the course of a day, sampled every 60 s.

BLH systems use some kind of power electronics to connect the battery with the internal wiring of the customer's house. As the Austrian electricity bills of private customers are usually based on active energy, power electronics such as inverters of photovoltaic systems are commonly optimized for providing active power to the electric grid. For simplicity's sake this work assumes that the BLH system is only capable in providing active power. In addition, according to the E-Control ordinance [30] smart meters must only be able to provide active power measurements. Hence databases used in this work should provide active power data. Whereas tracebase, AMPds, BLUED and the UMass Smart* databases provide these active power readings, the REDD dataset would necessitate further calculations to evaluate active power using the high frequency measurements of the current and voltage. The assumption of using active power also satisfies the use of a LLH system as the controllable load most likely will be an electric heating element which is a resistive load that only consumes active power.

The dataset used in this work is the one provided by tracebase. It offers a high sampling frequency and active power data that allows a perfect decomposition of the

generated load profile. Furthermore, tracebase offers readings of devices that are commonly used in Europe, which may influence the shape of the load profile compared to American devices. The AMPds, BLUED, UMass Smart* and REDD databases won't be considered in this work.

In order to analyze the possible savings incurred through using a BLH system under a time-based pricing scheme, some price information must be incorporated. Assuming dynamic pricing with hourly prices, i.e. 24 electricity prices a day the data used are provided by EXAA [3], the Energy Exchange Austria. These prices are wholesale prices of the control areas in Austria and Germany.

4.2.2 Data Preparation

Prior to using the data provided by these databases, a verification of the data should be mandatory. The sampling interval of the tracebase data varies from one second to several seconds within one dataset, which necessitates the interpolation as further calculations will use a one-second sampling interval. Luckily each measurement comes with an accompanying timestamp which allows the calculation of time between measurements. Assuming that each value at a specific time equals the average power since the last reading, the missing values can be interpolated by using the next measurement: e.g. a time series of *NAN, 1, 2, NAN, 3, NAN, NAN, 4, NAN* results in *1, 1, 2, 3, 3, 4, 4, 4, NAN*. Missing boundary values are filled by using an extrapolation process where the nearest value will be used to fill the data. In doing so, the time series above yields in *1, 1, 2, 3, 3, 4, 4, 4, 4*. This data preparation steps must be applied to all devices of interest in order to finally sum up all time series to a single aggregated load profile.

For further calculations the 15 minute sampling interval may also be of interest. Using the load profile from above, the 15 minute readings can be calculated by averaging (no moving average) $15\text{min} \cdot 60 \frac{\text{s}}{\text{min}} = 900\text{s}$ each. This arithmetic averaging process produces a new time series with the same amount of energy. For example a time series of *1, 3, 2, 4, 5, 6* would result in *2, 2, 3, 3, 5.5, 5.5* by averaging 2 seconds each.

A similar problem of missing information comes along with the EXAA price data from 1.10.2012 until 30.9.2013. Due to the clock change, hour 3 on 31st of March 2013 is missing. To fill the gap, the average of the previous and the subsequent hour is used. As per [4] on 13th of November 2012 the entire day is missing because of a breakdown of the electronic data processing center on the trading day, the 12th of November. These gaps are filled by hourly averaging the data of the previous and the following day.

4.2.3 Load Profile

Using the tracebase data necessitates the aggregation of appliances to simulate a household. This work distinguishes between two load profiles: a simple one for applying the NILM algorithm using only 7 devices, and the aggregation of 21 devices as listed in Table 4.2 where the devices for building the simplified load profile are indicated in bold.

In order to get a small variety of load profiles, 6 days will be analyzed. Devices that offer recordings over such a period were preferred, nevertheless the smartphone charger

Device	Labeling	Database Dates for Day 1 - Day 6
Charger-Smartphone	dev_D32328	6 times 20.11.2011
Coffeemaker	dev_D369E0	15.1.-20.1.2012
Cookingstove	dev_D33097	17.12.-21.12., 25.12.2011
Digital TV receiver	dev_D33097	3.12.-8.12.2011
Dishwasher	dev_B7E6F4	18.1.-23.1.2012
Freezer	dev_D36601	16.12.-17.12.2011, 20.1.-23.1.2012
Lamp 1	dev_11F01E	18.1.-22.1., 24.1.2012
Lamp 2	dev_72882E	10.5.-15.5.2012
Lamp 3	dev_C3E6D1	16.5.-20.5., 27.5.2012
Multimediacenter	dev_B7E43D	3.12.-8.12.2011
PC-Desktop	Desktop_Denis	1.1.-6.1.2012
Printer	dev_D3230E	21.11., 23.11.-27.11.2011
Refrigerator	dev_76C07F	11.6.-16.6.2012
Router	dev_B1B603	3.12.-8.12.2011
Subwoofer	dev_5534A4	13.1.-18.1.2012
Solar thermal system	_5525DD	16.12.-17.12.2011, 20.1., 21.1., 23.1., 24.1.2012
Toaster	dev_98ABD2	8.1.-9.1., 11.1.-14.1.2012
TV-LCD	dev_B8121D	13.1.-18.1.2012
Washing machine	dev_D31FFD	11.6.-12.6., 14.6.-15.6., 19.6., 21.6.2012
Water boiler	_55151A	3 times 24.-25.1.2012
Water kettle	dev_5AE2CA	1.2.-3.2., 5.2.-7.2.2012

Table 4.2: Device setup for building a load profile using tracebase [68], the devices used to build a simplified load profile are indicated in bold

and the water boiler only offered 1 or rather 2 recorded days, so the data were reapplied 6 or rather 3 times.

The energy consumption of the aggregated simplified load profile adds up to 1194 kWh a year, for day 1 (365 times day 1). Considering all 6 days the extrapolated annual energy consumption is 1131 kWh (60 times day 1 to 6 = 360 days, plus the days 1 to 5). Using 21 devices the energy consumption increases to 2228 kWh per year for day 1 and 2671 kWh for all 6 days. All of them are less than the average Austrian household's annual consumption of 3500 kWh, as per E-Control¹. A consumption between 1800 and 3000 kWh usually represents a household of one or two persons.

Figure 4.1 plots the load profiles for 3 of the 6 days analyzed using 21 devices.

The figure illustrates that the daily load profiles differ distinctly. The upper diagram shows day 1, the central diagram day 3 and the lower one day 6. Day 1 is characterized by a couple of high peaks, a higher demand during noon and some smaller peaks that

¹Average annual consumption as per E-Control, see <http://www.e-control.at/de/konsumenten/strom/strompreis/strompreis-monitor> (accessed on 8th of November 2013)

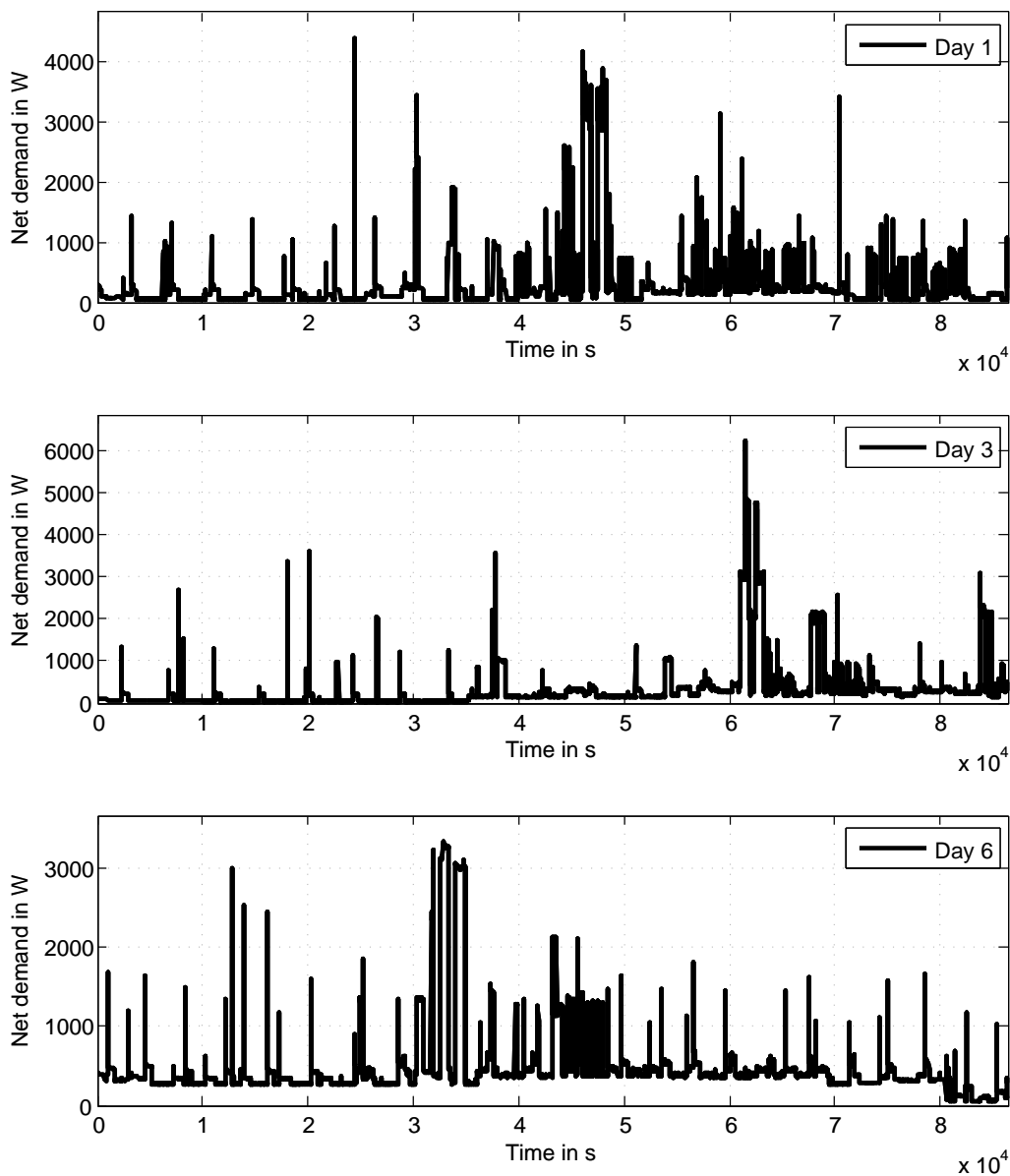


Figure 4.1: Load profiles using 21 devices for day 1, 3 and 6 based on data provided by tracebase [68]

occur quite frequently. Day 3 is characterized by a load of more than 6 kW in the afternoon and a higher demand during the evening hours. Day 6 is similar to day 1 but less chaotic with a higher base load that is caused by the washing machine.

Aside from a small water boiler used for dishwashing purposes, an energy-intensive electric boiler for supplying hot water for showering purposes is missing in both of the load profiles. For testing a LLH system such an element is mandatory. Therefore another appliance i.e. an electric boiler with a daily energy consumption between 2.5 kWh and 10 kWh will be additionally implemented for LLH system analysis.

4.2.4 Dynamic Pricing

The dynamic prices used to analyze potential savings when installing a BLH system base on averaging the hourly data provided by EXAA from 1st of October 2012 until 30th of September 2013. Figure 4.2 plots the prices used in this work.

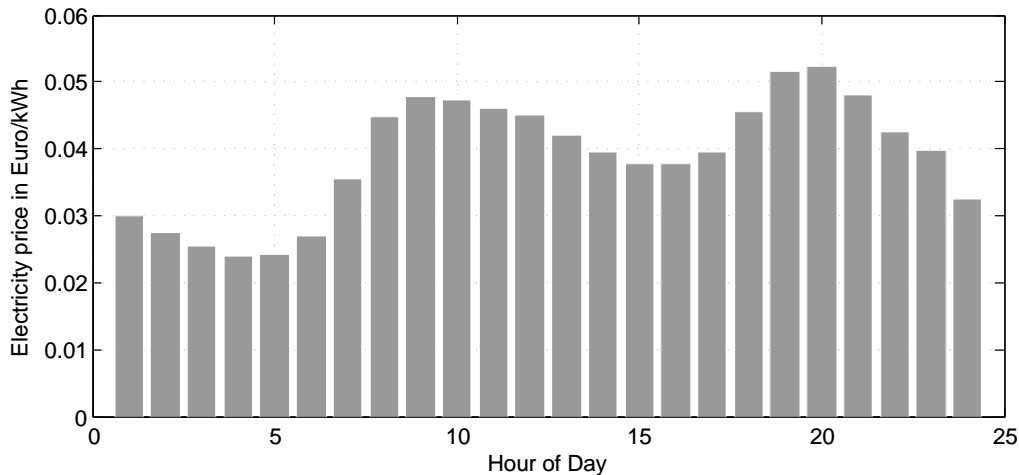


Figure 4.2: Dynamic electricity prices based on the EXAA spot market data [3]

4.3 Battery-Based Load Hiding

This section deals with the battery setup and the simulation model.

4.3.1 Battery Configuration

Inspired by the authors of the NILL algorithm [70] this work assumes the use of deep-cycle lead acid batteries with a minimum SOC of 20% and a maximum SOC of 90%, i.e. DOD is 70%.

The dimensioning of the battery for BLH algorithms depends on a variety of factors such as the shape of the load profile, the variance of the power, the demanded degree of privacy, the implemented algorithm etc. This work analyzes the following capacities: 10, 40, 70, 100, 120, 150, 200, 400 and 600 Ah.

The maximum charging and discharging current is assumed to be $0.3C$, i.e. for a 100 Ah battery the maximum current is set to 30 A, which may reduce the usable capacity compared to the nominal capacity (e.g. 100 Ah) which is usually the $0.1C$ or $0.2C$ capacity. This may be overvalued compared to commonly used load strategies, but in using BLH algorithms the charging current most likely will not be held constant at $0.3C$ for a longer period of time but instead vary between 0 and $0.3C$.

To simulate the BLH model a battery model provided by the SimPowerSystems library of Matlab is used. The following explanations of the battery model base on the descrip-

tions of <http://www.mathworks.de/de/help/phymod/sps/powersys/ref/battery.html>, accessed on 2nd of December 2013:

The model necessitates at least 4 parameters: the battery type, the nominal voltage that represents the end of the linear zone of the discharge characteristics, the rated capacity which is the minimum effective capacity of the battery and the initial SOC.

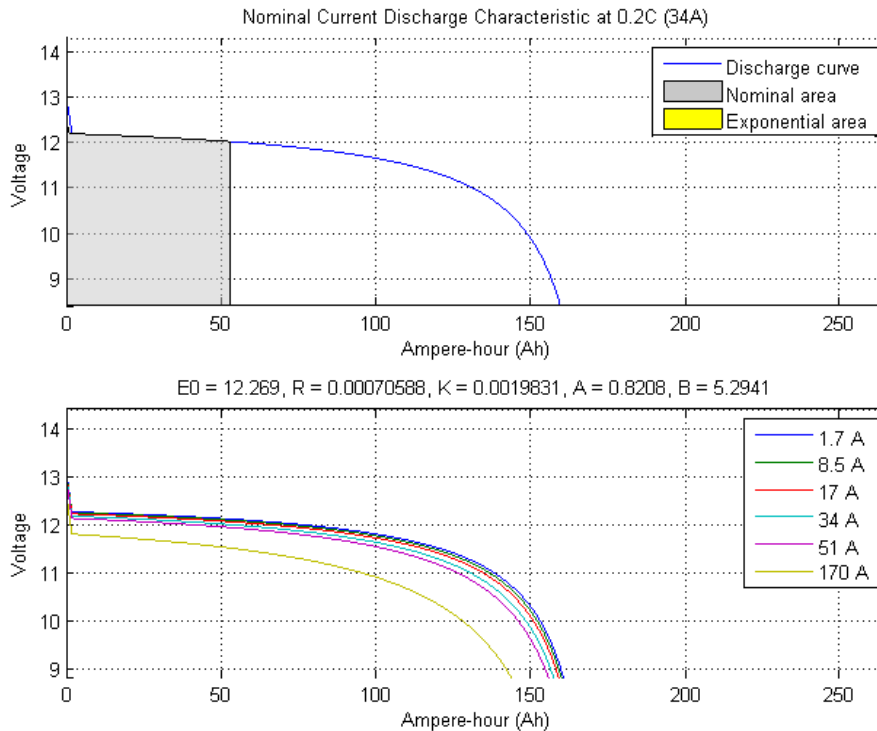


Figure 4.3: Discharge characteristics of a 12 V, 170 Ah lead acid battery

All other parameters can be set by Matlab automatically, e.g. the maximum capacity, fully charged voltage, nominal discharge current which is set to 0.2C automatically, internal resistance, the extracted capacity until the voltage drops under the nominal voltage and the voltage and capacity corresponding to the end of the exponential zone of the discharge characteristics. In this work each of these parameters will be set automatically. Figure 4.3 plots the discharge characteristics of a 12 V lead acid battery with a rated capacity of 170 Ah.

Referring to Mathwork's website, experimental validation of the model has shown a maximum error of 5% for a SOC between 10% and 100%, a charging current between 0 and 2C and a discharging current between 0 and 5C. Note that the model is based on several assumptions. For example it does not take temperature into account, there is no memory effect and, most significantly, the battery's capacity does not change with the amplitude of current. This means that the effect of different currents changing the battery's capacity (like it is plotted in the lower diagram in Figure 4.3) won't be considered in the model which may restrict the validity of the simulation results.

4.3.2 Simulation Model

We use Matlab 2013a in combination with the Simulink package and the SimPowerSystems library to simulate a realistic battery model.

The essential part of this work is the simulation of a BLH system. The basic principle of the model is illustrated in Figure 4.4. A inverter/charger-combination is connected to the utility and charges or discharges the battery. The operational mode of the inverter/charger is controlled by an intelligent control system. The three components battery, inverter/charger-combination and the control system form a BLH system.

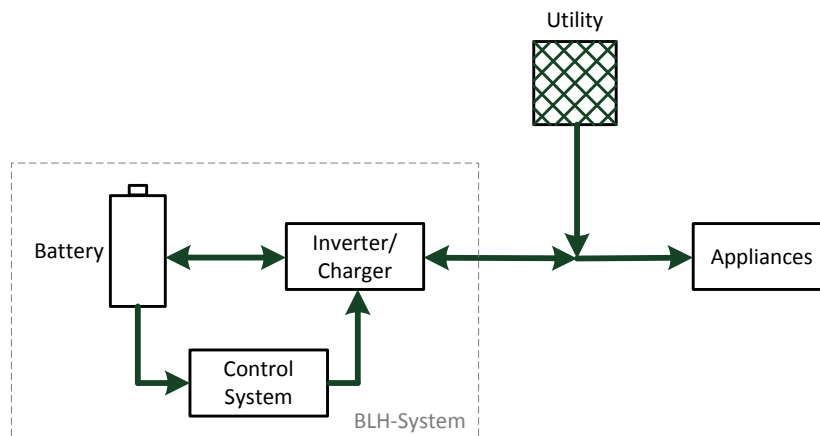


Figure 4.4: Simplified model of a BLH system

For simplification, this work assumes a purely resistive system considering active power only which allows the use of a DC system instead of an AC system. Furthermore, the inverter/charger-combination is idealized by two programmable current sources with zero losses. All other elements are assumed to be ideal as well. The reason for using a simulation model is the application of a realistic battery model that considers the actual SOC of the battery. Figure 4.5 plots the Simulink model.

The powergui box (1) is required by the SimPowerSystems library with some basic settings that must coincide with the Model Configuration Parameters of the Simulink simulation. (2) is the realistic battery model of SimPowerSystems. The time delay of 1 step (3) is necessary to avoid algebraic loops. Furthermore, the settings of the control system (4) for the following step depend on measurements of the current state, as a logical consequence the delay is mandatory. The control system contains the algorithm behind the BLH system and adjusts the level of the output currents i_{1} and i_{2} based on the measurements of the battery's voltage level, the SOC and the actual level of net demand. The programmable current source (5) represents the DC-side (e.g. 12 V DC) of the inverter/charger-combination of a BLH system, the current source (6) represents the AC- or utility-side (e.g. 230 V AC), which is simplified by another 12 V DC system in this simulation. If the output of the current source on the DC-side is positive, the source acts as a generator and the battery will be charged, if the current is negative the source acts as a load and the battery gets discharged. Therefore if the current

on the DC-side (5) is positive, the power flows from the utility to the battery. In the following, the AC-side must act as a load on the secondary branch to consume this energy. Basically $i_{-1} = -i_{-2}$, but in contrast to the AC-side the voltage level on the DC-side is not constant. To get the same power $p(t) = u(t) \cdot i(t)$ on both sides there must be a correction factor considering that effect. Thus, disregarding the direction of the current flow yields in $i_{-1}(t) = \frac{p_{net_demand}(t)}{u(t-1)}$ and $i_{-2}(t) = \frac{p_{net_demand}(t)}{u_{utility}(t)}$ whereas $u_{utility} = 12\text{ V}$ and $u(t-1)$ varies from approximately 10 V to 14 V depending on the SOC. (7) represents the workspace import of net demand in W in a one-second time series format. This input must be inverted as the household is represented as another programmable current source (8) and it can only act as a load so that the current must always be zero or below zero. Prior to controlling the current source the power (net demand) must be converted to a current, thus the calculations in (9). (10) represents the utility as a 12 V DC voltage source. Finally, the current measurements in (10) allow the use of scopes and the export to the workspace. Several variables will be exported to the workspace but for clarity reasons the *To Workspace*-blocks are hidden in Figure 4.5.

Upon beginning the simulation the system starts in stable state using NILL algorithm. Using BE- or NILL algorithm the initial value of the metered load equals net demand, whereas using the SF with *Lazy Stepping 2* yields in an appropriate quantized initial value.

The data produced by this Simulink simulation will be postprocessed for user-defined diagrams and to calculate the three measures RFM, RMSE and the F-measure.

4.3.3 Assumptions

Summarizing the *Evaluation Setup* of BLH this experiment is based upon the following assumptions:

- Load profile: using active power data provided by tracebase, assuming that the each measurement is the average power since the last measurement, quantized in 1 W steps, analyzing 6 independent days in total.
- Price data: data provided by EXAA, with missing information filled by averaging, the prices are the hourly means from 1st of October 2012 to 30th of September 2013.
- Simulation model of BLH: the DC simulation model uses a battery model provided by SimPowerSystems library but all other devices are assumed to be ideal.
- RFM: for calculating the relative feature mass only load changes of 5 W or more will be taken into account.
- F-measure: the F measure represents the effectivity of a specific NILM algorithm [24].

- 12 V Lead acid battery with an initial SOC of 55 %, the usable SOC is 20-90 % with a max. charging and discharging current of 0.3C, all other battery's parameter are set by Matlab automatically.
- Initial states: NILL algorithm starts in stable state, BE- and NILL algorithm start with metered load equals net demand.
- NILL algorithm: the measure for calculating the following stable state is $\alpha = 0.5$, when switching from stable state to high recovery state the battery will be discharged with 0.5 A, the algorithm changes from high recovery state to stable state if the battery's discharging current exceeds 5 A.

4.4 Load-based Load Hiding

This section addresses the load configuration, the algorithm setup and the simulation model when applying a LLH system.

4.4.1 Load Configuration

The controllable load is assumed to be an electric boiler. For simplification this work bases upon a fairly evenly distributed energy consumption of the electric boiler with a given target energy level of 5 kWh over the day (annual energy demand increases by 1825 kWh) which is simply another appliance in the load profile using tracebase data. The assumption of a target level yields in a constant energy consumption per day but not a constant temperature. If the boiler's temperature decreases dramatically, it may take some time to reach a high temperature level again, whereas a conventional temperature control would set the boiler's power demand to its maximum level.

The assumption of a constant energy demand is more similar to an electric boiler using off-peak electricity, however the target is not a given temperature but a specific energy consumption. Inspired by the Austria Email AG this work is based upon data of the electric heaters EWH-158-E and EWH-156-E with a volume of 150 l and a maximum power of 1.6 kW (rounded down) or rather 2.3 kW. As per [71] the standby energy consumption of these types are about 0.95 kWh per day, which means that 4.05 kWh will be available for the heating process which may be a plausible hot water consumption for a household of 2 persons.

This work also analyzes daily target energy consumptions of the electric boiler of 2.5, 7.5 and 10 kWh.

4.4.2 Noise Generation

In this paper a beta, a modified beta distribution and a truncated normal distribution will be used. In order to test different distributions, the parameter setup α , β , μ , σ , P_{max} and the target energy consumption will be varied. Furthermore the time of holding the boiler's load constant is set between 1 and 120 s. Longer time frames will not be

used as the NILM algorithm may derive the boiler's load and hence net demand more easily.

When applying the normal distribution, the expectation μ is set to $\mu_{set} = 208.3 W$ for an energy target of 5 kWh. Due to the asymmetric truncation from 0 to P_{max} the actual mean would be higher than μ_{set} . Hence the expectation (of the common normal distribution) is set to a smaller value and the expectation of the truncated distribution will be derived. This iteration process is done until the deviation between the new expectation and μ_{set} is below $10^{-5} W$. P_{max} is set to 1600 or 2300 W and the standard deviation σ to 300, 800, 1200 or 1600 W.

The beta distribution is based upon the parameters α and β . Again P_{max} is set to 1600 or 2300 W, α varies from 0.1 to 1.8 and β is derived by α and the expectation μ that is set to $\mu = \mu_{set}$: $\beta = \frac{\alpha - \alpha \cdot \mu}{\mu}$.

The modified beta distribution sets α constant but varies μ randomly between 0 and P for a random time frame with a maximum of one hour where randomization bases on uniformly distributed pseudorandom integers. The PDF allows realizations in $[0 P]$ where P is randomly set between $\frac{P_{max}}{4}$ and P . If μ is set higher than μ_{set} the boiler consumes more energy than it should. Therefore, when setting the following time frame and μ the energy gap of the realizations compared to the constant load μ_{set} is analyzed. If the gap exceeds $\pm 0.5 kWh$ the new expectation is limited to $[0 \mu_{set})$ or rather $(\mu_{set} P_{max}]$ depending on whether it was too high or too low. There is a high probability that the daily energy consumption differs from the target consumption but this gap shouldn't be too dramatic. The realized consumption lies in $[4.29 7.8] kWh$ for a target energy of 5 kWh taking the worst case into account.

4.4.3 Simulation Model

The simulation model of a LLH system is based on several simplifications. This paper uses not a dynamic model of the electric boiler but only the maximum power of the boiler of 1600 or 2300 W and a daily target energy consumption between 2.5 and 10 kWh without considering any further losses or devices. Thus, a Simulink simulation model is not necessary.

4.4.4 Assumptions

Summarizing the *Evaluation Setup* of LLH this paper is based upon the following assumptions:

- Load profile: using active power data provided by tracebase, assuming that the each measurement is the average power since the last measurement, quantized in 1 W steps, analyzing 6 independent days in total.
- Simulation model of LLH: no dynamic model, the modelling is solely based upon a maximum power level and a target energy consumption.

- F-measure: the F measure represents the effectivity of a specific NILM algorithm [24].

5 Results

This chapter presents the results of simulating the BLH and LLH systems. The most important measure when analyzing the effectivity of privacy protection is the F-measure, which describes the success rate of the NILM algorithm. Most likely the success rate of such a NILM algorithm is below 100% even without applying a load hiding system, as, for example, there may be situations when net demand could be realized by a variety of combinations of appliances that are turned ON. Figure 5.1 plots the F-measure of the original time series of net demand for the days 1-6 (simplified load profile), the dashed black line illustrates the mean. As the F-measure is already at a level of approximately 50%, even without applying any kind of obfuscation system, this suggests that the high sampling interval and the low number of appliances was chosen quite reasonably.

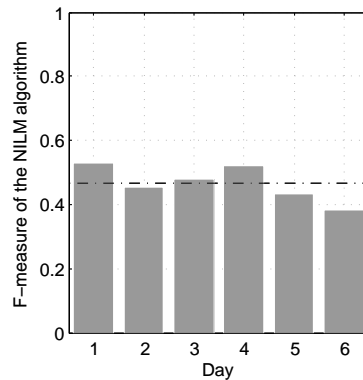


Figure 5.1: F-measure of the original time series of net demand

5.1 Battery-Based Load Hiding

This section specifies the results when using a battery-based load hiding system. Besides discussing different battery sizes this section compares the effectivity of increasing the capacity with an increase of the current rating. Furthermore potential savings and the availability of the components of such a system will be mentioned.

5.1.1 Net Demand vs. Metered Load

Figure 5.2 plots net demand, the metered load, the actual SOC and the charging/discharging current for day 1 when using BE algorithm, a battery capacity of 120 Ah und a current limit of 36 A.

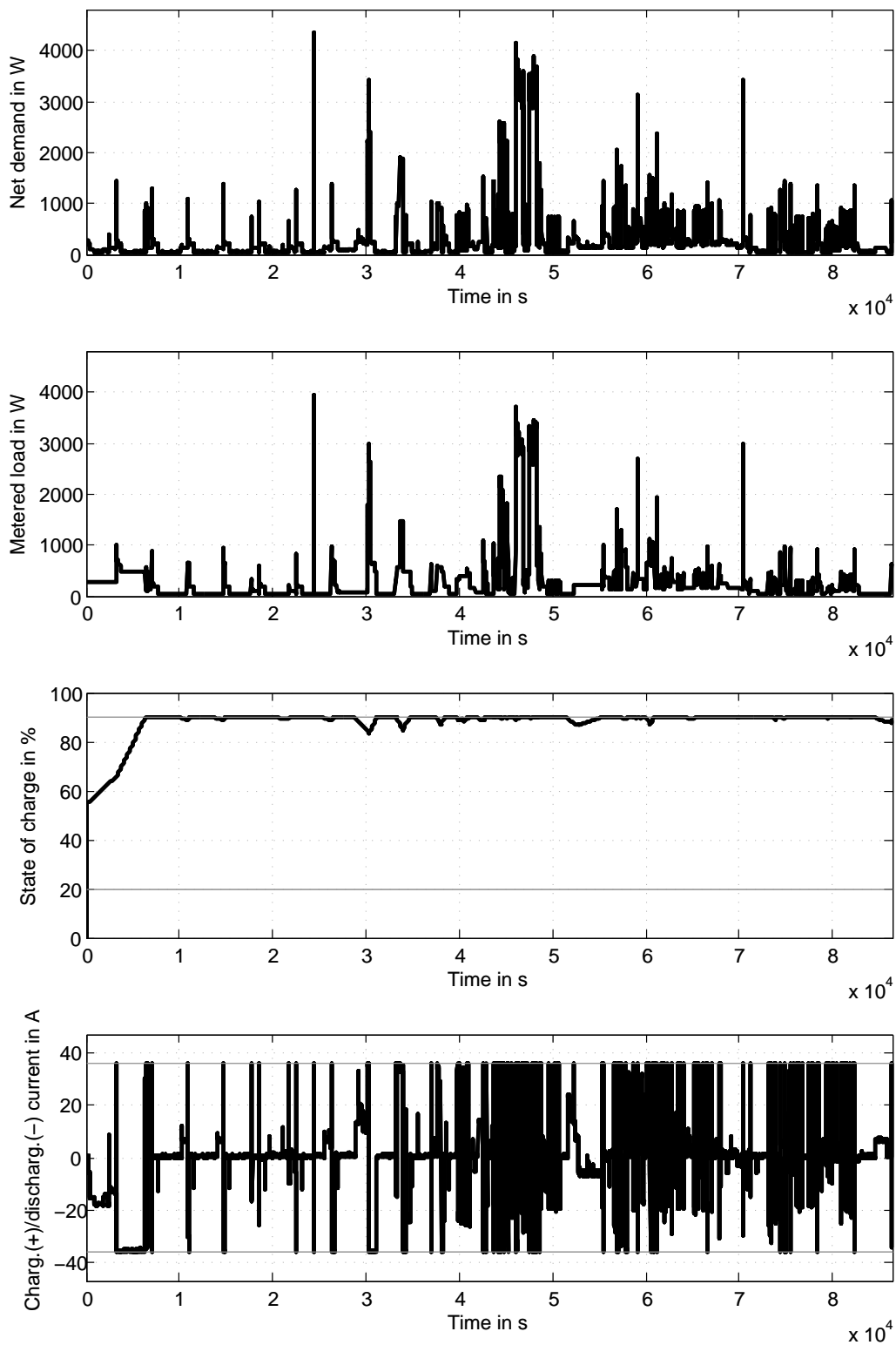


Figure 5.2: Results using BE algorithm for day 1 ($C=120$ Ah, $0.3C$)

BE algorithm tries to maintain a constant metered load as long as possible, i.e. until the battery is limited by the maximum current or SOC. Due to the maximum current rating, high peaks in net demand cannot be filtered out but only minimized by the maximum discharging current of 36 A. Small variations can be minimized but with an initial SOC of 55% the battery's SOC reaches its maximum of 90% very fast. As the SOC is at its maximum almost all the time BE algorithm suffers under a less effective functionality. The bottom diagram shows the charging/discharging current which is below 0 in situations where the battery gets discharged. The battery experiences the highest peaks whenever high peaks in net demand occur. Compared to the small current settings that emerge most of the time, periods where the battery suffers the maximum current rating are short.

When simulating NILL algorithm instead of BE algorithm using the same parameters leads to the metered load illustrated in Figure 5.3. In general the resulting load profile looks very similar compared to BE algorithm, so does the SOC and the charging/discharging current, hence they are not plotted here. For example a small difference between BE and NILL can be recognized at about 30000 s where the NILL algorithm yields to a smaller metered load after recovering from a peak load in net demand.

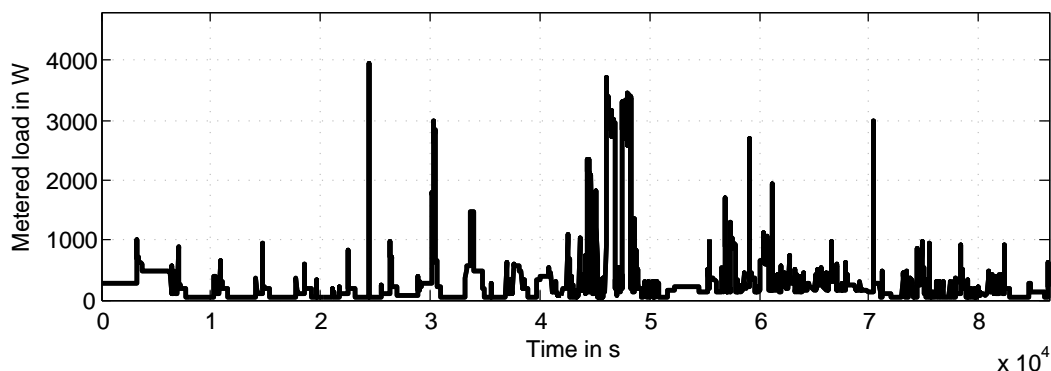


Figure 5.3: Metered load for NILL algorithm for day 1 ($C=120$ Ah, $0.3C$)

Figure 5.4 plots the results when using SF. In this case net demand gets quantized into steps that equal the battery's charging or rather discharging current multiplied by the voltage level ($p(t) = u(t) \cdot i(t)$).

The initial value of the metered load cannot be quantized as the simulation model bases on previous measurements at time $(t - 1)$. When starting the model there is no data available for $(t - 1)$, hence the initial value of the metered load is set to net demand. All further samples of net demand can be realized by two levels of quantization (net demand may also equal the quantization step, in that case the metered load is set to net demand). The SF tries to maintain the same level as long as possible. In situations where it must be changed, the choice whether to choose the upper or lower limit is set randomly as long as no limitation regarding the SOC occurs. Therefore, the output of SF is probabilistic which means that the metered load may differ from one computational run to another. The average level of the SOC is lower compared to BE- or NILL algorithm, which means

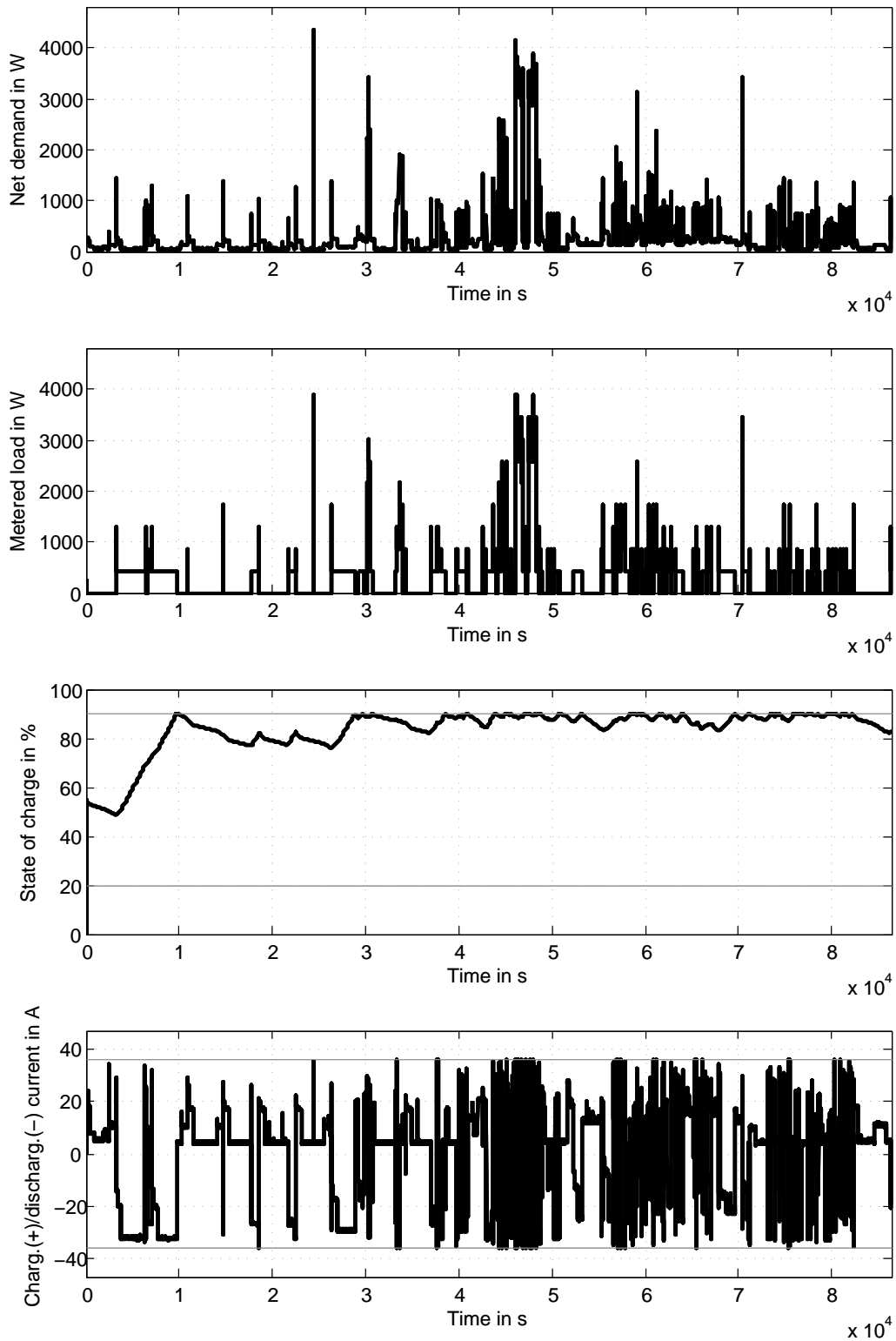


Figure 5.4: Results using the SF for day 1 ($C=120$ Ah, 0.3C)

that the algorithm can work with a higher efficiency as the quantization steps can be set randomly. Compared to BE or NILL, the battery experiences less maximum current peaks but a higher average absolute value which may decrease the battery's lifetime.

The next step is to increase the sampling interval from one second to 15 min. The SF provides the metered load that is diagramed in Figure 5.5. Whereas net demand is held constant for at least 15 min the sampling interval of the simulation model is still set to one second. Clearly short-time peaks in net demand that occur when using a one-second sampling interval diminishes when changing to 15 min. While net demand is already less chaotic the BLH system is able to hide most of the load variations. At the moment the SOC reaches the lower limit the metered load increases to the next higher quantization level to recharge the battery. The opposite happens when the battery reaches the upper level. Compared to the one-second data the battery's SOC varies more widely between the upper and the lower limit. The accompanying absolute value of the charging or rather discharging current is much higher than using a one-second resolution, but fortunately currents at their maximum rating are very rare.

There are 2 unexpected peaks between 40000 and 50000 s which are caused by the simulation model. The reason for these short outliers is the randomized setting of the quantization steps based on the actual current of net demand. While net demand in terms of power is constant for at least 15 min, the battery's current is not constant because the voltage level of the battery changes. So a situation may occur where the battery cannot maintain a given constant power level as the battery voltage changes and cannot maintain the same power would outrun the current limit, therefore the quantization step must be changed.

For example, the initial battery voltage has a level of 13 V and the quantization steps 4 and 5 may be feasible for a specific level of net demand of 645 W (the max. charging/discharging current is assumed to be 10 A, $P_{step4} = 4 \cdot 13 V \cdot 10 A = 520 W$, $P_{step5} = 5 \cdot 13 V \cdot 10 A = 650 W$). Now assume that the SF chooses the 4th step, hence the battery must provide the difference of $645 W - 520 W = 125 W$ and gets discharged. A discharge reduces the battery voltage, in this example it decreases to 12 V. Whereas with 13 V the battery was able to provide $13 V \cdot 10 A = 130 W$, now the maximum power of the battery is $12 V \cdot 10 A = 120 W$. Thus quantization step 4 decreases from 520 W to 480 W and step 5 from 650 W to 600 W. As net demand remains unchanged at 620 W the battery system cannot make up the difference of $645 W - 480 W = 165 W$ and the quantization step must be changed to step 5 or 6. Now when choosing step 6, the battery gets recharged again and the battery voltage increases, which may result in an opposite reaction. Such unfortunate situations result in short peaks.

To minimize this problem (it cannot be eliminated as long as there is a current but not a power rating) it would be possible to use a fixed voltage to calculate the quantization steps instead of using the battery voltage. In order to avoid new problems, the fixed voltage should be set to the minimum battery voltage that is allowed (and not its nominal value as that raises new problems). This would reduce the size of the quantization steps but also remove most of the short peaks that may occur, although their influence is marginal.

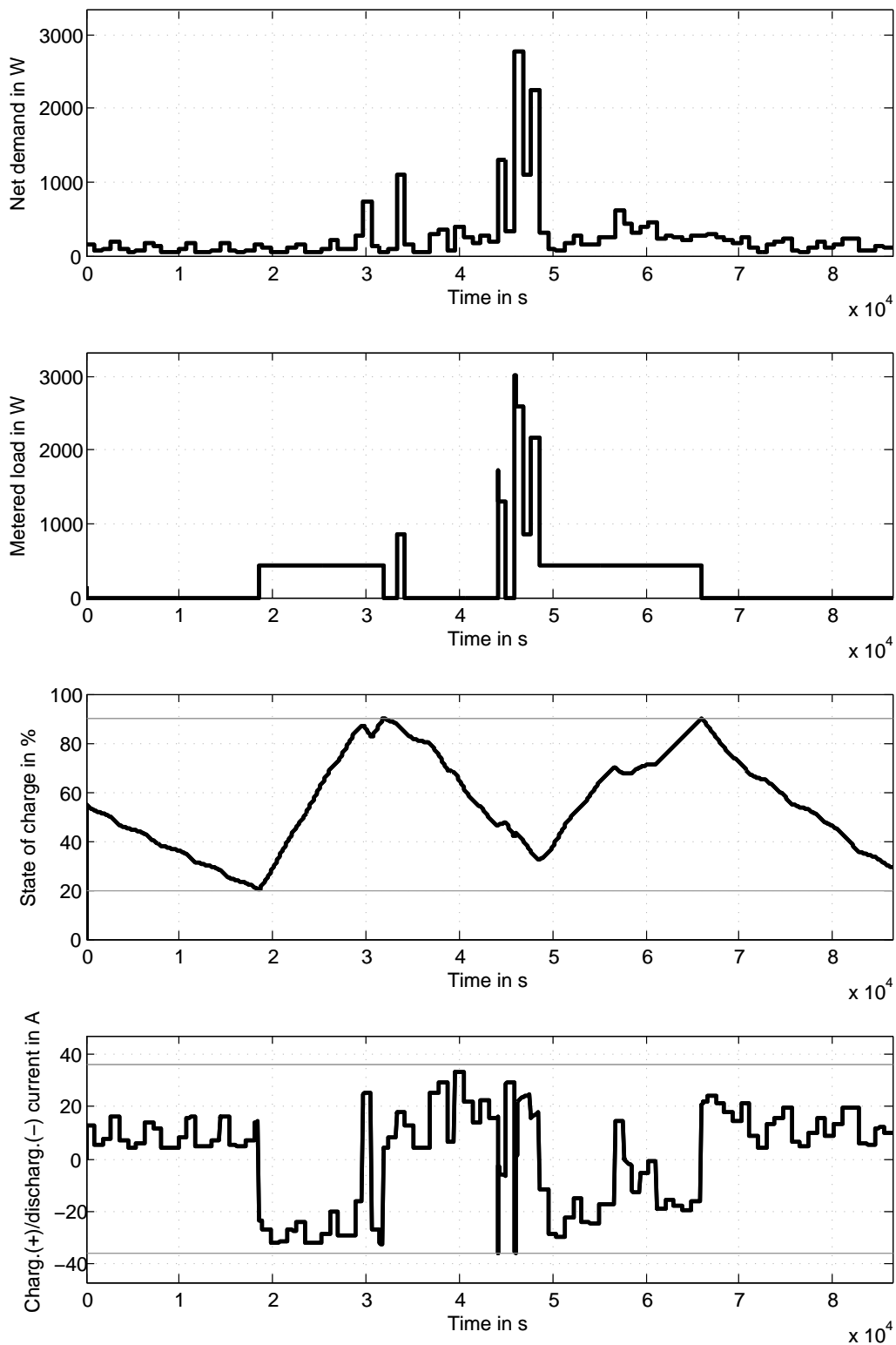


Figure 5.5: Results using the SF for day 1 based on a sampling interval of 15 min. ($C=120$ Ah, $0.3C$)

5.1.2 Battery Configuration

The previous section provided an overview of the output of a BLH system. In this section the effect of changing the battery capacity will be analyzed. The capacity is set to 10, 40, 70, 100, 120, 150, 200, 400 or 600 Ah.

Figure 5.6 plots net demand and the metered load under the SF for using a 40 Ah and a 400 Ah battery.

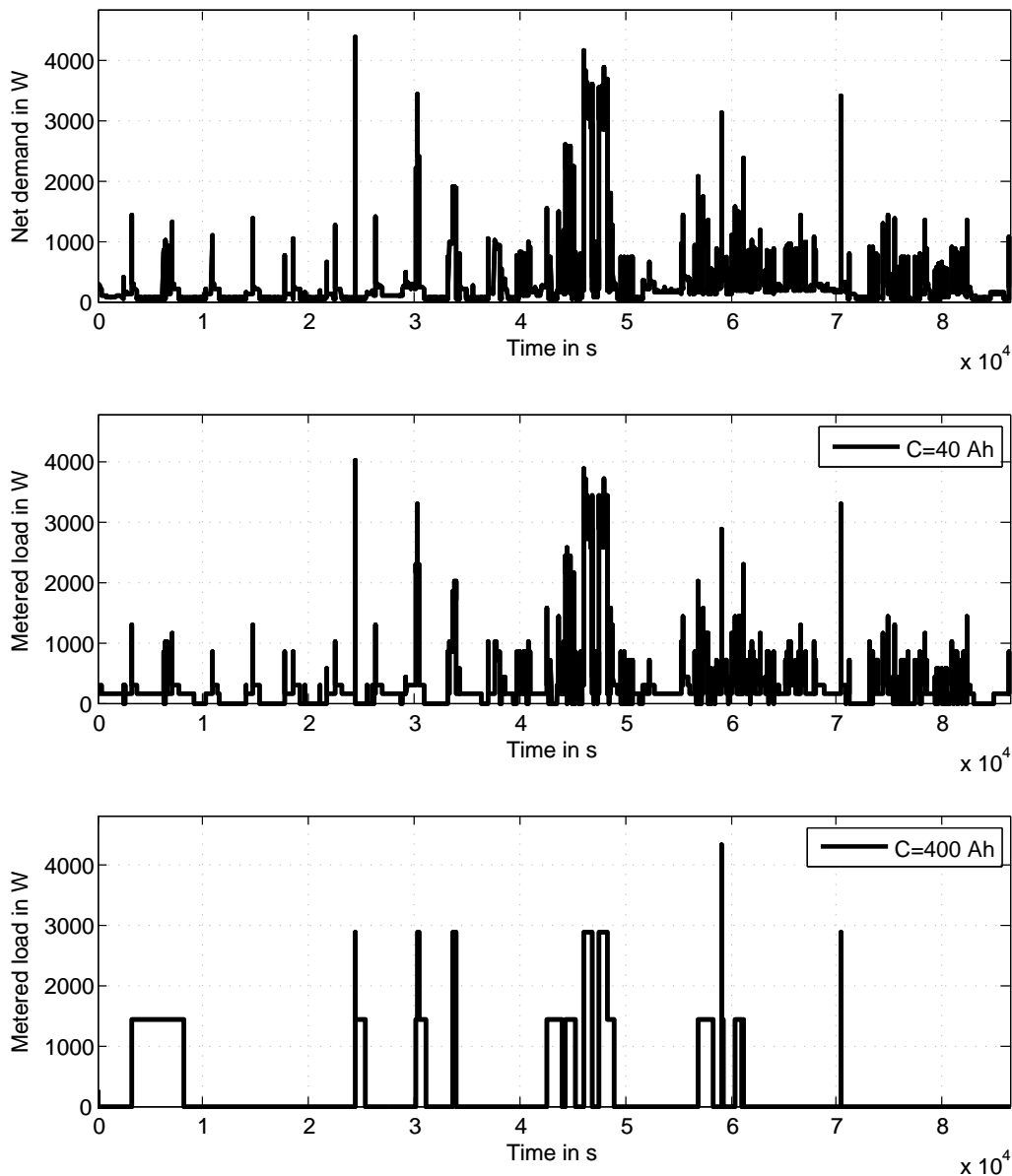


Figure 5.6: SF for day 1, using 40 Ah or rather 400 Ah (sampling interval: one second)

It is obvious that the level of distortion between net demand and the metered load increases with a higher capacity. Hence the success rate of NILM should be worse when

increasing the capacity. With a higher capacity comes increased quantization steps as the step size is set to the maximum charge rate which in turn is set to $0.3C$, i.e. for 40 Ah it is set to $12 A \cdot 12 V = 144 W$ and for 400 Ah it is set to $120 A \cdot 12 V = 1440 W$ roughly. For the remainder of this section all figures and results are based upon averaging days 1-6 unless otherwise stated.

Figure 5.7 plots the results of the NILM algorithm based on the simplified load profiles. The F-measure describes the success rate of the algorithm, smaller values are better from a load hiding point of view, e.g. if the F-measure is 0.3 about one third of the appliance's states can be detected correctly. The figure allows an overview of BE, NILL and SF considering different battery capacities. Whereas the NILL algorithm seems to be the most promising one for small capacities, for higher capacities SF is the best. From 10 to 100 or rather 120 Ah the fall of the F-measure is almost constant. Then a saturation process begins and the measure actually increases until 200 Ah where it drops to its minimum at 400 Ah. Using 600 Ah the metered load remains constant nearly all the time but unexpectedly the NILM algorithm again provides a higher success rate.

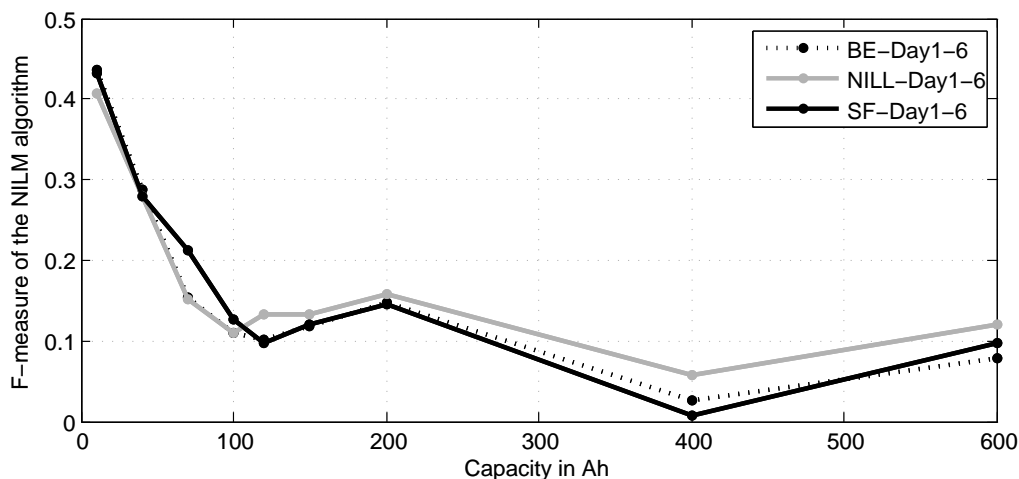


Figure 5.7: F-measure of the NILM algorithm after applying a BLH algorithm

A comparison of the RMSE using the simplified load profile is illustrated in Figure 5.8. A higher value means that there is a greater difference between net demand and the metered load, i.e. the higher the RMSE is the better the BLH should work. SF provides the most accurate results, but the difference is not very significant. Until a capacity of 400 Ah RMSE increases at an almost linear rate but the gradient shows some saturation effects when increasing to 600 Ah. When analyzing the more complicated load profile using 21 devices both the one-second and the 15 min readings yield very similar results without further remarkable insights. Therefore, they are not plotted in this work.

Finally, the RFM of the simplified load profile is diagramed in Figure 5.9. A higher value means a higher number of load changes of $\geq 5 W$ of the metered load compared to the original time series of net demand. A RFM greater 1 means that the number of load changes actually increased because of the BLH system. Values below 1 should

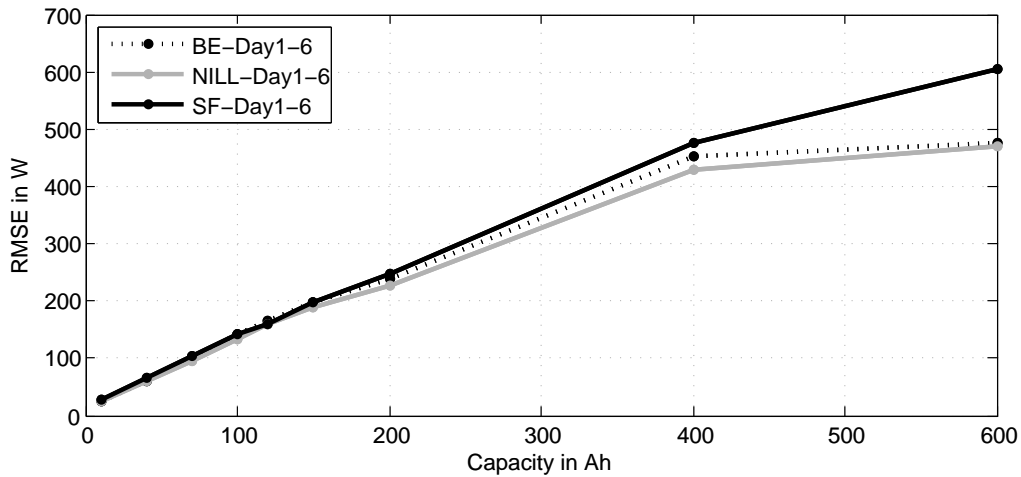


Figure 5.8: RMSE after applying a BLH algorithm

be beneficial as the metered load is more constant than net demand. Again the most desirable results come along with SF which provides the smallest values of RFM.

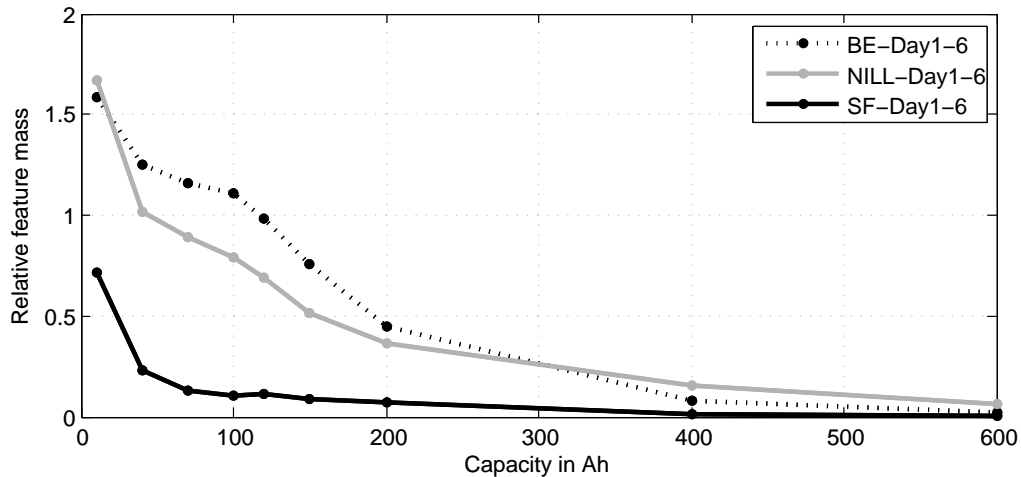


Figure 5.9: RFM of the simplified load profile using a sampling interval of one second

Figure 5.10 plots the same measure for the more complicated load profile and again SF offers the most desirable results. The average RFM is much smaller as the number of load changes of net demand is much higher compared to the simplified load profile.

When changing the sampling interval to 15 min. the BE algorithm provides the most desirable results for capacities up to 100 Ah, for higher capacities the SF is the most desirable, see Figure 5.11. Using the SF accompanies with high RFM values for small capacities. Even though net demand maintains constant when the battery's SOC gets too low or high the SF changes the quantization level to recharge or discharge the battery again.

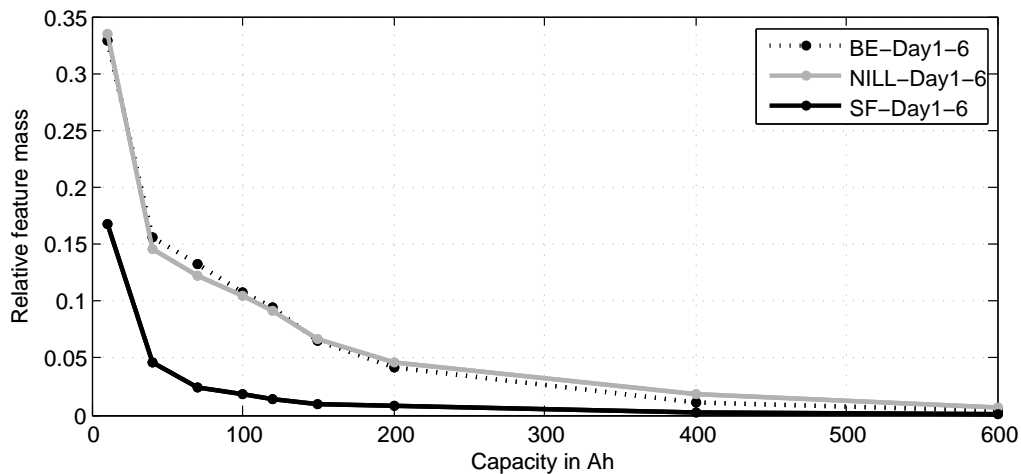


Figure 5.10: RFM using a sampling interval of one second

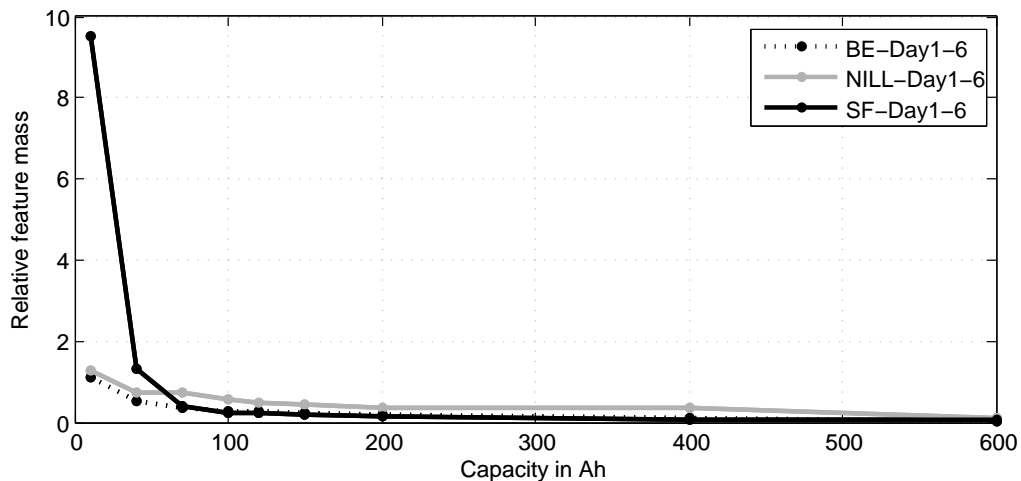


Figure 5.11: RFM using a sampling interval of 15 min

5.1.3 Current Ratings vs. Battery's Capacity

The previous section listed various results using different battery sizes. Whereas using a higher capacity allows the BLH system to provide the same amount of energy for a longer period of time until the SOC reaches its limit, a greater capacity allows a higher current rating in Amps using the same ratio of $0.3C$ too.

Regarding privacy protection the question arises whether the effect of doubling the current rating using the same battery outperforms doubling the capacity. For example, a comparison between a 100 Ah battery with a maximum current of 30 A which equals $0.3C$ and a 300 Ah battery with the same maximum current of 30 A that equals $0.1C$ in this case can determine the more significant effect. If there is no significant privacy protection improvement when using 300 Ah instead of 100 Ah, the battery's capacity rather than its current rating would appear to be the key factor when dimensioning a

BLH system but the current rating is.

The following results are based upon the 6 day average outputs of the SF. Table 5.1 lists the analyzed current ratings for a constant capacity of 120 Ah, the associated current in A and the accompanying capacity if the current rating is set to 0.3C.

Current rating in parts of 120 Ah	Current rating	Capacity when using 0.3C
0.02	2.4 A	not analyzed
0.025	3 A	10 Ah
0.05	6 A	not analyzed
0.1	12 A	40 Ah
0.175	21 A	70 Ah
0.2	24 A	not analyzed
0.25	30 A	100 Ah
0.3	36 A	120 Ah
0.375	45 A	150 Ah
0.5	60 A	200 Ah

Table 5.1: Comparing current ratings using a specific capacity with different capacities using 0.3C

Figure 5.12 plots the F-measure over different currents using both a constant capacity but a varying current rating (black) and furthermore a constant current rating but varying capacity (grey) for currents up to 60 A.

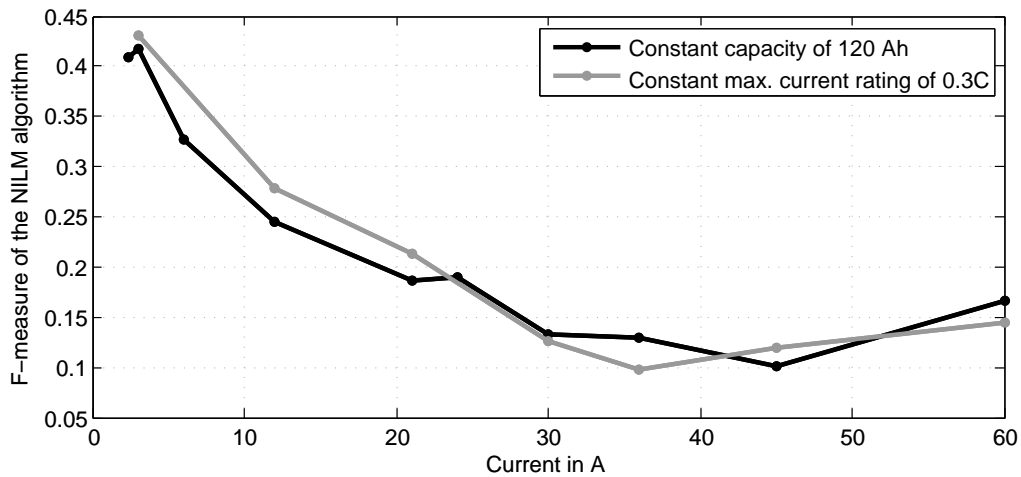


Figure 5.12: F-measure of the NILM algorithm depending on different currents to compare the effects of a fixed current rating vs. a constant capacity

The results are very similar which supports the significance of the current rating instead of different capacities. The results at 36 A correspond to 120 Ah and 0.3C,

therefore the F-measure should be equal. The reason for the observable gap is the probabilistic determination of the NILM algorithm but also of the SF that may yield to different results from one computational run to another (the simulation process was repeated). Below 36 A the black line (constant capacity) should perform better (smaller values of the F-measure) as the BLH system provides the same maximum current but a higher capacity. There is a vague trend that supports this idea but the trend is not very significant. The opposite should happen for currents that are higher than 36 A, but there is no evidence for this trend.

The same situation using a 600 Ah battery analyzing currents up to 180 A leads to Figure 5.13.

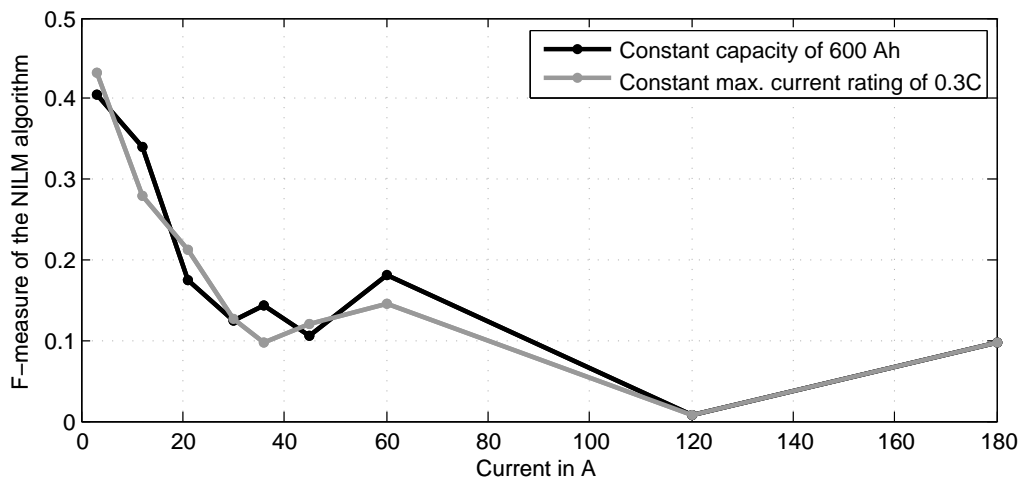


Figure 5.13: F-measure of the NILM algorithm depending on different currents to compare the effects of a fixed current rating vs. a constant capacity

Compared to the previous analysis there is even less evidence that the constant capacity provides better results. For a current of 180 A the results should again be the same (600 Ah, $0.3C=180$ A) and de facto they are the same.

The results of the RFM using the 120 Ah battery are plotted in Figure 5.14. Although the calculation of RFM is probabilistic as the SF base on some randomized settings the results using 36 A are the same. As expected for currents below 36 A the black line that corresponds to a constant capacity performs better, whereas for higher currents it performs worse. So in contrast to the F-measure RFM suggests that there is evidence that both not only the current rating but also the battery size are significant. Analyzing RMSE yields a similar result.

5.1.4 Potential Savings

Another question that may be of interest is whether a BLH system allows financial savings as the battery system tries to delay and flatten peak loads. Such peaks may occur while electricity prices are high assuming a dynamic pricing scheme. The electricity prices that are used here are wholesale prices without taxes or any additional charges.

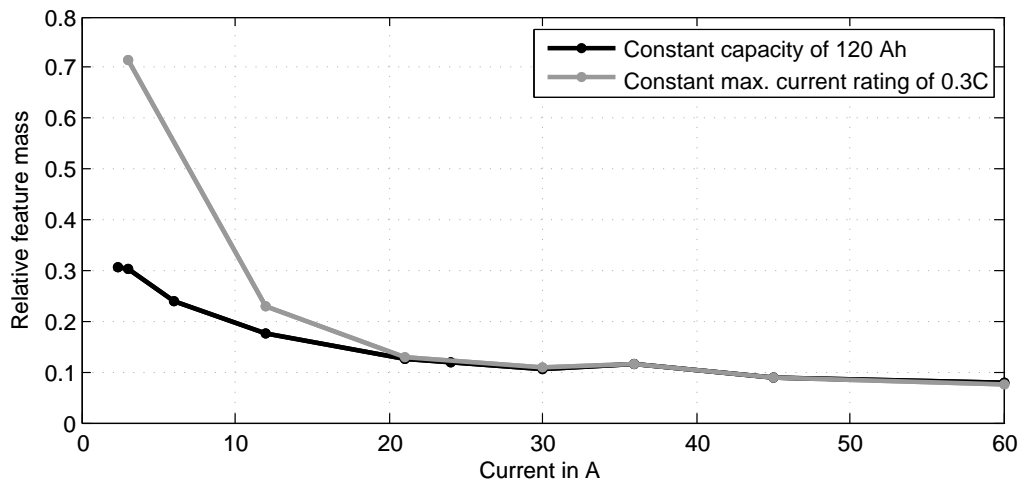


Figure 5.14: RFM for different currents to compare the effects of a fixed current rating vs. a constant capacity

Figure 5.15 plots possible savings when comparing net demand (simplified load profile) with the metered load under the same pricing scheme. Positive values describe real financial savings. Figure 5.15 suggests that a BLH system do not help cutting the electricity bill.

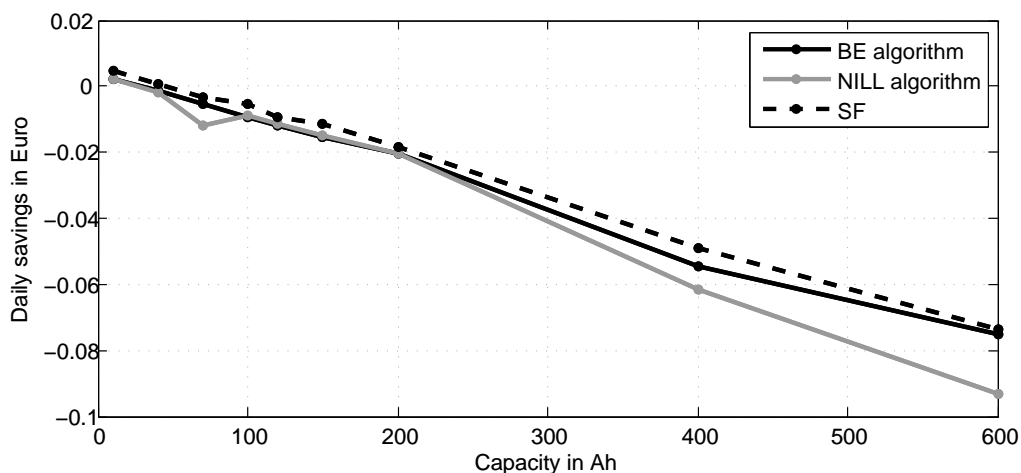


Figure 5.15: Potential savings using a 400 Ah BLH system

Unfortunately, this diagram is not significant as it does not consider that the battery's SOC at the end of the day may be higher than the initial value. Furthermore the simulation model disregards all kinds of losses. For example, using a 400 Ah battery the initial SOC is 27.5% smaller than the SOC at the end of the day when calculating the 6 day average of SF. This corresponds to an energy of roughly $E = 0.275 \cdot 400 \text{ Ah} \cdot 12 \text{ V} = 1.32 \text{ kWh}$. For comparative purposes note that the 6 day average daily consumption is 3.101 kWh. Assuming a uniformly distributed charging process, the mean wholesale

price of 0.0389 € leads to a correction factor for charging the battery to a higher level: $Correction = E \cdot price = 1.32 \text{ kWh} \cdot 0.0389 \frac{\text{Euro}}{\text{kWh}} = 0.051 \text{ Euro}$. The financial burden of using SF with a 400 Ah battery that is illustrated in Figure 5.15 is -0.049 €. Adding this correction factor would lead to daily savings of 0.2 Cent.

The problem in evaluating this correction factor is that such simplified calculations disregard that the battery voltage is not held constant to 12 V, the capacity changes when changing the charging or rather discharging current (this effect will also not be taken into consideration under the Simulink's battery model) and it assumes a uniformly distributed charging process over the day. An attempt to determine days where the initial SOC is the same as the SOC at the end of the day was unsuccessful, the SOC level increases at least 10% for all days and algorithms analyzed. This rising SOC level suggests that the initial SOC was set too low.

5.1.5 UPS Capability

When implementing a BLH system, the battery maybe is assumed to work as an uninterruptible power supply (shortened UPS) that provides energy in case of a blackout. Disregarding problems such as an issue of the battery system failing to supply all of the appliances the customer would like to operate, a brief overview of the average SOC of the battery should illustrate further possibilities of such a system as a beneficial side-effect.

Figure 5.16 plots the 6 day average SOC using the simplified load profile.

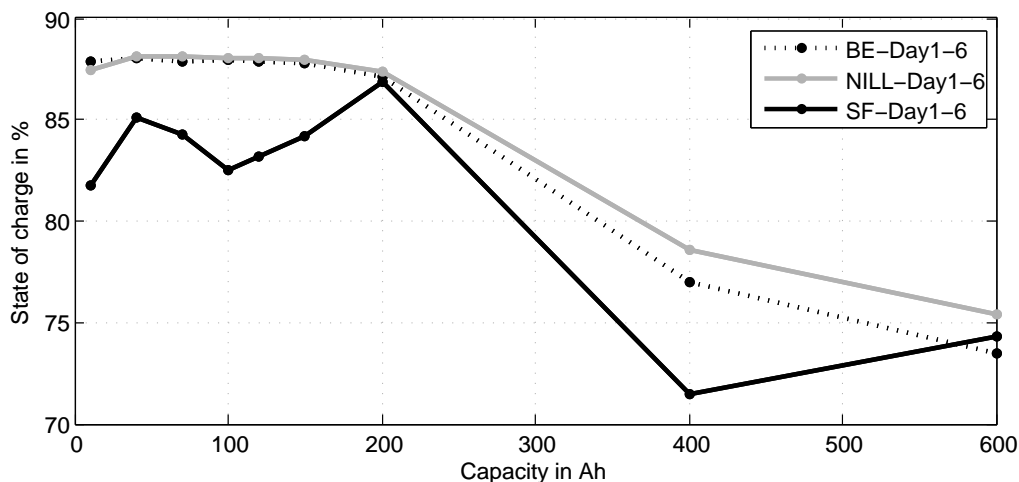


Figure 5.16: SOC using the simplified load profile and a one-second sampling interval

While the characteristics of BE- and NILL algorithm are very similar, SF provides the smallest values of the SOC. With regards to UPS compatibility, the performance of the SF is the worst but high SOC values accompany a high share of a fully-charged battery system, i.e. a state of 90%, which may significantly decrease the effectivity of the BLH algorithm. The general trend is that the SOC level decreases as the capacity increases, which is plausible as the battery's charging/discharging time increases heavily

under the same current setting in A. Note that the shape of the load profile is essential for SOC. Furthermore the randomization of the SF accompanies probabilistic variations of the SOC. Using the more complicated load profile leads to very similar results, hence they are not plotted here.

Figure 5.17 plots the results when applying a 15 min. sampling interval. NILL provides the highest and the SF the lowest levels of SOC. In general compared to the one-second interval the SOC is smaller ranging from about 55% to 82% roughly. As Figure 5.5 demonstrated the variation of SOC increased remarkable when changing from a one-second sampling interval to 15 min. Therefore, the battery will not longer remain at high levels of SOC for longer periods any more.

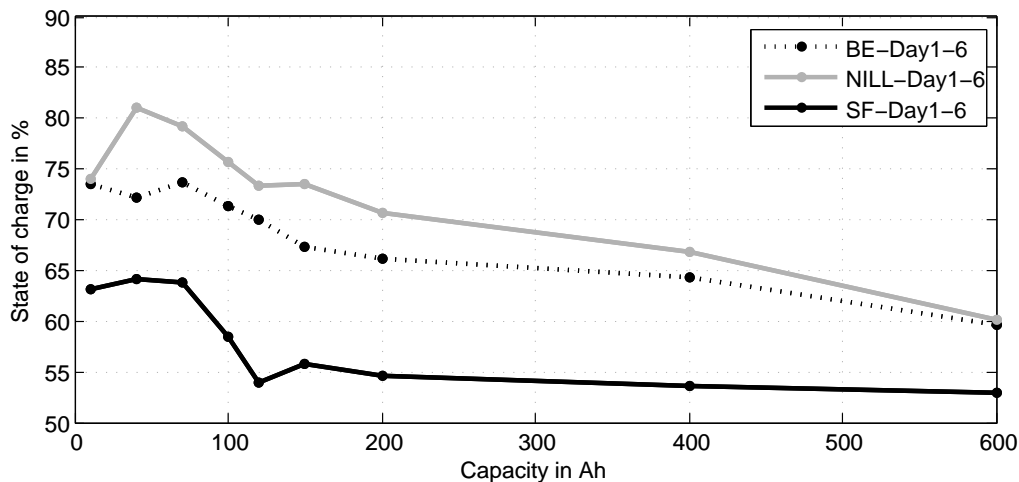


Figure 5.17: SOC using a sampling interval of 15 min.

5.1.6 Implementation

It cannot be ruled out that an implementation of a BLH system already exists, however during the course of this work no such a system could be identified. Hence, it may be of interest to explore the availability of the necessary components of a BLH system. Aside from the battery system, the most important components are the inverter and the charger which must be remotely controllable.

The following list shows companies that offer programmable inverter/charger-combinations are well known for their battery charging devices. These companies were contacted by mail to ask for devices that meet the specifications for the implementation of a BLH system (status: November 2013).

- Fronius International GmbH, contact person: Thomas Schuller: Fronius does not offer products with the required specifications thus far, but they have scheduled the development of such a device for their product portfolio for the end of 2014

- Mastervolt GmbH, contact person: Stefan Haslinger: Mastervolt forwarded the request to the local distributor DOMA elektroengineering GmbH. They did not reply to our request, instead they sent an offer for a inverter/charger-combination
- Sinergex Technologies L.L.C.: no reply
- Solar Business of Schneider Electric SA (formerly Xantrex Technology), contact persons: Azra Fadaee and Sandra Herrera: Schneider Electric offers inverter/charger-combinations with a communications device that allows some remote configurations and readings via a web interface but no complete remote control
- SMA Solar Technology AG: no reply
- Studer Innotec SA, contact persons: Serge Remy and Eric Werfeli: according to the contact persons, the Xtender series meets all requested specifications and allows complete remote control via RS-232 using Xtender serial protocol which is documented properly. Studer Innotec provides not only some example byte streams to program the device but also a command line tool named scom.exe that helps implementing the protocol.
- TBS Electronics BV, contact person: Daniel Schouten: in principle TBS Electronics offers programmable inverter/charger-combinations but the devices may be too slow for BLH systems. For example the devices require about 5 s to change from inverting to charging mode due to a build in stability check of the grid and besides that the charging current increases very slowly (it takes about 5-10 s to reach a stable state). Hence realtime remote control is not feasible.
- Victron Energy B.V., contact person: Ruurd ten Brink: no reply

An incomplete assortment of devices with the combined function of a inverter and a charger of different manufacturers with nominal output powers between 500 and 7000 VA (without the parallel connection of devices) is listed in Table 5.2. All of the devices are capable of being connected to the ENTSO-E¹ grid of 50 Hz. *Data from/to PC* should describe the possibility to read in data from measurements and to send various basic settings from the PC to the inverter/charger combination via a communications device. A basic setting includes the battery type, voltage level, max. charging current, the load strategy, etc. *Fit for BLH* describes the capability of a complete remote control of the device meeting the specifications for BLH systems. Some of the devices such as the ones from Mastervolt, Sinergex and SMA allow the use of remote panels to read and write data to and from the device using their own bus systems. The Xantrex Technology devices (while Xantrex is part of Schneider Electric, they have their own web presence) are not listed as they just provide systems for 60 Hz grids.

There is only one device that fulfills all specifications: the Xtender series of Studer Innotec, a company seated in Switzerland. A request for a list of examples that use

¹ENTSO-E: European Network of Transmission System Operators for Electricity

Device	Manufacturer	Data from/to PC	Fit for BLH	Interface
Compact	Studer Innotec			
Conext SX4024-230-50	Schneider Electric	X		RS485, LAN
Easy Plus 12/1600/70	Victron Energy			
Fusion	Sinergex Techn.			
Mass Combi	Mastervolt	X		RS232
Multi Plus 800VA-5kVA	Victron Energy	X		RS232, USB, NMEA 2000
Powersine	TBS Electronics	X		RS232, USB
Sunny Island 6.0H	SMA			
Tripp Lite APSX2012SW	Tripp Lite			
Xtender	Studer Innotec	X	X	RS232

Table 5.2: Assortment of charger/inverter-combinations

the Xtender serial protocol that allows remote control as well as a request for a quote remained unanswered.

5.2 Load-Based Load Hiding

This section deals with the results when applying a LLH system instead of the BLH system. Compared to the previous chapter there is an essential difference when analyzing the results. Whereas all BLH algorithms try to maintain a constant level of the metered load, the LLH algorithm tries to make the metered load even more noisy. Therefore the metric RFM in particular may no longer be significant. A sampling interval of 15 minutes will not be considered as the only meaningful metric is the F-measure, which only works properly with a one-second interval and the simplified load profile.

The parameter setup of α , σ and P_{max} is based upon some preevaluations. P_{max} is set to 1600 or rather 2300 W depending on the distribution function, α was set to 0.1, 0.3, 0.5, 0.7, 0.9, 1.3 and 1.8, but the most desirable results accompany α set to 1.8 and 0.7 depending on the time frame that describes the time the boiler's load is held constant. σ was set to 300 W, 800 W, 1200 W and 1600 W but 300 W and 800 W provided the best results.

Proposing a LLH system, this work does not aim to determine the ideal LLH algorithm but to provide a first attempt to analyze the potential of a LLH system.

5.2.1 Net Demand vs. Metered Load

Figure 5.18 plots net demand and the metered load after applying a LLH system using an underlying truncated normal distribution for day 1 with $P_{max} = 2.3 \text{ kW}$ and $\sigma = 800 \text{ W}$. The boiler's load is always held constant for 60 s and the target energy consumption (of the boiler) is set to 5 kWh.

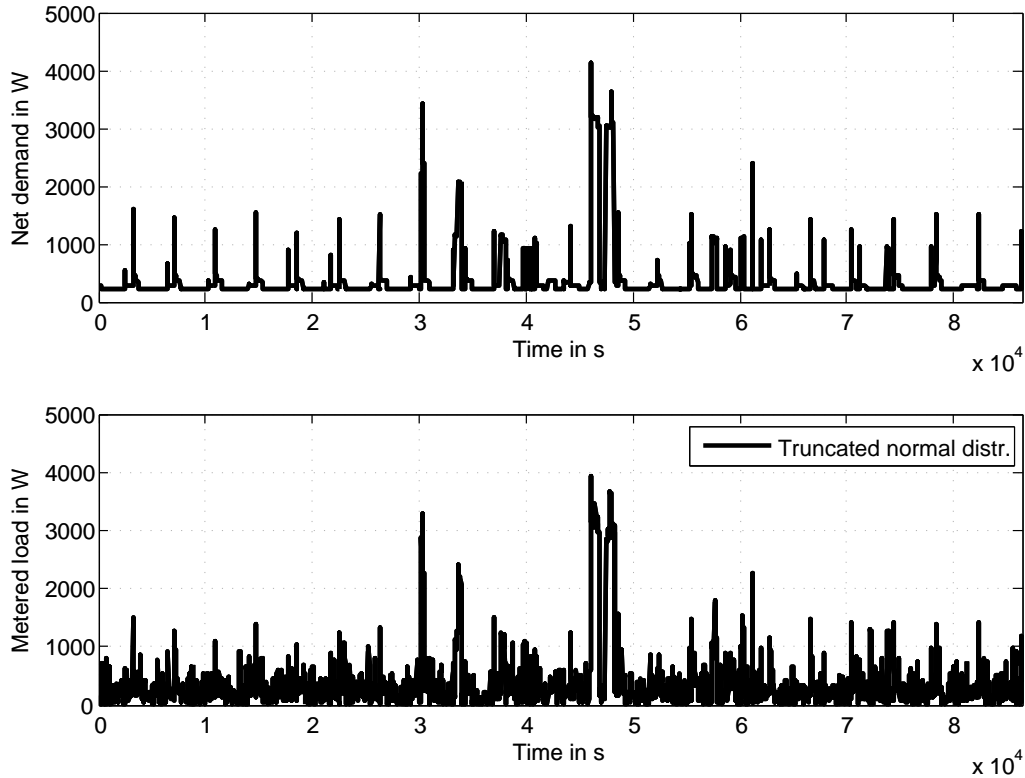


Figure 5.18: Net demand and the metered load using a truncated normal distribution (simplified load profile)

Net demand has an offset of 208.3 W which equals a constant load that yields in an additional consumption of 5 kWh per day to balance the energy consumption of net demand and the metered load. When looking at the metered load, smaller peaks disappear in the superimposed noise generated by the truncated normal distribution. As the boiler cannot supply energy, the minimum load of net demand cannot be reduced and clearly remains visible. Furthermore higher peaks appear almost as clear as without a LLH system.

Similarly Figure 5.19 plots the same situation when using the beta distribution ($P_{max} = 2.3 \text{ kW}$, $\alpha = 0.7$) or the modified beta distribution ($P_{max} = 1.6 \text{ kW}$, $\alpha = 0.9$).

While the results of the beta distribution look similar to the truncated normal distribution, the results of the modified beta distribution is distinguished from the others as it is less noisy. Furthermore, there are readings where the minimum load is clearly temporarily offset. For example such a situation can be observed at approximately 52000 s

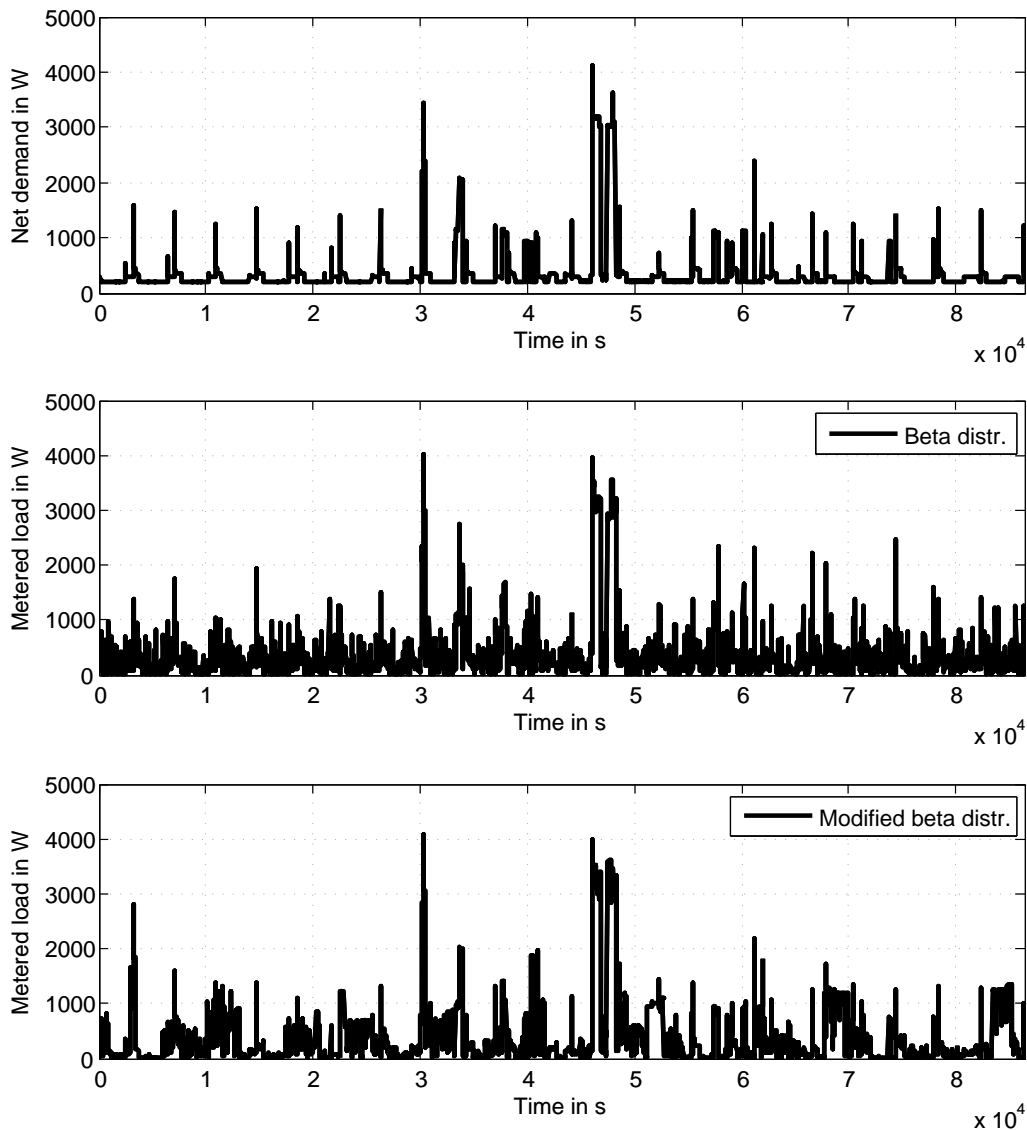


Figure 5.19: Net demand vs. metered load using different beta distributions (simplified load profile)

where net demand is relatively low but the metered load is at levels of about 1 kW. Furthermore, there are situations where the metered load is alike net demand as the noise produced by the modified beta distribution can occasionally be very small to maintain the target energy consumption at the end of the day. Thus, there may be time frames where the level of distortion is very low but on the other hand there are periods where the difference between net demand and the metered load is significant.

This may be beneficial as the NILM algorithm uses filters to pre-process the data before decomposition. The NILM input is always a filtered load profile using some kind of filter such as a median filter. Figure 5.20 plots the results after running a one-dimensional median filter with a window size of 360 s. When applying the filter,

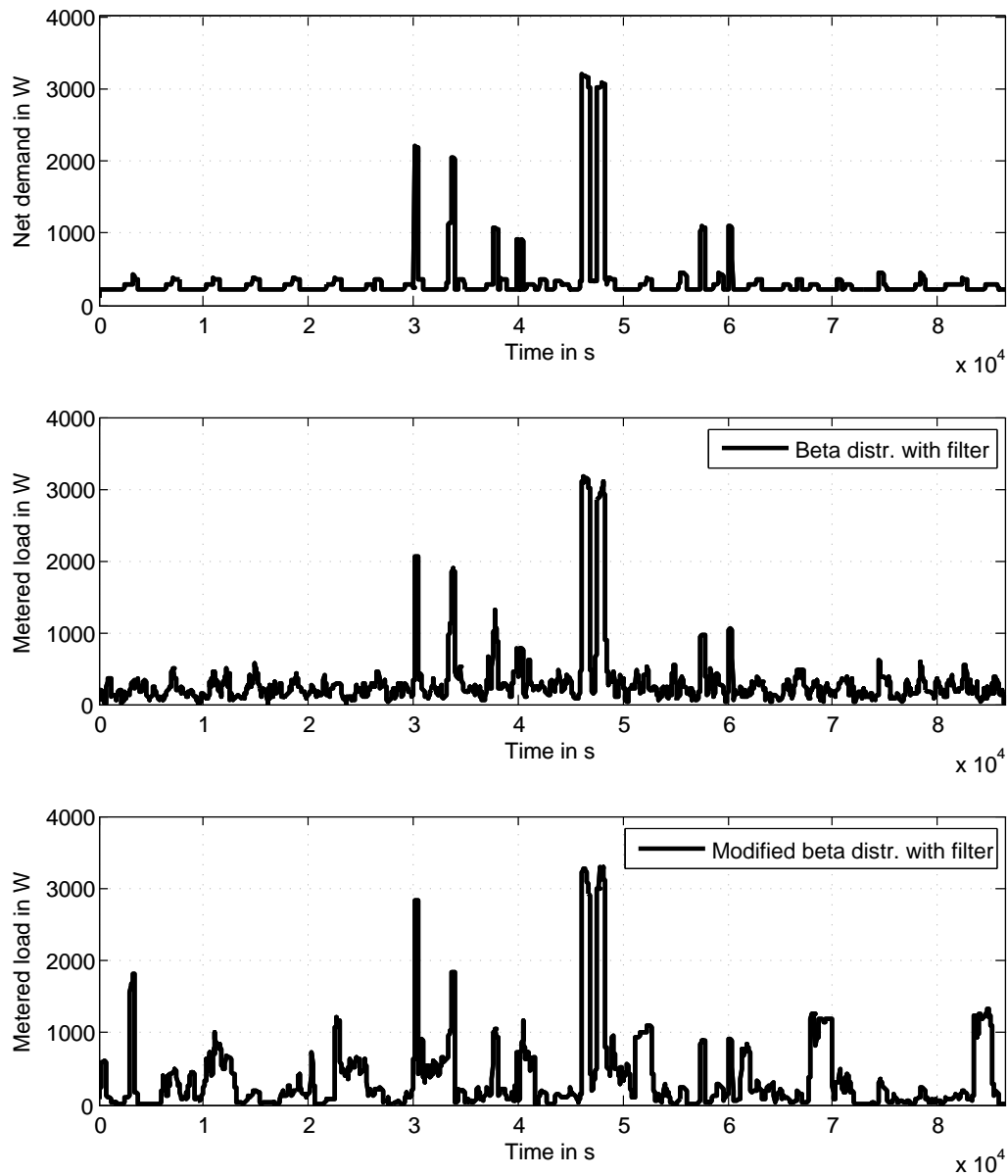


Figure 5.20: Filtered net demand and metered load using different beta distributions (simplified load profile, median filter)

less distinct peaks in net demand disappear but the artificial noise based on the beta distribution adds additional variations. In comparison the modified beta distribution creates noise that seems to be more significant with a number of much higher peaks. This may decrease the total success rate of the NILM algorithm. Therefore, none of the distributions succeed in hiding the higher peaks, and they may potentially even raise these peaks as the LLH system does not take the actual level of net demand into account.

5.2.2 Load Configuration

This section deals with the effect of varying the boiler's target energy ranging from 2.5 kWh to 10 kWh and the effect when increasing the time the boiler's load is held constant in a range from 1 s to 120 s. The following results are based upon averaging 6 days.

Figure 5.21 plots the F-measure of the NILM algorithm for different distributions over different target energy consumptions. The time frame where the boiler's load is held constant is set to 30 s. The distribution parameters are $P_{max} = 2.3 \text{ kW}$, $\sigma = 300 \text{ W}$ for the truncated normal distribution, $P_{max} = 2.3 \text{ kW}$, $\alpha = 0.7$ for the beta distribution and $P_{max} = 1.6 \text{ kW}$, $\alpha = 0.9$ for the modified beta distribution.

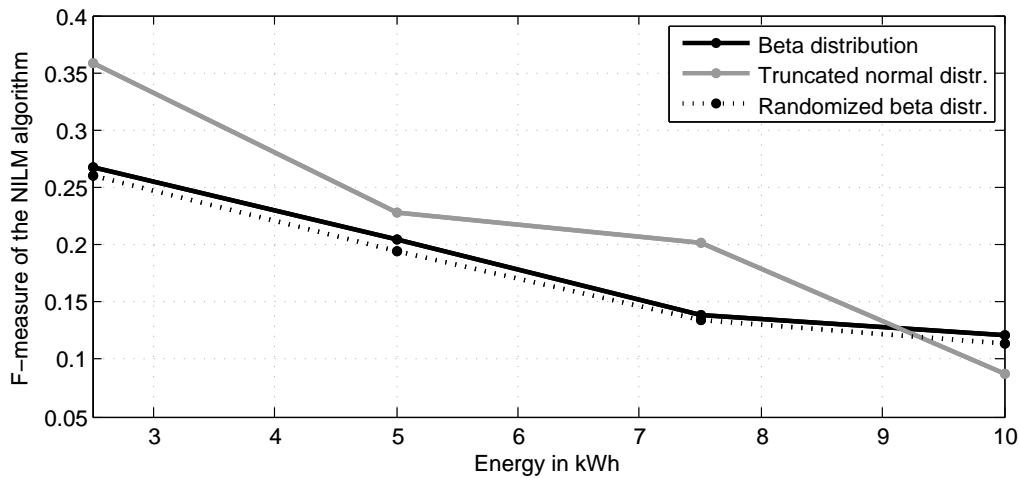


Figure 5.21: F-measure when holding the boiler's load constant for 30 s respectively

A downward trend is clearly visible as with higher energy consumption the amplitude of the artificial noise can be set much higher, therefore the distortion level increases. A saturation process is slightly visible beginning at 5 kWh. Aside from the 10 kWh level the randomized beta distribution provides the best results, the truncated normal distribution the worst. All 3 distributions provide F-measures of less than 30% for 5 kWh or beyond.

Increasing the time frame to 120 s yields the results plotted in Figure 5.22. In this case the truncated normal distribution performs best. Again there is a downward trend and a minor saturation process. The parameter setup is $P_{max} = 2.3 \text{ kW}$, $\sigma = 800 \text{ W}$ for the truncated normal distribution, the parameters of the beta and the modified beta distribution are the same.

The metric RMSE is diagramed in Figure 5.23 for using a time frame of 60 s. The parameters remain the same as with 30 s. The precise upward trend is almost linear for all distributions. Doubling the target energy from 2.5 kWh to 5 kWh does not duplicate the RMSE, suggesting that the level of privacy protection is already saturated. In general, the results of the F-measure and RMSE are similar, a higher target energy

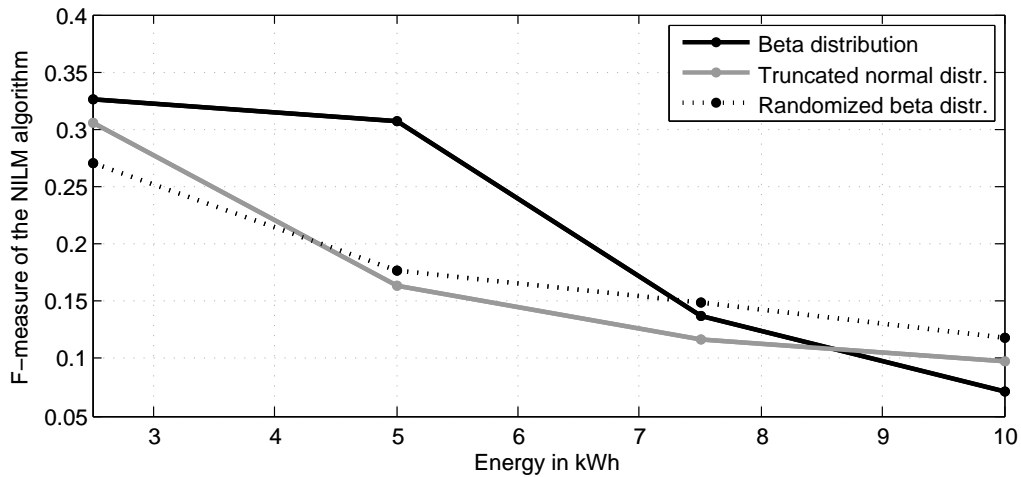


Figure 5.22: F-measure when holding the boiler's load constant for 120 s respectively

consumption increases the level of privacy protection but there is a small saturation process noticeable.

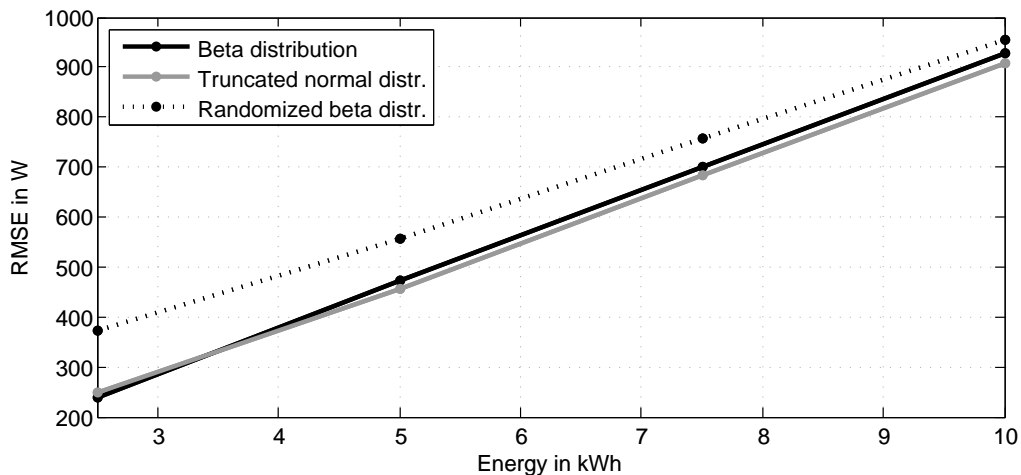


Figure 5.23: RMSE when holding the boiler's load constant for 60 s respectively

The idea of using a variety of time frames where the boiler's load is held constant should analyze potential improvements of the performance of the distributions. Figure 5.24 plots the F-measure for different time frames using the truncated normal distribution. The parameter setup is $P_{max} = 2.3 \text{ kW}$, $\sigma = 300 \text{ W}$ for 1 and 30 s and $P_{max} = 2.3 \text{ kW}$, $\sigma = 800 \text{ W}$ for 60 and 120 s. Aside from the expected downward trend the diagram suggests a longer time frame to increase the efficiency of the distribution. However, note that an even higher time frame may simplify the learning process of the NILM algorithm to filter the current load of the electric boiler.

In addition, analyzing the beta distribution over a longer time from does not necessarily provide more accurate results, as illustrated in Figure 5.25. Therefore, the proper

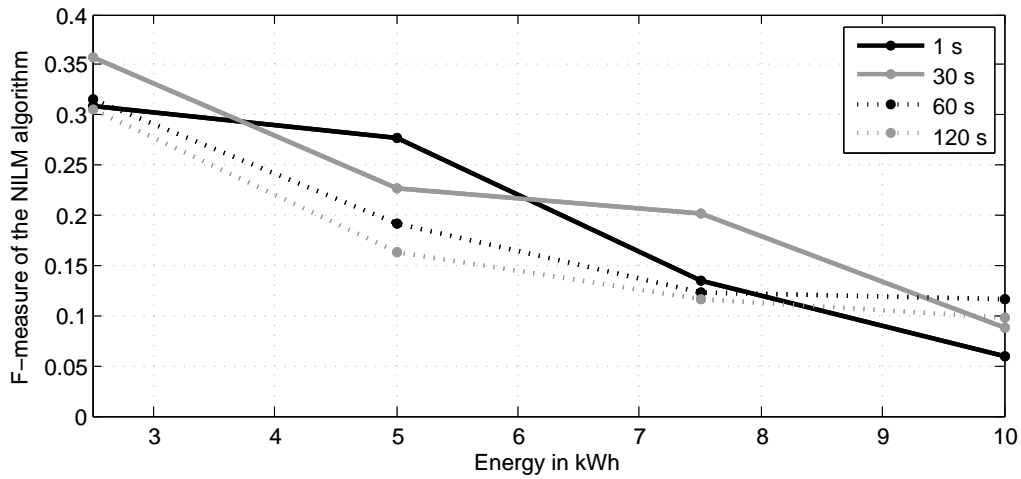


Figure 5.24: F-measure of the truncated normal distribution to analyze different time frames where the variable load is held constant

time frame depends on the distribution. Considering 1 s, 30 s, 60 s and 120 s, for a target energy consumption of 5 kWh the ideal time frame for the truncated normal distribution would be 120 s and 60 s for both of the beta distributions. The parameters are set to $P_{max} = 2.3 \text{ kW}$, $\alpha = 0.7 \text{ W}$ for 30, 60 and 120 s but $\alpha = 0.9$ for 1 s.

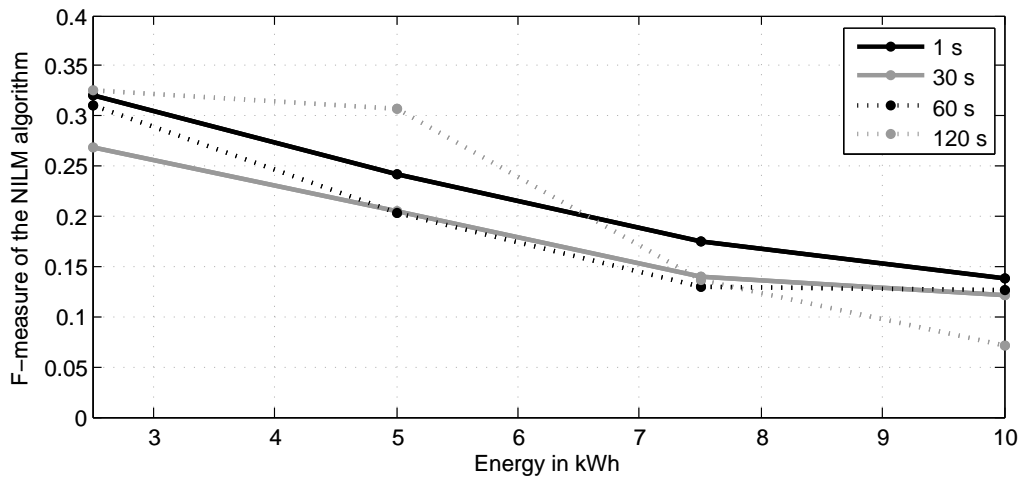


Figure 5.25: F-measure of the beta distribution to analyze different time frames where the variable load is held constant

All three distributions are based upon a target energy consumption of the electric boiler. As the distribution functions are based upon probabilities there is only a certain probability of reaching the exact target level. The probability of missing the target level increases if the time frame or the target level itself increases. Furthermore the modified beta distribution adjusts the expectation which yields in an even higher spread of data.

Figure 5.26 plots the histogram for all 6 days analyzed considering all 3 distributions, all 4 energy targets and all of the time frames analyzed (without any averaging). The larger part of the spread lies within the interval $\pm 1 \text{ kW}$. There is a positive skew of the distribution observable that is caused by the overrated expectation of the modified beta distribution. Thus, especially the modified beta distribution yields in realizations that outrun the target level.

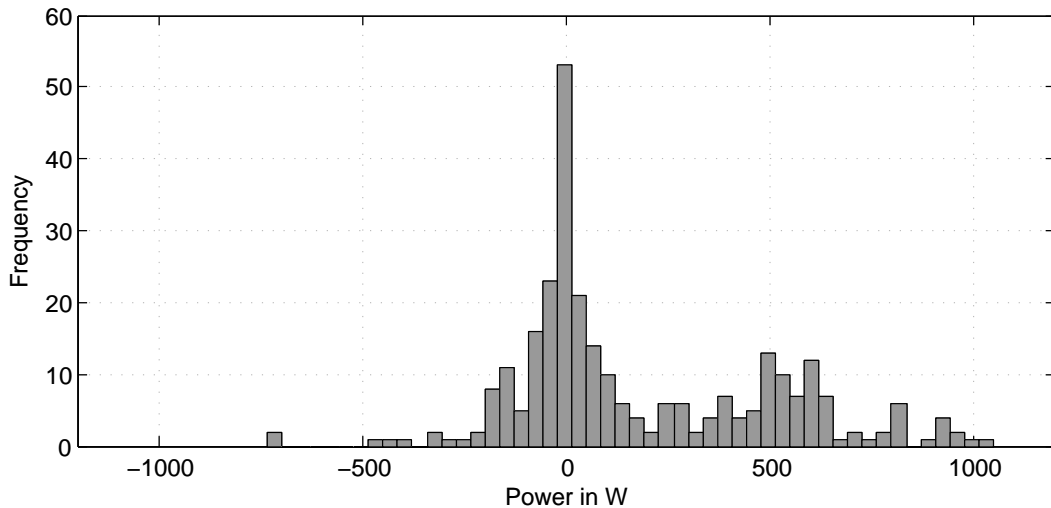


Figure 5.26: Histogram of the gap between the realized and the target energy consumption

5.2.3 Implementation

As with a BLH system, the implementation of a LLH system could be of interest. The essential parts when implementing such a system using an electric boiler are the boiler itself and an electronic device that allows to set the voltage level that is remotely controlled by a control system.

The first question when implementing such a system is whether an electric boiler allows for the adjustment of the voltage level or rather the power consumption. Without power control, an overview of load profiles in literature [53], [55] suggests that an electric boiler that is turned ON usually consumes constant power. Salehfar [42] models an electric boiler which allows for power control in a specific range but without considering the implementation of such a system. More practical is a paper proposed by Jia [67] that takes benefit of the structure of the North American power grid that bases on a split-phase electricity distribution system. Such a system allows for the switch between 110 V and 220 V when using two live conductors instead of a single-phase to grounded neutral setup.

Mr. Friedrich Stocker, an engineer of the Austrian boiler manufacturer Austria Email, confirmed that power controlling would be possible with regards to the boiler. According to Mr. Stocker the boiler acts as a purely resistive load that allows voltage control without

harming the boiler's lifecycle. He suggests the use of a phase-fired thyristor control to adjust the voltage level.

Devices such as the M028 power control provided by Kemo Electronic GmbH are very common and allow for power controlling up to 2.88 kVA [7].

Note that such phase-fired controllers may stress the electricity system with peak currents whereas a BLH system may unburden it as it tries to minimize peak loads in general. For further research such effects should be taken into account.

6 Comparison and Discussion

The previous chapter presented the results of the simulation process upon which this work is based. This section deals with further analysis and the discussion of the results and moreover the comparison of both load hiding approaches.

6.1 BLH Battery Setup

When implementing a BLH system one key element is the dimensioning of the battery system. Figure 6.1 plots the F-measure over the battery's capacity. As always, when deriving the F-measure the load profile is the simplified one and the results are based on the 6 day mean. There is a clear saturation process starting at 120 Ah. As a tradeoff between privacy protection and costs, not only of the battery but also of the inverter/charger combination, choosing a 120 Ah battery for this specific case seems to be reasonable.

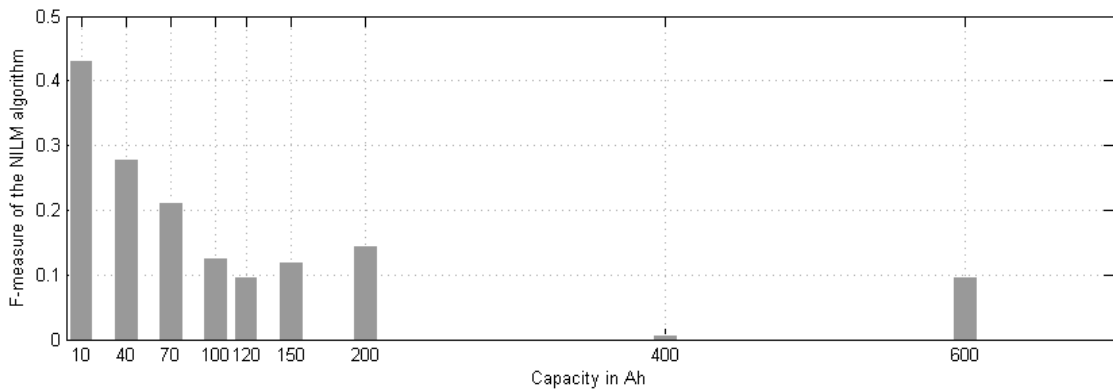


Figure 6.1: F-measure over different capacities using the SF, 6 day average

Figure 6.2 illustrates the comprehensible effect of an uptrend of the F-measure if the daily energy consumption increases when using SF for days 1 to 6. If demand increases, the obfuscation potential of the battery system decreases which results in a higher success rate of the NILM algorithm. A 120 Ah battery has a capacity of approximately $12 V \cdot 120 Ah = 1.44 kWh$. Day 3 has an energy demand of 2.5 kWh and the F-measure is below 5 %. Day 6 requires 3.68 kWh, which is more than twice the battery's capacity. Compared to day 3 (2.5 kWh) the success rate increased remarkable up to 20 %, but is still less than one third.

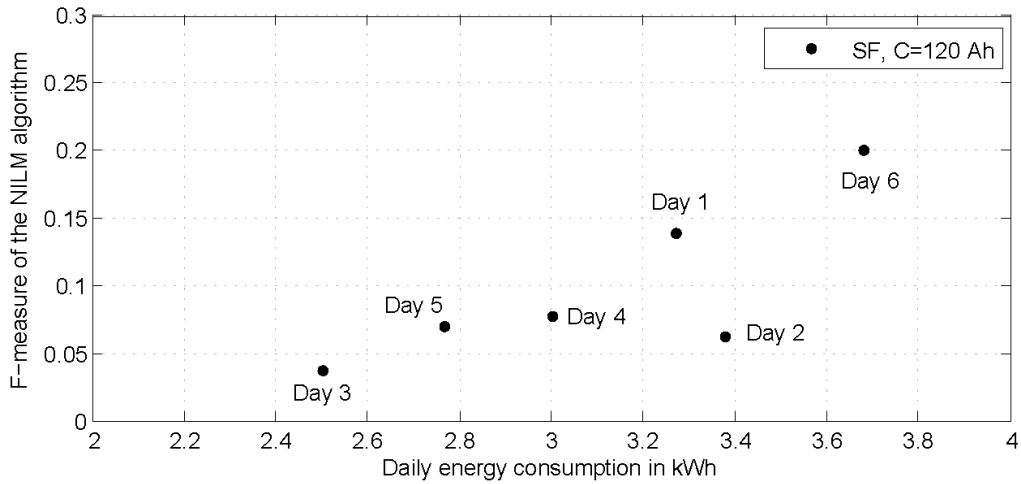


Figure 6.2: F-measure when using a 120 Ah battery and SF for 6 days

Another parameter that may influence the results is the empirical variance. If the variance would be 0, the metered load would already be constant which necessitates no further obfuscation system. A load profile with many high peaks, which results in a higher variance, may make it difficult to turn the load profile into a constant load. Conversely, the detection of the appliance's states may be more difficult for the NILM algorithm as well. The outlier at 3.38 kWh, which is day 2, has the highest empirical variance of the metered load of $2e+3 \text{ W}^2$ compared to $1.9e+3 \text{ W}^2$ for day 6 or $1.6e+3 \text{ W}^2$ for day 3, which supports the idea that a higher variance may reduce the success rate of the NILM algorithm. Furthermore day 4 with 3 kWh has a higher empirical variance ($1.8e+3 \text{ W}^2$) compared to the neighbour day 5 ($1.5e+3 \text{ W}^2$) and the same empirical variance as day 1.

The number of samples is far too limited for any kind of significant inference but with regards to the results a battery that can supply half of the daily energy may provide a satisfying privacy protection.

It is the current rating rather than the capacity which appears to be more significant. Averaging all 6 days, Figure 6.3 plots the F-measure when using a constant current rating of $0.3C$, but different capacities (10, 40, 70, 100, 120, 150, 200 Ah). The abscissa plots the F-measure when using a constant capacity of 120 Ah but different current ratings ($0.025C$, $0.1C$, $0.175C$, $0.25C$, $0.3C$, $0.375C$, $0.5C$). Hence, when considering the abscissa and the ordinate the maximum currents in Amps are the same, to analyze the significance of the capacity vs. the current rating.

If the battery size has no influence to the success rate of the NILM algorithm the F-measures should be the same in both situations. This is illustrated by the grey line with a gradient of 1. As all of the results are very close to that line and there is no obvious trend observable this suggests that the dimensioning of the battery is not essential. When analyzing the F-measure over a variety of capacities like it is plotted in chapter 5 the F-measure decreased significantly as the capacity increased. With regards to the

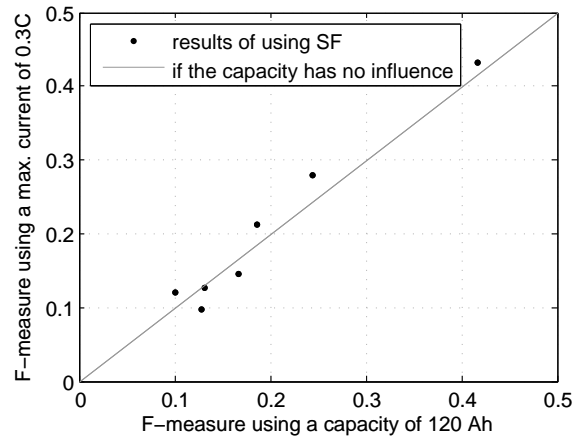


Figure 6.3: F-measure to compare the significance of the maximum current setting vs. the capacity

missing significance of the battery capacity, here this dependency can be attributed to the maximum current rating in A that changes with the battery capacity. In sum, the current ratings appear to be significant while the battery's capacity does not.

Inspired by [70] this work assumed the use of a deep-cycle lead acid battery. When observing the actual levels of the SOC, a high share of a fully charged battery can be observed. Conversely, situations in which the battery is fully discharged occur rarely and only when using high capacities of 400 Ah or more. This suggests that the use of a deep-cycle battery that allows a high DOD may not be necessary, a common car battery may provide a satisfactory performance. In addition, the algorithm's performance suffers in cases where the battery is fully charged especially when using BE- or NILL algorithm. Furthermore the level of SOC at the end of the day is consequently higher than the initial value. Hence the initial value of 55% was set too low.

Figure 6.4 plots the aggregated histogram of the battery's SOC for all 6 days analyzed when using a 120 Ah battery and SF.

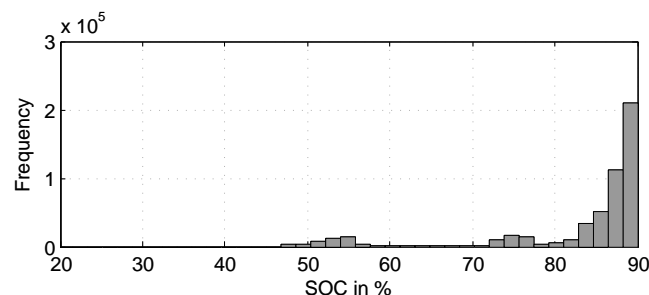


Figure 6.4: Histogram of the SOC when using a 120 Ah battery and SF for days 1 to 6

6.2 BLH Algorithms

This work applied three different BLH algorithms. All algorithms attempt to flatten net demand to provide a constant metered load.

The Best Effort algorithm idles the battery if the SOC is too high or too low, otherwise it always attempts to maintain a constant metered load by using the battery as a supplier or a load. If the battery cannot provide enough power, the battery charges or rather discharges with its maximum power anyway.

In contrast, the Non-Intrusive Load Leveling algorithm is much more complicated and distinguishes between 3 states of which the favored one is the stable state which is based upon the weighted average of the previous states. Based upon certain parameters the algorithm switches from one state to another if the SOC limits were to be violated. The NILL algorithm allows for some modifications of the parameter, this work is based upon the settings as proposed in [70] and [74].

The Stepping Framework is based upon quantizing net demand into a step function. The authors of the SF [74] propose several different approaches in reaching this target. The authors state that the best results are reached with *Lazy Stepping 2* which sets the actual step randomly, therefore this work considered this approach as the substitute of the SF.

The implementation of the BE algorithm and the SF would be much easier than the NILL algorithm as they do not necessitate extra calculations based upon previous states. Thus, the NILL algorithm requires some kind of memory whereas BE algorithm and the SF solely set the battery power based on the actual level of net demand and the SOC and current limitation of the battery.

Figure 6.5 plots the F-measure to compare all 3 algorithms using a 120 Ah battery.

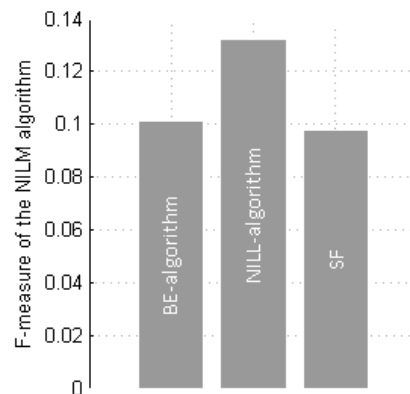


Figure 6.5: F-measure to compare all 3 BLH algorithms using a 120 Ah battery

As already discussed in chapter *Results*, the choice of which algorithm performs best is rather murky. In analyzing the F-measure, the NILL algorithm performs worst most often, Yang et al. [74] argues the same using other metrics. In general the SF performs

slightly better than BE, but the difference may not be significant. This inference holds for both when summarizing all results but also when throwing a glance onto this diagram that plots the situation for 120 Ah solely.

However the F-measure is based upon the decomposition of a specific NILM algorithm that uses state estimation but not edge detection. Therefore, RFM may be of interest as RFM is the only metric used in this work that takes load changes directly into account. Figure 6.6 plots the results for a 120 Ah battery. As with the F-measure, the results are the 6 day average. The performance of the SF is distinctly and visibly the most desirable. When using the simplified load profile (7 devices) or the higher sampling rate of 15 min. the RFM is higher as the number of load changes in net demand is significantly lower compared to the normal load profile (21 devices).

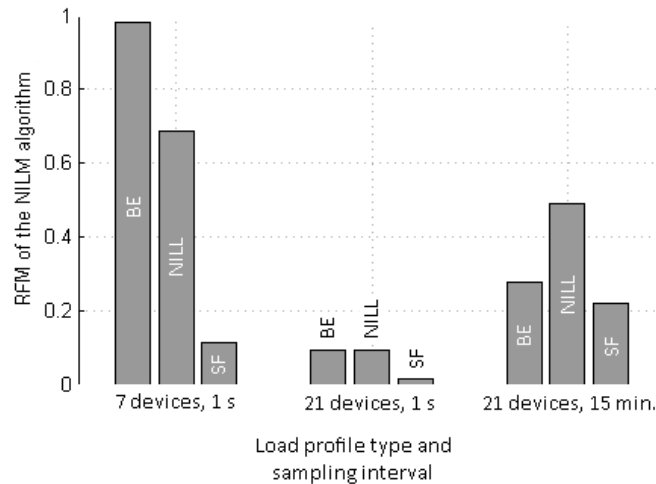


Figure 6.6: RFM of all 3 BLH algorithms for different load profiles using a 120 Ah battery

Note that the F-measure is not necessarily the best metric to describe the effectiveness of the NILM algorithm. Imagine a device such as an energy-intensive dryer that is turned OFF most of the time. If the algorithm estimates the appliance's state to be OFF all the time, the success rate, hence the F-measure is quite high. Even though the F-measure suggests a well performing algorithm, the information when the device is turned ON is completely lost. This information could be of particular interest, for example under a time-based electricity pricing scheme when using a program that recommends how to cut the electricity bill by changing the time of operation. Furthermore, when analyzing a smaller load like a smartphone charging device, the ON/OFF-states may be misjudged most of the time which results in a small F-measure. When calculating the overall F-measure, the smaller significance of the charger to the aggregated load profile will not be considered. Whereas the energy consumption of the dryer may be much higher than the consumption of the smartphone charger, the F-measure assumes all appliances to be comparable and does not consider different energy consumption levels. Therefore, it

may be meaningful to use an energy-based-weighting process or another metric.

6.3 LLH Algorithms

As a first proposal of a LLH system, various distributions that produce artificial noise were analyzed.

When analyzing 5 kWh as diagrammed in Figure 6.7 the modified beta distribution performs best while the common beta distribution performs worst. The parameter settings of the distribution were already described in chapter 5. Increasing the time frame where the boiler's load is held constant increases the level of privacy protection, hence it may be clever to test even longer frames, however then it may become easier to detect the boiler's actual load.. The best single result for 5 kWh accompanies with the truncated normal distribution using a time frame of 120 s.

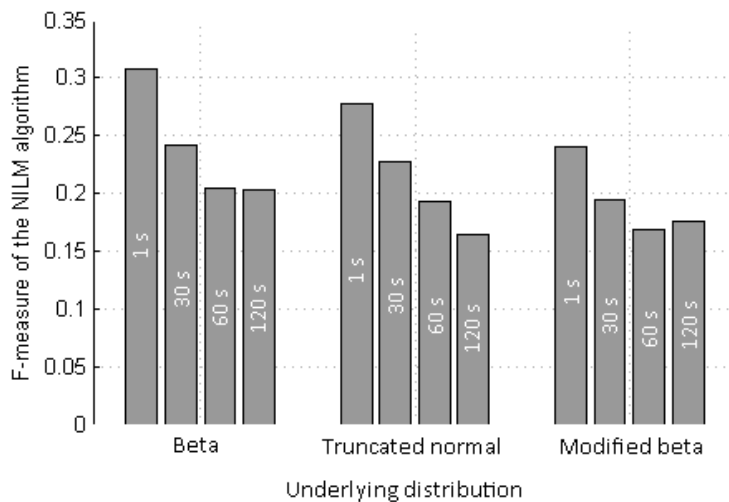


Figure 6.7: F-measure of different PDFs for an energy target of 5 kWh

Picking out the best results of each distribution leads to Figure 6.8. The best single result of 5.9% is provided by the truncated normal distribution for a target energy of 10 kWh. Whereas for a smaller energy target the modified beta distribution outperforms the common beta distribution the opposite happens for high energy consumption. In general, there is no clear evidence of which distribution performs best as it also depends on the daily energy target.

Implementing the beta distribution is easier than implementing the truncated normal distribution that requires an iteration process to meet the target energy. The modified beta distribution requires several randomization steps and the probability to outrun the target energy level is high in comparison to the other distributions.

As with BLH systems, the efficiency of a LLH system may decrease as the customer's net demand increases.

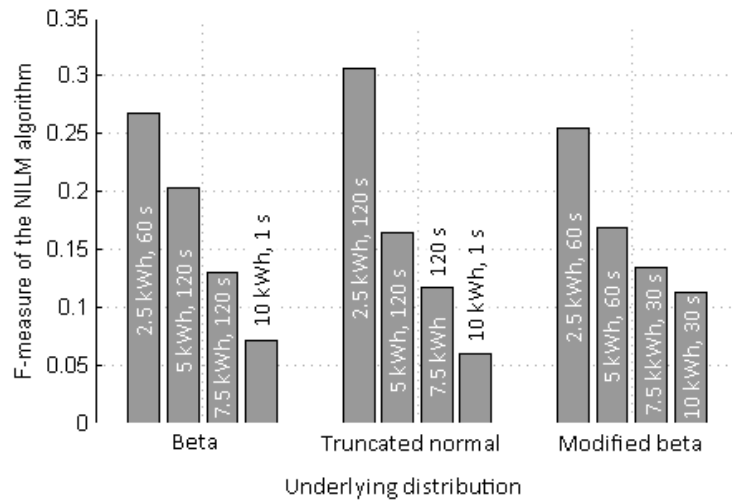


Figure 6.8: F-measure over a target energy for different LLH algorithms

6.4 BLH vs. LLH

When discussing methods to improve privacy protection via a load hiding system the question arises as to which one of the systems can provide better results. The metric RFM cannot be used for a comparison as the BLH and the LLH system follow different approaches to distort net demand.

Figure 6.9 plots the F-measure for the original time series of net demand, the best result of the LLH system and finally the best result of the BLH system for a 120 Ah battery.

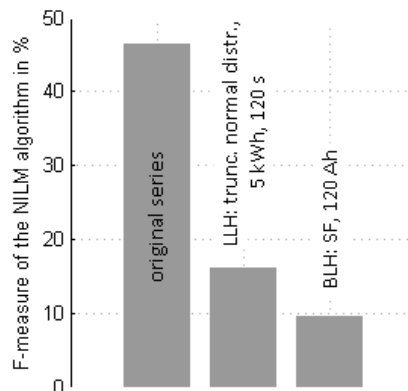


Figure 6.9: F-measure of the BLH (120 Ah battery) and LLH system (5 kWh target energy consumption)

With regards to LLH the plot assumes a daily target energy consumption of 5 kWh. Compared to the original series (46.6 %) the LLH system decreases the success rate of

the algorithm to about one third (16.4%) whereas the BLH system provides an even better performance of almost one-fifth (9.8%).

Figure 6.10, a plot of the RMSE for the same setup suggests that LLH can provide better results than BLH does.

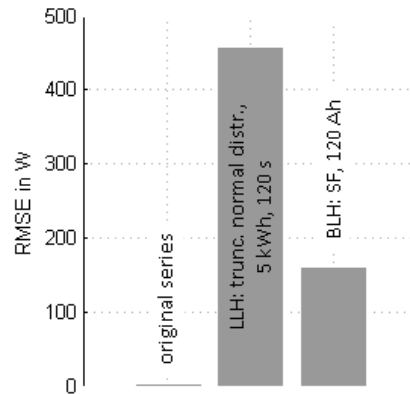


Figure 6.10: RSME of the BLH (120 Ah battery) and LLH system (5 kWh target energy consumption)

The reason for the improvement is that the LLH system can distort net demand by 5 kWh whereas the BLH system uses less energy. The BLH system could use the (usable) battery's energy of about $0.7 \cdot 120 \text{ Ah} \cdot 12 \text{ V} = 1.01 \text{ kWh}$ numerous times. The problem is that the BLH system remains at a high level of SOC most of the time, therefore the total energy that is stored into the battery plus the energy supplied by the battery is less than 5 kWh. Summing up the absolute value of the battery's energy consumption and supply yields in sort of an energy turnover of the battery. The 6 day mean of this turnover is about 2.18 kWh which is clearly less than the 5 kWh of the LLH system. Hence the LLH system can take benefit of the high energy consumption of the electric boiler, but either way the system was not able to provide a higher level of privacy protection when applying the NILM algorithm.

Finally Figure 6.11 plots the F-measure when looking for the best 6 day average results of BLH and LLH. BLH clearly outperforms LLH.

When comparing the expenses, the LLH system clearly outperforms BLH. Both the installation and maintenance costs of the BLH system exceed those of the LLH system. Whereas BLH necessitates a battery, some measuring units, an inverter/charger-combination and finally a controlling unit, the LLH system requires a variable load that could already be installed, an electronic device that allows for an output voltage or power level setting and finally a controlling device with some inputs of the electric boiler.

Neither the BLH system nor the LLH system can provide perfect privacy protection under a realistic setup. Under the assumptions (5 kWh target energy for LLH, 120 Ah battery for BLH) both systems are able to decrease the success rate of the NILM algorithm by about two-thirds or even more. A detection rate of about one third may

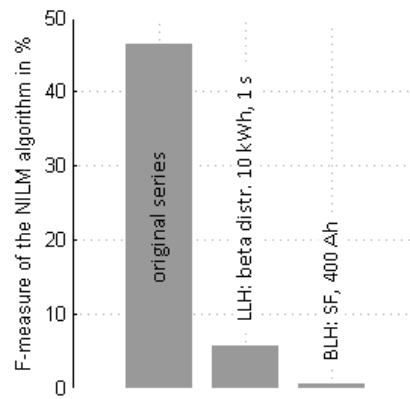


Figure 6.11: F-measures of the best results of the BLH and LLH system

already be satisfying as decomposing the appliance's states under such a quality of result is doubtful.

7 Conclusion and Outlook

This work presented various load hiding systems that could possibly prevent the invasion of an end-user's privacy after the installation of smart metering. State-of-the-art systems use a battery with an intelligent control system to charge and discharge the battery at strategic times. This allows for the flattening of the end-user's electricity demand. Therefore, three meaningful algorithms have been proposed thus far. Based on a simulation model, this thesis applied all three algorithms and quantified the effectiveness using the accuracy of a proper NILM algorithm to disaggregate the load profile. In addition, several related issues such as the battery dimensioning were discussed. Furthermore, an alternative solution of a load hiding system was suggested.

Summarizing the results, the latest proposal of a BLH algorithm named Stepping Framework performs best, and the NILL algorithm produced the worst results. The key factor when dimensioning the battery is the maximum charge/discharge rate of the current rather than the battery's capacity. A battery that provides approximately half of the user's daily energy consumption showed to be a novel tradeoff between battery size i.e., costs and privacy protection. In our case, a single 120 Ah, 12 V lead acid battery would have provided a sufficient level of privacy protection. Furthermore based on the high level of the battery's state of charge most of the time, the use of a deep-cycle battery would not be necessary, an ordinary automotive battery could provide a satisfactory performance and lifecycle. Even though the implementation of a BLH system may not be economically justifiable at the moment, all of the components that are required to build such a system, i.e. battery, inverter/charger-combination, measuring units and a controlling device are already readily available.

In order to develop a meaningful and more affordable alternative to BLH, this work further proposed a new load-based load hiding system. Such a LLH system adjusts the power level of a variable load like an electric hot water boiler to modify the domestic load profile. Whereas the BLH systems attempt to maintain a constant level of the metered load, the proposed LLH system attempts to superimpose artificial noise to make the load profile more chaotic. To produce this noise, three different underlying probability density functions were suggested and analyzed. There is no clear trend which one performs best, but the success rate of the NILM algorithm that decomposes the load profile can be reduced to about one third compared to the original time series of net demand. Compared to a BLH system the implementation of such LLH is easier as it requires only a variable load, a voltage/power-controller and a controlling unit without measuring net demand.

Finally a benchmark showed that the BLH system outperforms the LLH system. Clearly none of the systems will be able to provide a perfect level of privacy protection. The level of privacy protection may be more satisfactory if combined with other privacy

protection approaches such as anonymizing, aggregating and encrypting the end-user's data.

The following questions may be the subject of further research. Aside from the real implementation of load hiding systems, the combination of a BLH system with a photovoltaic system could be interesting. Furthermore, taking three-phase currents into account and analyzing more than just 6 days of data using a proper metric would help providing more significant conclusions. Setting the initial SOC more accurately, further research regarding potential savings, and the potential to unburden the electricity grid may help reducing the expense of installing such a system. Alternative storage units such as supercapacitors could increase the performance of such systems as the key factor of a BLH system seems to be the maximum charging/discharging current as opposed to the capacity. Moreover, a BLH system would be able to simulate the customer's presence at home. Determining the overall efficiency may decrease the practicality of a BLH system compared to other systems. With regards to LLH, a long-term simulation based on a novel dynamic model considering the temperature of the hot water could offer new insights to such a system. Moreover, enhancements of the algorithms may finally increase the level of privacy protection.

“The bottom line, says Rotenberg¹, is who controls the data. 'You may not have a lot of privacy concerns about whether you're using a toaster or a toaster oven,' he says, 'but you should be able to decide whether or not you reveal that information.' ”[12]

¹M. Rotenberg: director of the Electronic Privacy Information Center

Bibliography

- [1] Comparison Table of Secondary Batteries. http://batteryuniversity.com/learn/article/secondary_batteries. Online; accessed on 24th of February 2014.
- [2] Energy Storage. http://www.valldoreix-gp.com/en_energy_storage.html. Online; accessed on 24th of February 2014.
- [3] EXAA - Historische Marktdaten. <http://www.exaa.at/de/marktdaten/historische-daten>. Online; accessed on 20th December 2013.
- [4] Geschäfts- und Nachhaltigkeitsbericht 2012. http://www.exaa.at/exaa/annual-reports/exaa_de_gb_12_online_final.pdf. Online; accessed on 7th January 2014.
- [5] Handbook of batteries, Linden and Reddy - A short battery primer. <http://web.mit.edu/2.009/www/resources/mediaAndArticles/batteriesPrimer.pdf>. Online; accessed on 24th of February 2014.
- [6] HEV Vehicle Battery Types. <http://www.thermoanalytics.com/support/publications/batterytypesdoc.html>. Online; accessed on 24th of February 2014.
- [7] Kemo Electronic - Power Control Device E028 110 - 240 V/AC. <http://www.kemo-electronic.de/en/Light-Sound/Effects/Modules/M028-Power-control-110-240-V-AC-2600-VA.php>. Online; accessed on 16th January 2014.
- [8] Neostore compact. http://www.neovoltaic.com/de/produkte/neostore_compact. Online; accessed on 16th October 2013.
- [9] Stromspeicherung von VARTA Storage. <http://www.everto.at/produkte/solar-stromspeicher/>. Online; accessed on 16th October 2013.
- [10] Panasonic Develops New Higher-Capacity 18650 Li-Ion Cells; Application of Silicon-based Alloy in Anode. <http://www.greencarcongress.com/2009/12/panasonic-20091225.html>, 2009. Online; accessed on 24th of February 2014.
- [11] Energy Storage News - GE to Manufacture Molten Salt Sodium Nickel Chloride Batteries for Stationary Electricity Storage Applications. <http://www.energystoragenews.com/GE%20Plans%20to%20Manufacture%20Molten%20Salt%20Sodium%20Nickel%20Chloride%20Batteries%20for%20Mobile%20and%20Stationary%20Electricity%20Storage%20Applications.htm>, 2011. Online; accessed on 24th of February 2014.

- [12] A. Leo. Energy News - The Measure of Power. <http://www.technologyreview.com/news/401081/the-measure-of-power/>. Online; accessed on 22nd January 2014.
- [13] A. Molina-Markham, P. Shenoy, K. Fu, E. Cecchet, and D. Irwin. Private Memoirs of a Smart Meter. In *Proceedings of the 2nd ACM Workshop on Embedded Sensing Systems for Energy-Efficiency in Building*, BuildSys '10, pages 61–66, 2010.
- [14] A. Zoha, A. Gluhak, M.A. Imran, and S. Rajasegarar. Non-Intrusive Load Monitoring Approaches for Disaggregated Energy Sensing: A Survey. *Sensors*, 12(12):16838–16866, 2012.
- [15] AECOM Limited. Energy Demand Research Project: Final Analysis, June 2011.
- [16] K. Anderson et al. BLUED: A Fully Labeled Public Dataset for Event-Based Non-Intrusive Load Monitoring Research. In *Proceedings of the 2nd KDD Workshop on Data Mining Applications in Sustainability (SustKDD)*, Beijing, China, 2012.
- [17] S. Barker et al. Smart*: An Open Data Set and Tools for Enabling Research in Sustainable Homes. In *Proceedings of the 2nd KDD Workshop on Data Mining Applications in Sustainability (SustKDD)*, Beijing, China, 2012.
- [18] Bundesministerium für Wirtschaft, Familie und Jugend. Intelligente Messgeräte-Einführungsverordnung - IME-VO. <http://www.e-control.at/portal/page/portal/medienbibliothek/service-beratung/dokumente/pdfs/Intelligente-Messgeraete-Einfuehrungsverordnung%E2%80%93IME-VO.pdf>, April 2012. Online; accessed on 3rd October 2013.
- [19] C. Efthymiou and G. Kalogridis. Smart Grid Privacy via Anonymization of Smart Metering Data. In *Proceedings of the 1st IEEE International Conference on Smart Grid Communications*, pages 238–243, 2010.
- [20] C. Hiptmayr. Profil - Neue Stromzähler: Wie sich die Politik der Industrie beugt. <http://www.profil.at/articles/1243/560/344744/smart-meter-neue-stromzaehler-wie-politik-industrie>, 2012. Online; accessed on 20th February 2014.
- [21] C. Honsberg. Storage in PV Systems. Technical report, University of Delaware, 2008. Online; accessed on 15th October 2013.
- [22] C. Thoma, T. Cui, and F. Franchetti. Secure Multiparty Computation Based Privacy Preserving Smart Metering System. In *Proceedings of the North American Power Symposium (NAPS)*, pages 1–6, 2012.
- [23] C.M.K.C. Cuipers and E.J. Koops. Het wetsvoorstel 'slimme meters': een privacytoets op basis can art. 8 EVRM. Technical report, Universiteit von Tilburg, 2008.

- [24] D. Egarter, V.P. Bhuvana, and W. Elmenreich. Appliance State Estimation Based on Particle Filtering. In *Proceedings of the 5th ACM Workshop on Embedded Systems For Energy-Efficient Buildings*, BuildSys'13, pages 1–2, 2013.
- [25] D. Hütter. Spitzenlastbepreisung und intelligente Zähler. Master's thesis, Institut für Elektrizitätswirtschaft und Energieinnovation der Technischen Universität Graz, 2010.
- [26] D. Hütter and H. Stigler. IEWT 2011 - Auswirkungen von zeitvariablen Preisstrukturen auf den Spitzenleistungsbedarf in Österreich. http://eeg.tuwien.ac.at/eeg.tuwien.ac.at_pages/events/iewt/iewt2011/uploads/fullpaper_iewt2011/P_19_Huetter_Daniel_31-Jan-2011,_8:31.pdf, 2011. Online; accessed on 4th October 2013.
- [27] D.P. Varodayan and A. Khisti. Smart meter privacy using a rechargeable battery: Minimizing the rate of information leakage. In *Proceedings of the IEEE International Conference on Acoustics, Speech and Signal Processing, ICASSP*, pages 1932–1935, 2011.
- [28] D.U. Sauer, M. Leuthold, D. Magnor, and B. Lunz. Dezentrale Energiespeicherung zur Steigerung des Eigenverbrauchs bei netzgekoppelten PV-Anlagen. Technical report, RWTH Aachen University, 2011.
- [29] E-Control. Erläuterungen zur IMA-VO 2011. http://www.e-control.at/portal/page/portal/medienbibliothek/strom/dokumente/pdfs/IMA-VO_Erlaeuterungen.pdf, 2011. Online; accessed on 3rd October 2013.
- [30] E-Control. Intelligente Messgeräte-AnforderungsVO 2011 - IMA-VO 2011. http://www.e-control.at/portal/page/portal/medienbibliothek/strom/dokumente/pdfs/IMA-VO_BGBL_2011_II_339.pdf, October 2011. Online; accessed on 3rd October 2013.
- [31] E. Klaassen, Y. Zhang, I. Lampropoulos, and H. Slootweg. Demand Side Management of Electric Boilers. In *Proceedings of the 3rd IEEE International Conference on Innovative Smart Grid Technologies*, pages 1–6, 2012.
- [32] E.L. Quinn. Privacy and the New Energy Infrastructure. *Center for Energy and Environmental Security Working Paper No. 09-001*, 2008.
- [33] E.L. Quinn. Smart Metering & Privacy: Existing Law and Competing Policies. *A Report for the Colorado Public Utilities Commission*, 2009.
- [34] E.M. Valeriote, T.G. Chang, and D.M. Jochim. Fast Charging of Lead-Acid Batteries. In *Proceedings of the 9th Annual Battery Conference on Application and Advances*, pages 33–38, 1994.
- [35] Ernst & Young. Kosten-Nutzen-Analyse für einen flächendeckenden Einsatz intelligenter Zähler, July 2013.

- [36] F. Li, B. Luo, and P. Liu. Secure Information Aggregation for Smart Grids Using Homomorphic Encryption. In *Proceedings of the 1st IEEE International Conference on Smart Grid Communications*, pages 327–332, 2010.
- [37] F. Skopik. Security Is Not Enough! On Privacy Challenges in Smart Grids. *International Journal of Smart Grid and Clean Energy*, 1:7–14, 2012.
- [38] F.D. Garcia and B. Jacobs. Privacy-friendly Energy-metering via Homomorphic Encryption. In *Proceedings of the 6th International Conference on Security and Trust Management*, STM’10, pages 226–238, 2011.
- [39] G. Ács and C. Castelluccia. I Have a DREAM!: Differentially Private Smart Metering. In *Proceedings of the 13th International Conference on Information Hiding*, IH’11, pages 118–132, 2011.
- [40] G. Kalogridis, C. Efthymiou, S.Z. Denic, T. Lewis, and R. Cepeda. Privacy for Smart Meters: Towards Undetectable Appliance Load Signatures. In *Proceedings of the 1st IEEE International Conference on Smart Grid Communications*, pages 232–237, 2010.
- [41] G.W. Hart. Nonintrusive appliance load monitoring. In *Proceedings of the IEEE*, volume 80, pages 1870–1891, 1992.
- [42] H. Salehfar, P.J. Noll, B.J. LaMeres, M.H. Nehrir, and V. Gerez. Fuzzy Logic-Based Direct Load Control of Residential Electric Water Heaters and Air Conditioners Recognizing Customer Preferences In a Deregulated Environment. In *IEEE Power Engineering Society Summer Meeting*, volume 2, pages 1055–1060, 1999.
- [43] I. Buchmann. What is the perfect battery? <http://www.buchmann.ca/article4-page1.asp>, 2001. Online; accessed on 24th of February 2014.
- [44] I. Buchmann. Charging the lead-acid battery. http://www.id1.ku.edu/ARA/AARPS/Documents/Batteries&Chargers/Battery_U_13_Charging.pdf, 2006. Online; accessed on 7th November 2013.
- [45] I. Mendaza, B. Bak-Jensen, and Z. Chen. Electric Boiler and Heat Pump Thermo-Electrical Models for Demand Side Management Analysis in Low Voltage Grids. *International Journal of Smart Grid and Clean Energy*, 2(1):52–59, 2013.
- [46] J. Dixon, M. Ortúzar, E. Arcos, and I. Nakashima. ZEBRA plus ultracapacitors: A good match for energy efficient EVs. Technical report, Pontificia Universidad Católica de Chile.
- [47] J. Liang, S.K.K. Ng, G. Kendall, and J.W.M. Cheng. Load Signature Study Part I: Basic Concept, Structure, and Methodology. *IEEE Transactions on Power Delivery*, 25(2):551–560, 2010.

- [48] J. Liang, S.K.K. Ng, G. Kendall, and J.W.M. Cheng. Load Signature Study Part II: Disaggregation Framework, Simulation, and Applications. *IEEE Transactions on Power Delivery*, 25(2):561–569, 2010.
- [49] K. Kursawe, G. Danezis, and M. Kohlweiss. Privacy-friendly Aggregation for the Smart-grid. In *Proceedings of the 11th International Conference on Privacy Enhancing Technologies*, PETS’11, pages 175–191, 2011.
- [50] K. Vanthournout, R. D’hulst, D. Geysen, and G. Jacobs. A Smart Domestic Hot Water Buffer. *IEEE Transactions on Smart Grid*, 3(4):2121–2127, 2012.
- [51] K.C. Armel, A. Gupta, G. Shrimali, and A. Albert. Is Disaggregation the Holy Grail of Energy Efficiency? The Case of Electricity. *Energy Policy*, 52(C):213–234, 2013.
- [52] J.J.C. Kopera. Inside the Nickel Metal Hydride Battery. http://www.cobasys.com/pdf/tutorial/inside_nimh_battery_technology.pdf, 2004. Online; accessed on 24th of February 2014.
- [53] L. Paull, D. MacKay, H. Li, and L. Chang. A Water Heater Model for Increased Power System Efficiency. In *Proceedings of the Canadian Conference on Electrical and Computer Engineering*, pages 731–734, 2009.
- [54] L.O. Valden and R. Stoiber. Key Technologies for battery Electric Transportation. Technical report, 2012. Online; accessed on 24th of February 2014.
- [55] M. Orphelin and J. Adnot. Improvement of Methods for Reconstructing Water Heating Aggregated Load Curves and Evaluating Demand-Side Control Benefits. In *Proceedings of the IEEE Transactions on Power Systems*, volume 14, pages 1549–1555, 1999.
- [56] M. Shaad, A. Momeni, C.P. Diduch, M. Kaye, and L. Chang. Parameter identification of thermal models for domestic electric water heaters in a direct load control program. In *Proceedings of the 25th IEEE Canadian Conference on Electrical and Computer Engineering*, pages 1–5, 2012.
- [57] M. Zeifman and K. Roth. Nonintrusive Appliance Load Monitoring: Review and Outlook. *IEEE Transactions on Consumer Electronics*, 57(1):76–84, 2011.
- [58] M.A. Lisovich, D.K. Mulligan, and S.B. Wicker. Inferring Personal Information from Demand-Response Systems. *IEEE Security and Privacy*, 8(1):11–20, 2010.
- [59] M.L. Marceau and R. Zmeureanu. Nonintrusive load disaggregation computer program to estimate the energy consumption of major end uses in residential buildings. *Energy Conversion and Management*, 41:1389–1403, 2000.
- [60] P. Murphy et al. Enabling Tomorrow’s Electricity System. *Report of the Ontario Smart Grid Forum*, 2010.

- [61] NIST. Framework and Roadmap for Smart Grid Interoperability Standards, Release 1.0 (Draft). Technical report, National Institute of Standards and Technology, U.S. Department of Commerce, 2009.
- [62] P. Amann, G. Huber, J. Reißner, and J. Petrasch. Domestic Hot Water Heater for Active Demand Side Management and Efficiency Improvements. Technical report, Energy Research Center, Vorarlberg University of Applied Sciences, 2013.
- [63] P. Bertoldi, B. Hirl, and N. Labanca. Energy Efficiency Status Report 2012 - Electricity Consumption and Efficiency Trends in the EU-27. Technical report, European Commission - Joint Research Centre - Institute for Energy and Transport, 2012.
- [64] P.L. Joskow and C.D. Wolfram. Dynamic Pricing of Electricity - Draft. Technical report, 2011.
- [65] PricewaterhouseCoopers Austria. Studie zur Analyse der Kosten-Nutzen einer österreichweiten Einführung von Smart Metering, June 2010.
- [66] R. Anderson and S. Fuloria. On the Security Economics of Electricity Metering. In *WEIS*, 2010.
- [67] R. Jia, M.H. Nehrir, and D.A. Pierre. Voltage Control of Aggregate Electric Water Heater Load for Distribution System Peak Load Shaving Using Field Data. In *Proceedings of the 39th North American Power Symposium*, pages 492–497, 2007.
- [68] A. Reinhardt et al. On the Accuracy of Appliance Identification Based on Distributed Load Metering Data. In *Proceedings of the 2nd IFIP Conference on Sustainable Internet and ICT for Sustainability*, pages 1–9, 2012.
- [69] S. Makonin, F. Popowich, L. Bartram, B. Gill, and I.V. Bajic. AMPds: A Public Dataset for Load Disaggregation and Eco-Feedback Research. In *Proceedings of the Annual Electrical Power and Energy Conference (EPEC)*, pages 1–6, 2013.
- [70] S. McLaughlin, P. McDaniel, and W. Aiello. Protecting Consumer Privacy from Electric Load Monitoring. In *Proceedings of the 18th ACM Conference on Computer and Communications Security, CCS '11*, pages 87–98, 2011.
- [71] Staff of Austria Email AG. Operation and Maintenance Instructions. http://www.austria-email.com/fileadmin/content-en/Products/Wall-mounted_electric_water_heater/Haengespeicher_kompakt_EWH/228843-12_Elektrospeicher_-en.pdf, 2013. Online; accessed on 5th December 2013.
- [72] Staff of Lab-Volt Ltd. Lead-Acid Batteries - Courseware Sample. http://www.labvolt.com/downloads/download/86351_f0.pdf, 2010. Online; accessed on 7th November 2013.

-
- [73] W. Labeeuw and G. Deconinck. Non-intrusive detection of high power appliances in metered data and privacy issues. Technical report, Katholieke Universiteit Leuven, Department of Electrical Engineering, 2011.
- [74] W. Yang, N. Li, Y. Qi, W. Qardaji, S. McLaughlin, and P. McDaniel. Minimizing private data disclosures in the smart grid. In *Proceedings of the 18th ACM Conference on Computer and Communications Security, CCS '12*, pages 415–427, 2012.
- [75] Z.J. Kolter and M.J. Johnson. REDD: A Public Data Set for Energy Disaggregation Research. In *Proceedings of the SustKDD Workshop on Data Mining Applications in Sustainability*, 2011.
- [76] Z.J. Kolter and T. Jaakkola. Approximate Inference in Additive Factorial HMMs with Application to Energy Disaggregation. In *Proceedings of the International Conference on Artificial Intelligence and Statistics*, volume 22 of *JMLR Proceedings*, pages 1472–1482, 2012.